Master’s Thesis – Master Energy Science

RESILIENT DECARBONIZATION STRATEGIES FOR DISTRICT HEATING:

A TECHNO-ECONOMIC ANALYSIS OF AMBIENT AND WASTE HEAT SOURCES CONSIDERING ECONOMIC RISKS DUE TO UNCERTAINTY IN FUTURE ENERGY PRICES AND WASTE HEAT AVAILABILITY

Nyasha Grecu

Student ID: 5273528

May 31, 2024

Supervisors:
Dr. Wen Liu, Utrecht University
Dr.-Ing. Ralf-Roman Schmidt, AIT Austrian Institute of Technology GmbH

Second reader:
Dr. Javanshir Fouladvand, Utrecht University

Internship organization:
AIT Austrian Institute of Technology GmbH
Giefinggasse 4
1210 Vienna
Austria

ABSTRACT

District heating (DH) systems can contribute substantially to the decarbonization of the heating sector by enabling the implementation of sustainable heating solutions on a large scale and the use of heat sources that are difficult to integrate on a small scale. This includes ambient heat (AH) and waste heat (WH), two heat sources with large, untapped potential. However, DH systems with AH and WH are subject to economic risks arising from uncertainty in the future development of key factors such as energy prices and WH availability. Accordingly, this thesis evaluated the technical and economic performance of AH and WH sources employed for the resilient decarbonization of DH networks considering economic risks due to uncertainty in future energy prices and WH availability.

Specifically, a model was developed that simulates DH systems with and without AH and WH sources and evaluates the levelized cost of heat (LCOH) across a wide range of energy price scenarios and WH cessation scenarios. WH cessation scenarios reflect the possibility that the WH source is no longer available due to bankruptcy, relocation, or a change in processes such that internal heat recovery increases. The model was applied to various DH system configurations (defined by the heat supply technologies in the DH system and their capacities) in the context of both a general model and a case study application for a small city in northwestern Poland. The mean LCOH and standard deviation across energy price and WH cessation scenarios provided a measure of average cost and associated economic risk of the configurations analyzed.

Results indicate that the average cost and economic risk of DH systems is strongly influenced by the DH system configuration. Additionally, results show that a tradeoff exists between average cost and economic risk. The inclusion of industrial WH in DH systems is beneficial to the techno-economic performance of DH systems in terms of average cost and often also economic risk. However, this is largely due to the assumptions that industrial WH has a relatively low price, the price remains constant across energy price scenarios, and the probability of WH cessation is relatively low. Another key research outcome is that the presence of AH and WH sources in DH systems leads to a reduction in economic risk in the face of future uncertainties. Increased supply side flexibility in the form of a greater variety and installed capacity of heat supply technologies, also leads to reduced economic risk.

These outcomes highlight the importance of the careful consideration of heat supply technologies and DH system configurations, accounting for uncertainty in the future development of key factors, such as energy prices and WH availability, in the resilient decarbonization of DH systems.

ACKNOWLEDGEMENTS

I would like to express my gratitude to my supervisors, Dr. Wen Liu and Dr.-Ing. Ralf-Roman Schmidt, whose guidance, support, and feedback were instrumental in shaping this work. I would also like to thank my colleagues at AIT for the valuable insight and advice they provided, which significantly contributed to the progress of this research.

A heartfelt thank you to Valentin Hübner for his continued support and insightful feedback during the process of completing this thesis. I am immensely grateful to Talya Grecu, Sabine Grecu, and Dorin Grecu for their endless support and encouragement, not only throughout this thesis but also during my entire university career. Lastly, I would like to thank all the friends and family members who have also been there to support and encourage me throughout this process.

TABLE OF CONTENTS

LIST OF ABBREVIATIONS

AH	Ambient heat
AIT	Austrian Institute of Technology
CAPEX	Capital expenditures
CCS	Carbon capture and storage
CO_2	Carbon dioxide
COP	Coefficient of performance
CHP	Combined heat and power
DEA	Danish energy agency
DSM	Demand side management
DH	District heating
EU	European Union
HOB	Heat only boiler
HP	Heat pump
ISD	Integrated surface database
KPI	Key performance indicator
LCOH	Levelized cost of heat
MCS	Montecarlo simulation
NOAA	National Oceanic and Atmospheric Administration
NCEI	National Centers for Environmental Information
OPEX	Operational expenditure
O&M	Operation and maintenance
PDF	Probability density function
PV	Photovoltaic panels
SQ	Sub question
TESCA	Techno-economic system and computational analysis
UU	Utrecht University
WH	Waste heat
WWTP	Wastewater treatment plant

LIST OF TABLES

LIST OF FIGURES

1 INTRODUCTION

1.1 BACKGROUND AND SOCIETAL RELEVANCE

To mitigate climate change and its negative effects, the European Union (EU) has set the legally binding target of becoming a climate neutral society by 2050 [1]. This extends to the energy sector and, within that, the heating sector. Heat needed for space heating and hot water makes up a large portion of energy demand (and associated emissions), and is still largely fossil fuel based [2], [3]. In the EU, 40% of total final energy demand comes from the heating and cooling sector, with 75% supplied by fossil fuels [4]. This makes decarbonizing the heat sector incredibly relevant for achieving EU targets and mitigating climate change.

District heating (DH) networks can play a key role in heat decarbonization [5]. This is because they enable the implementation of sustainable heating solutions on a large scale and the use of heat sources that are difficult to integrate on a small scale, such as ambient heat (AH) and waste heat (WH) [6], [7]. The use of heat pumps (HPs) in DH networks can provide greater flexibility by increasing the coupling of the electricity and heat sectors [8], [9], [10]. This will become increasingly relevant with greater penetration of intermittent renewable energy in the future [9]. HPs also allow for the integration of lower temperature heat sources that could not be used otherwise, especially AH but often also WH [4]. Further advantages are that DH networks are mature systems that can provide flexible, economical, and reliable heating solutions [5]. However, current DH systems are still largely fossil fuel based [2]. In 2017, 48% of the EU-27 DH mix consisted of fossil fuels, with 25% coming from natural gas, 16% from hard coal, 5% from lignite (brown coal) and 2% from oil [11]. Although this is often WH from fossil CHP processes, the reliance of DH systems on fossil fuel sources creates a need for a comprehensive and thorough evaluation of DH decarbonization options and the role they can play in the future.

Various heat supply technologies can be used for decarbonizing DH systems [2], [5]. These include biomass, geothermal energy, solar thermal energy, AH, WH, waste incineration, and large-scale HPs [12], [13]. Furthermore, thermal storage, greater coupling of the electricity and heat sectors, and reduced DH operating temperatures can also contribute to DH decarbonization [12]. Two options with large, untapped potential are the use of AH and WH for DH. AH refers to heat found in water bodies, air near the earth's surface, and ground a few meters belowground [14]. It can be combined with large-scale HPs to obtain heat at temperatures suitable for DH. WH is heat that is produced as a byproduct in processes such as cooling of datacenters or high temperature industrial processes and that would otherwise be dissipated into the environment [15]. Depending on the temperature of the WH source and the DH network, it may also require coupling with HPs [16].

The decarbonization of DH systems using AH and WH requires large investments in sustainable heat supply technologies including heat exchangers, HPs, and piping infrastructure, as well as storages etc. Different temperature AH and WH sources have different benefits and risk factors. For AH sources, there is high certainty they will still be available in the future. However, they have low temperatures, especially in the winter, and therefore rely on HPs. This results in low coefficient of performances (COPs), higher investment costs due to the HP, and increased dependence and vulnerability to electricity prices [17]. High temperature WH from industrial processes has relatively low investment and operation costs as no HP is necessary. However, there is greater uncertainty surrounding its future availability as there is a chance that industrial activities change (i.e., with industry decarbonization) or are discontinued (i.e., if the company relocates) [18]. Medium temperature WH such as from service sector cooling also requires a HP, and therefore has higher investment cost. However, COPs are higher than for AH sources and, depending on the source, future availability may be more certain compared to high temperature WH sources.

Thus, in analyzing which options are best to invest in, it is not only important to consider overall cost but also the system's resilience in the face of future uncertainties. This is because the development of key factors, such as energy prices or WH availability, impacts DH system costs. Thus, economic risks, in the form of variations in the expected cost of the system, arise from the uncertainty in the future development of these factors. This is a key consideration of this thesis, which aims to understand the potential role of AH and WH in the resilient decarbonization of DH networks, considering the uncertainty in the future development of energy prices and WH availability. Focus is placed on energy prices and WH availability as these are two key sources of uncertainty for future DH systems with AH and WH.

1.2 SCIENTIFIC RELEVANCE

This section provides an overview of the scientific relevance of analyzing the potential of AH and WH sources for contributing to the resilient decarbonization of DH systems considering future uncertainty. See Section 2 for an in-depth discussion of existing literature and analysis of individual studies.

Various papers have analyzed the technical and economic performance of DH systems with AH and/or WH sources (see section 2.1). Of these, most focus on DH systems with AH sources coupled with large-scale HPs, [3], [4], [7], [8], [19], [20], [21] while only a limited number of studies consider DH systems with WH [6], [21], [22], [23] or DH systems with both AH and WH [5], [12], [17], [24]. Of studies including both, only one has AH and WH as the main focus of the analysis [17], while the others just include AH and WH as two of the multiple heat supply technologies in the DH system being studied [5], [12], [24]. Furthermore, no study focuses on the analysis of AH and WH on a general level, considering the different types of AH and WH sources available and their potential contribution to the robust decarbonization of DH systems. Moreover, if accounting for uncertainties, studies conducting techno-economic analysis on DH systems with AH and/or WH mostly use either sensitivity analysis or scenario analysis [3], [4], [5], [6], [8], [9], [17], [22], [23], [24]. These approaches do not allow for the consideration of the expected probability of the distribution of uncertain inputs, i.e., quantifying the uncertainty. Furthermore, sensitivity analysis only considers the effect of varying a single parameter at a time rather than the combined effect of the simultaneous variations in multiple parameters, or considering interdependent uncertainty parameters, which more accurately reflects uncertainty in real-world situations. In contrast, the use of other approaches to uncertainty modelling, such as Monte Carlo simulation (MCS), allows for the quantification of uncertainty in such a way that these expected probabilities are accounted for. Moreover, they allow for the simultaneous variation in multiple key input parameters, reflecting uncertainty in various parameters. This has been exemplified and applied by studies focusing on uncertainty modelling for heat supply technologies and DH systems, largely using MCS (see section 2.2). However, of these studies, those analyzing individual heat supply technologies have mainly focused on fossil-fueled CHP plants [25], [26], [27], [28], [29], and those studying systems with multiple technologies have mainly compared centralized DH systems to decentralized ones without DH [3], [18], [30]. Finally, only a limited number of papers explicitly modelled future DH systems despite the importance of this in designing robust decarbonization strategies for DH systems [5], [8], [12], [17], [18], [20], [24], [31] (see section 2.3).

Thus, the literature gap this thesis seeks to address is twofold:

- First, is the lack of a **techno-economic analysis that focuses on AH and WH** as heat supply sources for DH on a general level, comparing different types of AH and WH and how they perform in contributing to the decarbonization of DH systems.
- Second, is the lack of a study that focuses on **quantifying the economic risk** associated with DH systems with AH and WH, which arises from uncertainty in the future development of key factors, such as energy prices and WH availability.

1.3 Research question

Accordingly, the research question this thesis aims to answer is:

What is the technical and economic performance of employing AH and WH supply technologies for the resilient decarbonization of DH networks considering uncertainty of future energy prices and WH availability?

The techno-economic performance of DH networks employing AH and WH sources is measured in terms of average costs and associated economic risk. It is calculated taking into consideration future DH systems and uncertainty in the development of future energy prices and WH availability, as these were identified as two key sources of uncertainty for future DH systems with AH and WH. The research question is broken down into the following sub-questions (SQs):

- SQ1: What is the average cost of DH system configurations[1] both incorporating and excluding AH and/or WH in future DH systems and how do they compare?
- SQ2: What is the level of economic risk arising from uncertainty of future energy prices and WH availability for technology configurations both incorporating and excluding AH and/or WH in future DH systems and how do they compare?

The temporal scope of the thesis is a twenty year study period starting in 2050, the year the EU aims to become climate neutral [1]. In addition to the analysis of the role of AH and WH in DH decarbonization on a general level, a case study is conducted which considers the DH system of a small city in northwestern, Poland.[2] This case study is part of an ongoing Horizon Europe project, HeatMineDH. This results in a third SQ:

- SQ3: What is the technical and economic performance of employing AH and WH supply technologies for the resilient decarbonization of the DH network of a small city in northwestern Poland considering uncertainty of future energy prices and WH availability?

[1] DH system configuration refers to the heat supply technologies in a DH system and their capacity.
[2] The city is not named for confidentiality reasons.

1.4 ROADMAP

The remainder of this thesis is structured as follows:

Section 2 provides an overview of relevant literature on the subject, first considering studies evaluating the techno-economic performance of AH and WH technologies in DH systems, then studies focusing on uncertainty modeling of heat supply technologies and DH networks, and finally the consideration of future scenarios within these studies.

Section 3 outlines the methodology employed in the thesis. First, a detailed explanation of the methodological steps is provided followed by a comprehensive description of the general model and case study. These descriptions include an overview of the system modelled, an explanation of key input data and model parametrization, the definition of system configurations analyzed, and an account of the methodological steps' application.

Section 4 presents the results of the general model, followed by those of the case study application.

Section 5 analyzes and discusses the results. Initially, an synthesis of key findings from the general model and case study is presented. Subsequently, results are analyzed in the context of literature. Then, limitations of the study are discussed, followed by potential directions for future research. The section ends with a discussion of insights and recommendations for stakeholders.

Finally, section 6 concludes this work with a summary of key results, conclusions, and their implications.

2 LITERATURE REVIEW

The following section provides an overview of literature relevant to this thesis' aim of investigating the techno-economic potential of AH and WH supply technologies in contributing to the resilient decarbonization of DH networks, considering uncertainty of future energy prices and WH availability. Existing literature has been categorized into the following three topics:

1. **Techno-economic analysis**: studies evaluating the technical and economic performance of AH and WH technologies in DH systems, providing insights into what types of systems have been analyzed and their viability.
2. **Uncertainty modelling**: studies modelling uncertainty and economic risk associated with heat supply technologies and DH networks, providing insight into key factors that influence their techno-economic performance and the impact of these factors.
3. **Future scenarios:** studies that specifically model and forecast future DH systems with AH and/or WH sources, providing insight into what future scenarios could look like.

These three topics are at the core of the research focus of this thesis, and thus the literature review is structured accordingly.

2.1 TECHNO-ECONOMIC ANALYSES

This section reviews literature analyzing the techno-economic performance of AH and WH in DH systems. A distinction is made between studies focused on AH coupled with large-scale HPs, studies analyzing medium to high temperature WH that are either coupled with a HP or not based on their temperature, and those that consider systems with both large-scale HPs and WH. A distinction is also made between analyses assessing the technologies individually and those assessing the technologies as part of a configuration of sustainable heat technologies.

Ambient heat with large-scale heat pumps

AH refers to heat found in water bodies, air near the earth's surface, and ground a few meters belowground [14]. Due to their relatively low temperatures, AH sources need to be combined with large-scale HPs to supply heat at a high enough temperature for DH. HPs are powered by electricity and use a closed process to extract heat from a low-temperature heat source and convert it to a higher temperature [32]. The term 'large-scale' is used to highlight that the HPs referred to are in the MW range and at a scale large enough to provide heat to a DH system (in contrast to HPs at an individual household level).

Of studies analyzing AH combined with large-scale HPs, many focused on optimal operation. For example, Abokersh et al. compared different control strategies for HPs in a DH system with solar collectors, a seasonal thermal storage, a domestic hot water storage, and an auxiliary natural gas heater [19]. They found that the HP operation strategy has a significant effect on the economic performance of the system, with one of the two control strategies analyzed consistently leading to a lower levelized cost of heat (LCOH) across scenarios analyzed regardless of the different scenario aims (minimizing cost vs. minimizing natural gas use). Bach et al. studied the integration of drinking water, sewage water, and sea water HPs in Copenhagen's DH system, comparing their integration in the DH distribution vs. transmission network, and the use of a variable or fixed COP in modelling the HPs. The COP was found to play a key role in determining the HPs' operational hours [8]. When connected to the higher temperature transmission network, the COP is lower, increasing the cost of heat from the HP, and reducing the full load operating hours. Similarly, using a variable COP when modelling HPs as it improved their cost competitiveness when the COP was relatively high and thus influenced the operating hours [8]. Other studies focused on the flexibility HPs provide by increasing the interconnection of the electricity and heat sectors. Fambri et al. analyzed flexibility provision by groundwater-based HPs in Turin's DH system and found that not only does the HP improve the balance of the electricity distribution system but has greater profitability when doing so [9]. Østergaard et al. compared a system with seawater-based HPs and storage to a biomass-based DH system and found that HPs increased renewable energy integration but, unlike Fambri et al, that they were less attractive from a business economic perspective [7].

Other studies included HPs in a system with an array of technologies. Fitó et al. studied the robustness of a decentralized, electricity-based system (connecting the national electricity grid with decentralized photovoltaic panels (PV), HPs, electric batteries, and thermal storage per building) compared to a centralized, heat-based system (consisting of a DH network connected to the same technologies at a larger scale, as well as a gas boiler, biomass CHP, solar thermal collectors, and geothermal plant). The two most impactful parameters on total cost were space heating demand and the COP of the HPs. The heat-based system was found to have overall lower costs across all carbon constraint scenarios studied and be more robust as it was less sensitive to changes in space heating demand, HP COP, and carbon constraints. Lamaison et al. analyzed a system with a biomass generator, HP, and heat storage, optimizing for levelized cost of energy, sizing, and operation [33]. Results indicated that the combination of the three technologies is an attractive configuration for DH systems. For optimal operation, the HP was used in combination with daily storage with the HP operating at low electricity prices and the storage being utilized at high electricity prices. In scenarios with limited biomass availability a seasonal storage was required [33]. Kontu et al. found the competition with combined heat and power (CHP) plants decreases the viability of HPs in medium- or large-scale DH systems with heat only boilers (HOBs) and CHPs compared to small-scale ones with only HOBs [4]. This highlights that the configuration and size of the system analyzed influences the operation and cost effectiveness of HPs in the system However, the inclusion of a HP reduced variable costs across all system sizes as they can be used when electricity prices are low. For the same reason, the HPs lead to even greater cost reductions in low electricity price scenarios [4]. Yang et al. compared the economic performance of solar assisted ground source HPs to solar thermal energy storage and natural gas, biomass, and electric boilers [20]. As with Kontu et al, results also indicated that the LCOH was dependent on the system configuration considered. Furthermore, results indicated that the economic competitiveness and environmental benefits of systems with electric heating through electric boilers or HPs is highly dependent on electricity prices and the electricity mix considered. Yang et al. also highlight the possibility of a negative impact of electric heating on the electricity grid as it more than a doubled electricity demand in the case study considered (Harbin, China), which could place a significant burden on the electricity grid [20].

In summary, studies focusing on the integration of large-scale HPs in DH networks highlight that the operation strategy and COP directly influences their operation and the cost of the system. Additionally, the configuration and size of the system in which the HP is included also affects the technical and economic performance of HPs in DH systems. Moreover, HPs are found to increase flexibility and renewable energy integration. Finally results generally indicate that systems with HP are more cost effective relative to systems without HPs, however this is not always the case.

Waste heat

WH is heat that is generated as a byproduct in processes such as cooling of datacenters or high temperature industrial processes that would otherwise be released into the environment [15]. To serve as a heat source for DH, it may require coupling with large scale HPs depending on the temperature of the WH source and DH network [16].

Fewer studies focused on WH compared to HPs. Specific WH sources analyzed included WH from a petrochemical cluster in Sweden [6], a wastewater treatment plant (WWTP) and steelwork combined with HPs in Northern Italy [21], and deep cooling of biomass boiler flue gases and a WWTP combined with HPs in Salaspils, Latvia [22]. Bühler et al. considered a wide range of WH sources, analyzing the following sectors: gravel and stone, oil refinery, food, sugar, wood, pulp, and paper, chemical and pharma, cement bricks and rockwool, concrete products, asphalt, metal, metal products. As with HPs, some studies analyzed WH individually [6], [23] while others included WH as one of multiple technologies in a system [21], [22]. A couple studies included future uncertainty in their analysis. Bühler et al. investigated sensitivity of their results to plant lifetime to reflect uncertainty in the availability of WH in the future [23]. Morandin et al. speculated there would be greater internal heat recovery in the future and modelled scenarios where half and all the WH is available for DH [6]. Multiple studies also considered the temporal mismatch between WH availability and DH demand. Bühler et al. found that it results in a 30% decrease in the potential of WH sources to replace fossil fuel heating sources, but this can be reduced to 10% if the WH source is coupled with a heat storage [23]. Similarly, Pakere et al. found that WH integration has the potential to phase out natural gas but that it needs to be coupled with thermal storage to ensure peak demand can be met [22]. Overall, results indicate that WH sources can act as a cost-effective heat supply source for DH networks, and often perform even better than the alternative without WH. Of the wide range of WH sources analyzed by Bühler et al., most were less expensive than both solar DH and the average Danish DH cost, with the least expensive WH coming from the building material, oil refinery, and food production sectors [23]. Morandin et al. found that WH from the petrochemical sector can be profitable currently as well with an assumed reduction in available capacity due to increased internal heat recovery in the future [6]. Pakere et al. found a lower LCOH for the decarbonized scenarios with WH compared to the reference scenario without WH [22]. Spirito et al. reported higher investment costs as more WH is included in the system due to investments needed for HPs coupled to the steelwork and WWTP. However, when accounting for monetized climate change cost, configurations with greater WH inclusion also perform best economically [21].

Ambient and waste heat

Some studies analyzed system configurations that included both HPs and WH. Gonzalez Salazar et al. analyzed paths for replacing coal in Berlin’s DH system, considering river water HPs, industrial WH, waste incineration, geothermal energy, biomass, solar thermal energy, and gas turbines. They calculated optimal operation to minimize costs and found that while DH is more cost effective than decentralized heating, costs largely depend on fuel prices and regulatory frameworks [12]. Specht et al. compared four systems for decarbonizing DH in Leipzig based on: (1) natural gas with carbon capture and storage (CCS), (2) hydrogen, (3) biomass, WH, and solar and (4) electricity. They optimized hourly dispatch based on lowest cost and calculated the LCOH. The latter two scenarios had lower costs than the first two, indicating that systems with more diversified portfolios have a more robust LCOH [24]. Su et al. compared technologies and pathways planned for DH decarbonization in the Helsinki metropolitan area, including HPs, WH from data centers, biomass, geothermal energy, waste incineration, and thermal storage [5]. Like Gonzalez Salazar et al. and Specht et al., they also determined the lowest cost operation strategies. They found that carbon dioxide (CO_2) emissions are expected to decrease significantly until 2030 but average heat production costs will increase significantly, nearly tripling. This is largely due to the investments in new low-carbon technologies. Additionally, there is a significant reduction in revenue from electricity from CHP plants. Nonetheless, WH use from the datacenter is found to be profitable even with high investment costs [5]. Yuan et al. investigated future 100% renewable energy systems, focusing on the tradeoff between industrial WH and HPs when optimizing cost, operation, and CO_2 emissions. They argued a tradeoff exists because additional industrial WH use can hinder renewable energy penetration and therefore flexibility, while increased HPs lead to a more expensive system due to higher initial investment. They found that the optimal mix is not fully reliant on HPs or industrial WH but rather a combination of both energy sources [17].

Future and uncertainty in techno-economic analyses

Most studies model DH systems partially or fully composed of sustainable heat supply technologies. They compare different configurations or scenarios to analyze DH decarbonization pathways and their techno-economic potential. These alternative scenarios are often compared to current DH systems. Most studies model current counterfactual 'snapshots,' but some model future scenarios. Studies considering the future, mostly model different levels of renewable energy penetration in for example 2030 or 2050 [5], [8], [12], [17], [20], [24], [31]. Uncertainties related to future developments are accounted for through the modelling of different scenarios or sensitivity analyses. For example, Gonzalez-Salazar et al. modelled future scenarios with 80% and 95% greenhouse gas (GHG) emission reductions relative to 1990 while Bach et al. conducted a sensitivity analysis to changes in biomass prices, electricity prices and HP capacity [8], [12]. Yang et al. used Monte Carlo simulation (MCS) to model uncertainty in future economic parameters [20]. In studies not considering the future, uncertainties are also often analyzed using scenarios or sensitivity analysis [6], [22], [23] For example, Morandin et al. modelled a future scenario with a 50% reduction in available WH due to increased internal recovery [6] while Pakere et al. modelled a low and high price scenario [22]. Bühler et al. conducted a sensitivity analysis to measure the effect of changes in the discount rate, investment horizon, cost of WH. and electricity prices [23]. The use of scenarios or sensitivity analysis to model uncertainties fails to account for the expected probability of different future developments in prices and heat supply availability. Furthermore, sensitivity analysis only measures the isolated effect of changing a single variable rather than the combined effect of changing multiple variables simultaneously, which more accurately represents reality.

2.2 UNCERTAINTY MODELING

Risk assessment methods can be classified as semi-quantitative or quantitative. Semi-quantitative methods include multi-criteria decision making and scenario analysis. Quantitative approaches include mean variance portfolio theory, real options analysis, MCS, and (stochastic) optimization techniques [34]. As discussed above, multiple studies on the techno-economic potential of AH and WH sources reflect the uncertainty in key input parameters in using a sensitivity analysis to test the effect of variations in input parameters on the output being analyzed [3], [8], [23], [24], [35]. Various papers analyzing AH and WH also take a semi-quantitative approach and model different scenarios [4], [6], [12], [22]. For papers with a quantitative approach, MCS is a common method. This section provides an overview of papers focusing on risk assessment of heat supply technologies and DH networks. First, studies on the economic risk of individual heat supply technologies are considered, then, studies on the economic risk of systems with multiple heat supply technologies are examined, next, studies modeling risks other than economic risks are discussed, and finally, a summary is provided.

Economic risk of individual heat supply technologies

Studies using MCS to analyze economic risk of individual heat supply technologies mainly focus on CHP plants. Besides DH [36], [37], [38], hospitals [25], [29] or small offices [27] are also considered as heat sinks. For the CHP plant fuel, some studies consider biomass [37], [38], municipal solid waste [37] or coal [36] but most analyze natural gas [25], [26], [27], [28], [29], [36]. Two of the studies considering fossil fuels analyze low carbon technologies, namely CCS [36] and integrated reforming combined cycle power plants [26]. In addition to CHP, other heat supply technologies considered have been a biomass boiler [39], wastewater HP [40], and WH from data center [41]. However, these are limited in comparison to the number of studies on CHP plants. Most studies vary economic variables like electricity prices, fuel prices, O&M costs, and investment costs but some also vary technical parameters like lifetime, efficiency, heat demand, and availability. To model expected availability, approaches included modelling scheduled and unscheduled shutdowns in the MCS simulation [36] or varying plant lifetime to account for uncertainty in future availability [28]. In defining the uncertainty of input parameters; some studies define a range based on a mean value and standard deviation [36], [37], while other apply probability distributions such as normal distributions [25], triangular distributions [26] or varying distributions [38].

Key conclusions from the analyses vary. Bartela et al. analyzed a coal CHP with and without CCS and found that the unit with CCS had a higher risk associated with it because of higher investment costs and lower electricity generation efficiency, but was more robust in the face of high uncertainty in future GHG emission allowances [36]. Swing Gustafsson et al. compared decentralized HPs to a DH network coupled with a CHP with different fuels and found that although the HPs performed better on average, the configuration that performed better varied based on the exact input variables. They therefore concluded that which technology is better is case specific and modelling must account for local conditions [37]. Urbanucci and Testi found that the influence of uncertainty on the optimal size and cost of a CHP is significant, and that not accounting for uncertainty led to an overestimation of size and of cost savings [29]. Maribu and Fleten highlight that deterministic models fail to account for the flexibility a CHP can provide in the face of volatile electricity prices, and that CHPs are attractive when this is considered because of their ability to respond to high prices [27]. Regardless of differences in the parameters varied and technologies analyzed, all studies agreed that the modelling of uncertainty allows for the inclusion of more information and knowledge on uncertainties, and thus allows for the quantification and consideration of risk associated with investment in heat supply technologies.

Economic risk of systems with multiple heat supply technologies

Multiple studies have also analyzed the economic risk associated with systems consisting of multiple heat supply technologies. This allows for the comparison of different types of energy or heating systems. This is often systems with and without a DH network. For example, as mentioned in section 2.1, Fitó et al. compared a decentralized, electricity-based system (connecting the national electricity grid with decentralized PV, HPs, electric batteries, and thermal storage per building) to a centralized, heat-based system (consisting of a DH network connected to the same technologies at a larger scale, as well as a gas boiler, biomass CHP, solar thermal collectors, and geothermal plant) [3]. They conducted a multi-objective (costs and CO_2 emissions) optimization of the sizing and operation of each system and tested the robustness of the systems through a sensitivity analysis. The centralized heat-based system was found to be more robust as it was less sensitive to changes in space heating demand, HP COP, and CO_2 emissions constraints. The parameter with the greatest impact on the system design was the maximum CO_2 emissions constraint [3]. Marx et al. compared individual heating systems to an interregional DH network, using MCS to model the uncertainty in future energy prices and WH availability. Uncertainty in WH availability was modelled by using the probability that a company goes bankrupt as a proxy [18]. As for Fitó et al., the individual heating system was found to be less robust. This was because the interregional DH network was able to optimize the supply portfolio using industrial WH at stable prices, HPs at low electricity prices and CHP at high electricity prices, making the cost of the system less dependent on uncertainties in future energy prices. In contrast, uncertainties in energy prices had a greater influence on the economic risk associated with the individual heating systems as they were based on biomass boilers and individual HPs and could less flexibly respond to volatility in energy prices [18]. Verschelde and D'haesleer also compared heating systems with and without a DH network, using machine learning to find the decision boundary for when a system with a DH network is chosen compared to one without. They found that important parameters were linear heat density and the cost of alternative heat technologies. Furthermore, results showed that the decision boundary cannot be based on a single parameter and rather depends on multiple criteria [30].

MCS varying fuel and energy carrier prices has also been used to study the flexibility of energy hubs with various supply technologies, storage options, and/or demand side management (DSM) in the face of volatile market prices. This allows for a valuation of investments in different system configurations which accounts for strategic and operational flexibility and the ability of the system to respond to volatile energy prices [42], [43]. Kienzle et al. studied an energy hub consisting of a CHP with heat storage, DSM, and both storage and DSM. The addition of heat storage and DSM led to increased investment costs but also reduced economic risk, measured by the percent standard deviation of the system's present value. The highest investment cost and lowest risk was found for the system with both heat storage and DSM. This reflects the ability of the energy hub with multiple technologies to provide greater flexibility and robustness in the face of volatile energy prices [42]. Volodina et al. compared three DH system configurations consisting of a datacenter coupled with a HP, a CHP and both accounting for uncertainty in heat demand and energy prices using stochastic ordering [44]. They compared net present value and emissions associated with each design under a green scenario where net zero emissions are reached quickly, a market scenario with limited government intervention, and a neutral scenario between the two. The dispersion of the results is used as an indicator of the risk, and indicated that a HP combined with WH form a datacenter used to supply both baseload and seasonal demand was most robust [44]. Zhang et al. combined various uncertainty analysis methods, using stochastic simulation, uncertainty analysis, and sensitivity assessment to analyze heating and cooling pathways. Specifically, they modeled individual heating, fourth generation DH, fifth generation DH, and ultra-low temperature DH systems under uncertainty in demand, equipment efficiency, equipment cost and electricity prices. They found that the factors to which systems with DH were most sensitive to are heat demand and electricity prices. In contrast, the individual heating system was more sensitive to equipment efficiency and investment costs [35].

Risks other than economic risks

Uncertainty analysis has also been used in relation to DH for modelling risks other than economic risk. This includes the reliability of fuel supply under uncertainty in fuel demand using MCS [45], the failure probability of DH piping using deterministic probability analysis [46], and the optimal design of a CHP plant in terms of type, size, and operation under uncertainty in temperature, energy demand, and prices [47]. Lygnerud and Werner studied the risk posed to industrial WH recovery from industries terminating their activity. For the 107 Swedish WH recovery projects studied, the main reasons for stopped heat delivery (accounting for 6% of annual average heat recoveries) were industry activity discontinuation or substitution by another supply source. Key risk factors identified where small delivery amounts or the use of HPs for low temperature WH [48].

Summary

To summarize, papers looking at individual technologies mostly analyze investment uncertainty related to CHP plants, and mostly CHP fueled by natural gas. Only two studies consider AH and WH, specifically a wastewater HP and WH from a datacenter [40], [41]. Studies analyzing systems with multiple heat supply technologies compare different types of energy and heating systems, and often compare centralized systems with DH to decentralized systems without DH. The majority of studies look at the uncertainty related to economic parameters like energy prices, O&M costs, and investment costs, but technical parameters such as technology efficiency and HP COPs are also studied. Most studies do not analyze future developments but rather variations in parameters for current systems. Only a couple studies model into the future, utilizing different projections to estimate future energy prices and adjusting plant lifetime or using probability of bankruptcy to model future WH availability. Results largely indicate that flexible systems perform better once uncertainties are considered since they are better able to respond to variations in key input parameters [3], [18], [27], [43]. The reduction of risk with increased flexibility may be associated with reduced overall costs [18] but may also result in higher overall cost for example due to higher investment costs for the flexible components [43]. Exactly how a system performs depends on the input parameters therefore it is important to consider potential variations in these and why risk modelling is highly valuable. All papers advocate for the use of risk modelling as it allows for the consideration of uncertainties in assessing heat supply technologies and DH systems and quantification of the risk associated with them. It thus provides a more accurate and holistic depiction of the performance of different heat supply technologies and systems and can lead to more informed and robust decision making for investors.

2.3 FUTURE SCENARIOS

This section reviews the modelling of future DH systems in the papers reviewed. The consideration of future decarbonization of DH systems is mostly present in the modeling of counterfactual scenarios with a greater or full share of sustainable heat supply technologies relative to current systems. Only a limited number of papers explicitly modelled future DH systems [5], [8], [12], [17], [18], [20], [24], [31]. To do so, most papers use existing energy models such as Balmorel [8], EnergyPLAN [17], [31], IRPopt [24], energyPRO [5], and TRNSYS[20], while others develop their own models [12], [18]. The development of future prices is estimated using different projections such as fuel price scenarios from the International Energy Agency's World Energy Outlook [8], projections from models fitted with historical energy price data [18], calculations based on expected energy generation mixes [20], or estimates from MICOES, an electricity market model developed at Leipzig University [24].

Only a few papers consider changes in future WH availability [6], [16], [18], [23], [28], [49]. In doing so, the approaches taken are mostly relatively simple. Morandin et al. studied the use of WH from the petrochemical sector and estimated there would potentially be greater internal heat recovery in the future, so modelled a scenario where only 50% of the WH was available for DH in addition to one where 100% was available [6]. Bühler et al. reflected uncertainty in WH availability by varying the lifetime of the system, considering industrial WH [23]. Marx et al. used the probability that a company goes bankrupt as a worst-case scenario and applied it to each company for each year modelled to reflect the uncertainty in future WH availability. This, along with energy prices, were modelled as variable inputs in a MCS to reflect uncertainty in future developments [18]. Thus, Morandin et al. model the uncertainty in the quantity of WH available in the future while Bühler et al. and Marx et al. consider uncertainty in the duration of the availability and the potential scenario where WH unexpectedly ceases to be available [6], [18], [23]. Nielsen et al. estimated WH available from WWTPs, data centers, metro tunnels, and service sector cooling in 2050 by applying multiplication factors that reflect how the availability is expected to change relative to the present. WH form data centers and cooling of the service sector was expected to increase while that from WWTP and metro tunnels was expected to stay constant [16]. Pelda et al. estimated industrial WH available in 2050 based on primary energy use and considered future efficiency improvements [49]. Nielsen et al. and Pelda et al. estimate the quantity of WH available in the future but neither modelled the uncertainty related to this availability or the techno-economic potential and economic risk of these heat supply technologies [16], [49]. This contrasts with Morandin et al., Bühler et al., and Marx et al. who explicitly model the uncertainty in WH availability within their techno-economic analyses.

To the best of my knowledge, only one study has thoroughly considered and calculated the impact of future industry decarbonization on WH availability [50]. Manz et al. quantified the amount of WH available in the EU under an industry decarbonization scenario with 95% GHG emission reductions from the study 'Industrial Innovation: Pathways to deep decarbonization of industry.' Uncertainty was considered by modelling two different scenarios (one where energy intensive materials are produced domestically and one where they are imported) and variations in DH temperatures. However, other than these two scenarios, varying possibilities for how industry might decarbonize and the associated amount of WH available were not considered. Furthermore, the study only estimated WH availability and its spatial synergy with current DH areas but did not analyze its economic viability or associated economic risk.

2.4 LITERATURE GAP

As highlighted in section 2.1, various papers have carried out a techno-economic analyses on DH systems with AH coupled with large-scale HPs and, to a lesser extent, on DH systems with WH. There is a limited number of studies focusing on DH systems with both AH with HPs and WH. For most of these, AH and WH are just two of the multiple heat supply technologies included in the DH system being analyzed and not the main focus of the analysis. Only Yuan et al. focused on the use of AH with HPs and industrial WH as heat supply sources but based the study on the assumption that there is a tradeoff between the two [17]. Furthermore, Yuan et al. only consider seawater and geothermal based HPs, and specific industrial WH sources available in Aalborg, Denmark. No study has a focus on evaluating AH and WH on a general level, considering the different types of AH and WH sources available and their potential contribution to the robust decarbonization of DH systems. Additionally, if accounting for uncertainties at all, most papers conducting techno-economic analysis on DH systems with AH, WH, or both use either sensitivity analysis or scenario analysis. These methods do not allow for modelling of the expected probability surrounding these uncertainties, such as the probability of different future developments in prices and WH availability. Furthermore, sensitivity analysis only measures the isolated effect of variations in a single variable rather than the combined effect of variations in multiple variables simultaneously, which more accurately represents reality. Nonetheless, the potential of modelling this uncertainty and quantifying the economic risk associated with DH systems and specific heat supply technologies is there, as evidenced by the papers reviewed in section 2.2 which have this as a focus. There is a consensus that the use of risk modelling allows for the consideration and quantification of uncertainties associated with heat supply technologies and DH systems and the risk associated with them. This allows for a more accurate depiction of the techno-economic performance which also shows the economic risk arising from uncertainty in key factors. This can lead to more informed investment decisions for the robust decarbonization of heating systems. However, of these papers, those modelling individual heat supply technologies largely focus on CHPs fueled by fossil fuels, and those modeling systems configurations with multiple heat supply technologies largely compare systems with and without DH. There is no paper focusing on DH systems with AH and WH heat supply technologies and the economic risk associated with investments in them. Finally, only a limited number of studies explicitly consider future DH systems (see section 2.3) despite the need for this in designing future DH systems that can provide robust decarbonizations solutions for the heating sector.

This thesis aims to model and understand the technical and economic performance of employing AH and WH supply technologies for the resilient decarbonization of DH networks considering uncertainty of future energy prices and WH availability. Its focus lies on AH and WH supply technologies and the various sources that they encompass and compares a wide variety of different DH system configurations and sizes which incorporate or excluded AH and/or WH sources. Furthermore, it places a focus on modelling the uncertainty in the development of future energy prices and WH availability and quantifying the economic risk that arises from this uncertainty. Variations in energy prices and WH availability are studied as they were identified as two key sources of uncertainty for future DH systems with AH and WH sources. The uncertainties are modelled in such a way that variations in both energy prices and WH are considered at the same time, and that the expected probability of future developments is considered. Moreover, it specifically models a future DH system. Thus, the research gap this paper aims to address is twofold: it not only specifically focuses on AH and WH as heat sources for DH systems and how they compare to each other, but also on modelling the uncertainty in future development of energy prices and WH availability and the economic risk associated with it. Furthermore, the general model developed is also applied to a concrete case study for a small city in northwestern Poland with both AH and WH sources. To the best of my knowledge, no study has been conducted which analyzes the techno and economic performance and economic risk associated with AH and WH sources in a Polish DH system.

In doing so, this thesis will build on Marx et al.'s methods. Marx et al. applied MCS to a seasonal energy balance model of an interregional DH network and individual heating systems to quantify the economic risk arising from uncertainty in electricity and biomass prices and WH availability, Thus, they focus on modelling uncertainty and quantifying economic risk in a techno-economic analysis for heating systems. Though their focus is different to that of this thesis, they include industrial WH as one of the heat supply sources for the interregional DH network and specifically model uncertainty in both future energy prices and WH availability [18]. Thus, their methods can serve as a guideline in modelling uncertainty in energy prices and WH availability when applied to the case of DH systems with AH and WH sources.

3 METHODOLOGY

3.1 OVERVIEW

To analyze the techno-economic performance and risk associated with the use of AH and WH sources in future DH networks, a fully renewable DH system was modeled for the year 2050. Techno-economic performance was measured by using LCOH as a key performance indicator. Uncertainties in future developments were considered by analyzing variations in both system design parameters and external factors. Variations in system design parameters were modelled by varying the type of heat supply technologies included in the model and their size/capacity. Variations in stochastic external factors were modelled through deterministic sampling of energy price scenarios, and an analysis of possible WH fall out scenarios (i.e., due to bankruptcy or relocation). An overview of the methods used is shown Figure 3.1.

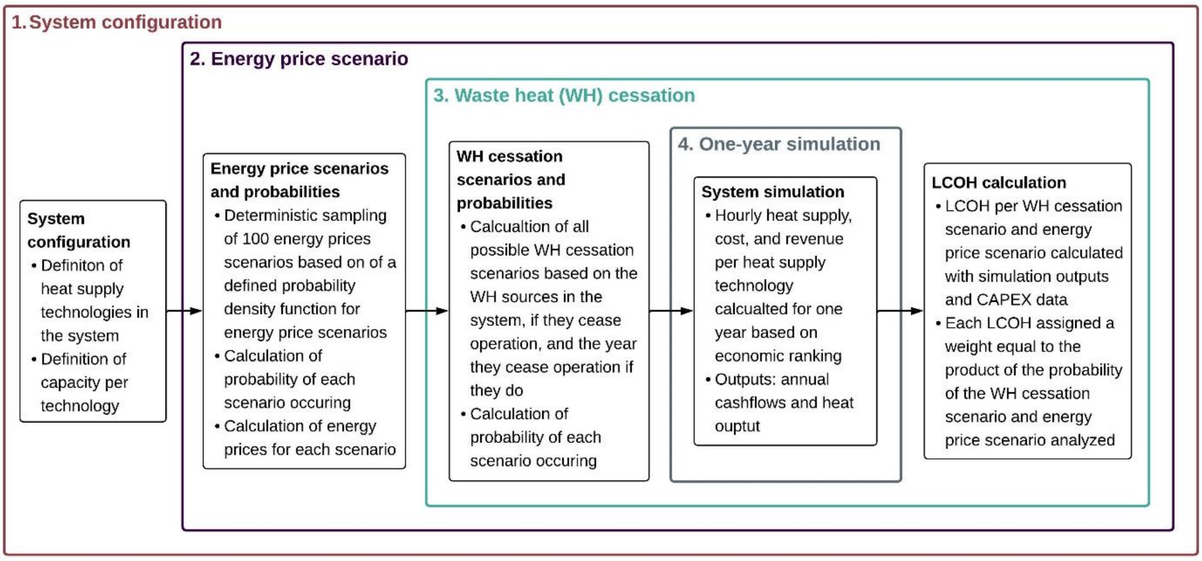

Figure 3.1 Methodology overview

The methodology applied consisted of four levels of analysis: (1) system configuration, (2) energy price scenario, (3) WH cessation scenario, and (4) one-year simulation. Specifically, the steps taken for each level were:

1. Defining the system configurations to be compared.
2. Defining a weighted sample of energy price scenarios based on deterministic sampling of a defined probability density function (PDF) of energy price scenarios. For each system configuration, simulating all energy price scenarios in the weighted sample.
3. For each energy price scenario, calculating all possible WH cessation scenarios and their probability of occurring. A WH cessation scenario is defined by the number of WH sources in the system, whether they cease operation during the study period analyzed, and the year they cease operation if they do. The weight of the WH cessation scenario is equal to its probability of occurring.

4. For each WH cessation scenario and year in the study period, running a one-year simulation to determine annual heat production and variable operational costs per heat supply technology. Then combining these outputs with fixed operational costs and investment costs to calculate the LCOH for each WH cessation scenario and price scenario. Each LCOH is assigned a weight equal to the product of the weight of the WH cessation scenario and the weight of the price scenario being considered.

Thus, for each system configuration the result a weighted sample of LCOH values that reflects the effect of uncertainty in future energy prices and WH availability. This allows for an assessment of the overall economic performance of each system as well as the economic risk associated with it (quantified through the spread of the distribution).

The methods were developed using a general model and applied to a concrete case study for a small city in northwestern Poland. The following section delineates the methodology employed in the thesis. First, the levels of analysis outlined above are explained in greater detail, then, their application in the general model is described, and finally, the case study is explained.

3.2 Methodological steps

3.2.1 System configuration

In the system configuration level, the system designs to be analyzed and compared to each other are defined. This refers to the type of heat supply technologies included in the DH system and what their capacities are. The capacities of the heat supply technologies are selected in such a way that peak demand of the DH network can be fully met.[3]

WH price

The price for WH is influenced by local conditions and parties involved, and can be agreed on bilaterally between the DH operator and the WH provider [18]. Thus, for the purposes of this thesis, it was categorized as a system design parameter and assumed to be constant over the study period. However, as its exact value in the future is uncertain and it influences total costs and the attractiveness of utilizing WH, a sensitivity analysis was conducted varying the WH price.

3.2.2 Energy price scenario

Deterministic sampling was used to analyze and quantify the economic risk arising from uncertainty in the future development of energy prices. Energy price scenarios were represented by a price lambda (λ), a variable ranging from 0 to 1 with 0 representing a minimum price scenario and 1 a maximum price scenario. First, a PDF was defined to reflect the uncertainty in the value of the price lambda. Subsequently, deterministic sampling was used to obtain a weighted sample of 100 energy price scenarios based on the PDF defined. Energy prices were calculated based on the energy price scenario and assigned a weight equal to the probability of that scenario occurring (based on the PDF defined).

[3] Redundancy in terms of N-1 security is not considered.

Then, in combination with the system configuration being analyzed, the energy prices were used as inputs for the one-year simulation and the LCOH of the system was calculated for all WH cessation scenarios for every price scenario in the weighted sample. This resulted in a weighted sample of LCOH values that accounts for uncertainty in future energy prices and WH availability. An overview of the deterministic sampling methodology and its connection to the rest of the methodology employed in the thesis is presented in Figure 3.2.

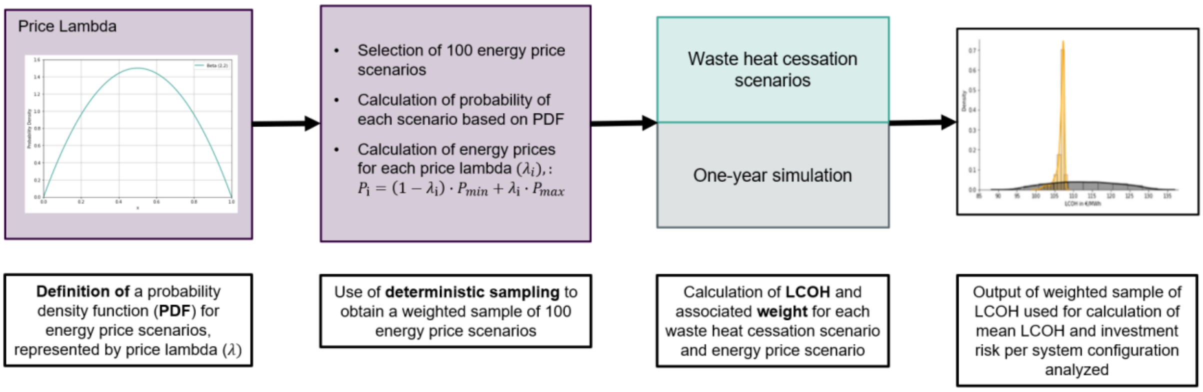

Figure 3.2 Outline of energy price scenario methodology (figure inspired by [18].)

For this thesis, the energy sources, and therefore prices, identified as the most relevant were biomethane, biomass, and electricity. This is because biomethane and biomass can replace fossil fuels such as natural gas and coal which are used to power heat supply technologies like CHPs and boilers in current DH systems. Similarly, electricity is relevant for electricity production from CHPs, as well as electric heat supply technologies such as electric boilers and HPs. Electricity is therefore especially relevant for AH and low to medium temperature WH sources which need to be combined with HPs to supply heat at a high enough temperature for a DH network.

To define the PDF for energy price scenarios, the same approach was taken as Marx et al. [18], who assumed a correlation between energy prices and used a Beta (2,2) distribution[4] to define the PDF for all energy prices considered. However, while Marx et al. included the energy price scenario as one of the stochastic input parameters for their MCS, this thesis took a deterministic sampling approach to obtain a weighted sample of energy price scenarios.

The energy prices considered by Marx et al. were those of biomass, natural gas, and electricity. They assumed a correlation between biomass and natural gas prices since biomass is a key substitute for natural gas in heating and this correlation has been evidenced in recent years (a 0.9 correlation index was found for the period of January 2015 to June 2023). They also assumed a correlation between natural gas and electricity prices. Currently electricity prices and natural gas prices are strongly linked as natural gas generators are frequently the price setting power plants in the electricity merit order. This could decrease in the future with greater renewable energy integration and higher CO_2 prices [18],.

[4] A Beta (α, β) distribution is a distribution between 0 and 1 with a probability density function defined as: $f(x|\alpha,\beta) = constant \cdot x^{\alpha-1}(1-x)^{\beta-1}$. It is frequently utilized for stochastic variables between 0 and 1 [18].

However, Marx et al. argued that since natural gas has a high share in electricity and heat generation, biomethane uptake as a substitute is currently low, and market-readiness of balancing technologies for renewable energy intermittency is limited, the correlation is expected to continue for the foreseeable future. This thesis models a greenfield scenario for 2050, and thus excludes natural gas as a fuel source. In its place, biomethane is incorporated as it is a carbon-neutral direct alternative for natural gas [51]. It is assumed that biomethane would mirror the price trajectory of natural gas as it is a direct substitute, albeit with an overall higher cost due to its carbon neutrality. Thus, following the logic of Marx et al, this thesis assumes a correlation between biomass, biomethane, and electricity prices in the future.

The energy price scenarios considered were represented by the price lambda (λ), a variable ranging between 0 and 1. A price lambda of 0 corresponds to the minimum energy price scenario while a price lambda of 1 corresponds to the maximum price scenario. The PDF of the price lambda was defined by a Beta (2,2) distribution, as shown in Figure 3.3. The beta distribution represents the assumptions that an average price scenario is expected to be most probable and that the minimum and maximum price scenarios are equally probable. Moreover, it accounts for the assumption that values below the minimum scenario or above the maximum scenario are irrelevant. In contrast, a normal distribution tends to infinity and would lead to excessively high or low prices [18].

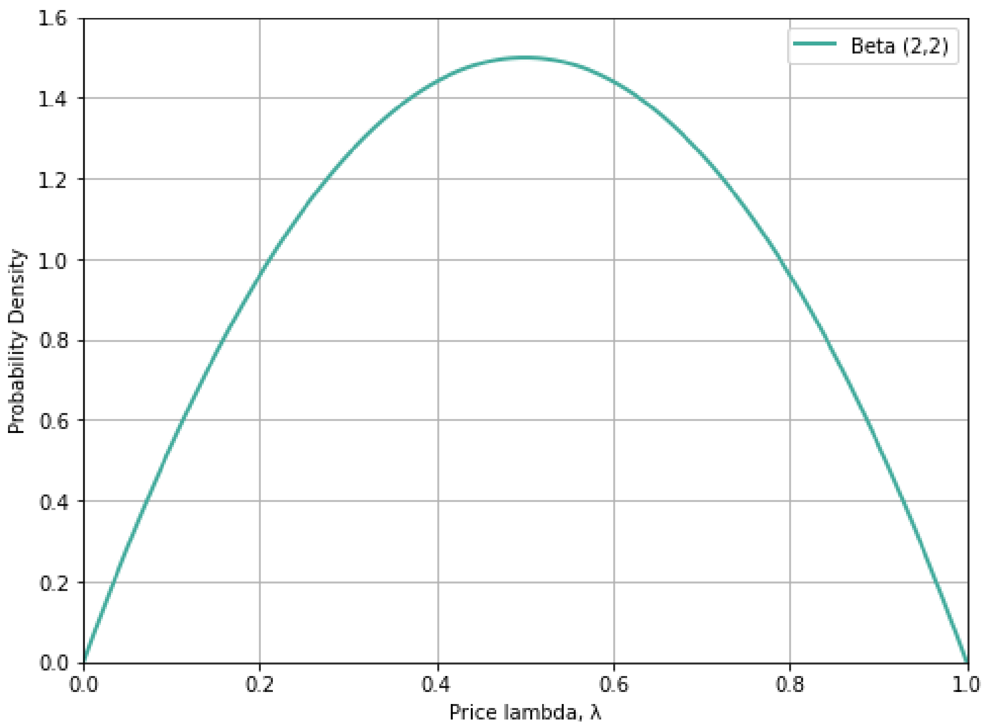

Figure 3.3 Beta (2,2) probability density function for price lambda

The price lambda was combined with minimum and maximum energy prices to calculate the energy prices in that scenario as follows:

$$P_\lambda = (1-\lambda) \cdot P_{min} + \lambda \cdot P_{max}$$

Where:

P_λ	=	energy price in scenario with price Lambda λ [€/MWh]
λ	=	price Lambda (drawn from Beta (2,2) distribution)
P_{min}	=	minimum energy price [€/MWh]
P_{max}	=	maximum energy price [€/MWh]

The minimum and maximum prices can either be static for the duration of the analysis period or a timeseries of a higher temporal resolution. For a given energy price scenario the same lambda was applied to all energy prices. This ensured that the correlation between energy prices is accounted for.

For the analysis, deterministic sampling was used to obtain a weighted sample of 100 energy price scenarios. Specifically, 100 price lambda values equally spaced between 0 and 1 were taken and assigned a weight equal to the probability of that price lambda occurring as defined by the Beta (2,2) distribution.

3.2.3 WH cessation scenarios

When WH is supplied from commercial or industrial processes, there is uncertainty regarding the future availability of the WH. There is a risk that the WH ceases to be available for the DH system, i.e., if the company goes bankrupt, relocates elsewhere, or decarbonizes its processes in such a way that WH is recovered internally.

To quantify the risk of WH sources ceasing to be available, the same proxy was taken as Marx et al. [18]. They calculated a 0.76% probability of a company going bankrupt in Austria each year by dividing the number of annual bankruptcies by the total number of companies in the country. This probability was then applied to every WH provider in their model for each year modeled. The year the WH ceases to be available (if it does) was included as one of the stochastic parameters in their MCS. However, in contrast to Marx et al.'s method, for each energy price scenario modelled, this thesis considered all possible scenarios of when WH providers cease to be available rather than a single WH cessation scenario per energy price scenario.

For each WH source, the cessation scenario is defined by whether the WH ceases to be available and, if yes, in what year. Thus, if a period of length T years is analyzed, there is T+1 cessation scenarios per WH source analyzed. One for each year the WH can cease to be available, and one for the scenario in which it does not drop out at all. With an increase in the number of WH sources, there is an exponential increase in the total number of possible WH cessation scenarios, as each scenario for a single WH source can be combined with each possible scenario of every other WH source in the system. If there is no WH sources included in the initial system configuration, there is only a single scenario possible. Specifically, the total number of WH cessation scenarios can be calculated as follows:

$$N = (\mathrm{T}+1)^{\mathrm{w}}$$

Where:

N	=	total number of WH cessation scenarios
w	=	number of WH sources in initial system configuration
T	=	length of study period analyzed [years]

As mentioned above, the probability of WH sources ceasing to be available out is modelled through an annual WH cessation probability of 0.76%. It is assumed that the annual cessation probability is constant throughout the entire study period considered. Thus, for each WH source, the probability of the WH cessation scenario occurring can be calculated as follows:

$$p(x) = \begin{cases} (1-\sigma)^{x-1} \cdot \sigma, & 1 \le x \le T \\ (1-\sigma)^{T}, & x = 0 \end{cases}$$

Where:

$p(x)$	=	probability of WH cessation scenario x
x	=	WH cessation scenario represented by a value ranging from 0 to T: 0 if WH does not cease operation within the study period, otherwise the year the WH ceases operation (value between 1 and T)
σ	=	annual WH cessation probability [0.0076]
T	=	study period analyzed [years]

The probability of a scenario happening with multiple WH sources in the system is the product of the probabilities of cessation scenario of each WH source:

$$p(x_1, \dots, x_n) = \prod_{i=1}^{n} p(x_i)$$

Where:

x_i	=	cessation scenario of WH source i
n	=	number of WH sources
$p(x_1, \dots, x_n)$	=	probability of WH cessation scenario (with scenario x_i per WH source i)
$p(x_i)$	=	probability of x_i

For each of the 100 price scenarios modelled, all possible WH cessation scenarios and their associated probabilities are calculated. Then for each WH cessation scenario, the LCOH for that scenario is calculated. The WH scenario is assigned a weight equal to the probability of the WH scenario happening. Thus, the LCOH of a given WH cessation scenario and a given price scenario has a weight equivalent to the product of the weight of the WH cessation scenario and the weight of the energy price scenario.

$$w(\lambda, X) = w(\lambda) \cdot w(X)$$

Where:

$w(\lambda, X)$	=	weight of energy price scenario λ and WH cessation scenario X
$w(\lambda)$	=	weight of energy price scenario λ
$w(X)$	=	weight of WH cessation scenario X

This results in a weighted sample of LCOHs for every system configuration considered.

3.2.4 One-year simulation

To calculate the LCOH of each WH cessation scenario, it is necessary to understand annual heat production and cashflows per heat supply technology in the DH system over the study period analyzed. To achieve this, a fully renewable DH system was modeled for the year 2050. A detailed explanation of the DH system and input data specific to the general model and case study is given in sections 3.3 and 3.4 respectively, but a description of the simulation model is provided below.

Model inputs are the type of heat supply technologies included in the system and their capacities, annual residential heat demand, energy prices of electricity and other fuels, and temperatures of AH and WH sources in the system and the DH network. The model steps through hourly timesteps over the course of a year and determines the amount of heat supplied by each heat supply source based on a defined operation strategy. This is an economic ranking where the full capacity of the lowest cost source is used until demand is fully met. The model output is the hourly production from each heat source, based on which total annual cashflows are calculated. This consists of variable O&M costs, electricity and fuel costs, and electricity revenues for the CHP (if present in the system). Revenue from the heat supplied by the DH system is not considered. Total annual heat production can also be calculated, which is equal to total demand as the system configuration is defined in such a way that demand is always fully met.

The one-year DH system simulation was modelled using a tool developed at AIT called Techno-Economic System and Component Analysis (TESCA). TESCA is a simulation tool developed in python which uses object-oriented programing to define component classes which represent different technologies such as solar panels and batteries. Each component has specific attributes and methods associated with it. These components are the building blocks for the system simulations carried out.

For a system simulation, specific instances of the components are defined through key attributes such as capacity and efficiency. Furthermore, an operation strategy for the components is determined. The model then runs through a step wise simulation of a designated timestep length over the duration study period where the behavior of the components is determined by the operation strategy defined. Data on the operation of each component is tracked and stored during the simulation. Additionally, TESCA has built in economic analysis functionalities, which can be used in combination with the simulation outputs to evaluate the economic performance of the system.

Thus, TESCA allows for the analysis of "electrical, thermal and gas systems, as well as system combinations, from a technical and economic perspective"[52]. Due to its quick calculation times, it is also compatible with sensitivity and risk assessments through MCS or deterministic sampling. So far, TESCA has primarily been used for simulating electrical systems and only used for modeling individual heating systems. Thus, the thermal components already modelled were individual HPs, a heat exchanger, and a layered heat water storage. However, for this thesis, TESCA was expanded and further developed to model DH systems. Specifically, the components modelled for the DH system are a CHP, HOB; large-scare HP, and high temperature WH. Since a HP was already included in TESCA for modeling individual household systems, it was only adjusted as needed for modelling of large-scale HPs and compatibility with the operating strategy defined. The other three technologies were newly added in the TESCA framework. The TESCA economic analysis functions were used to calculate variable operational expenditures (OPEX) during the one-year simulation and, combined with fixed OPEX and capital expenditure (CAPEX) values, to calculate the LCOH over a multiple year study period (See section 3.2.5). An overview of the one-year simulation is presented in Figure 4.3.

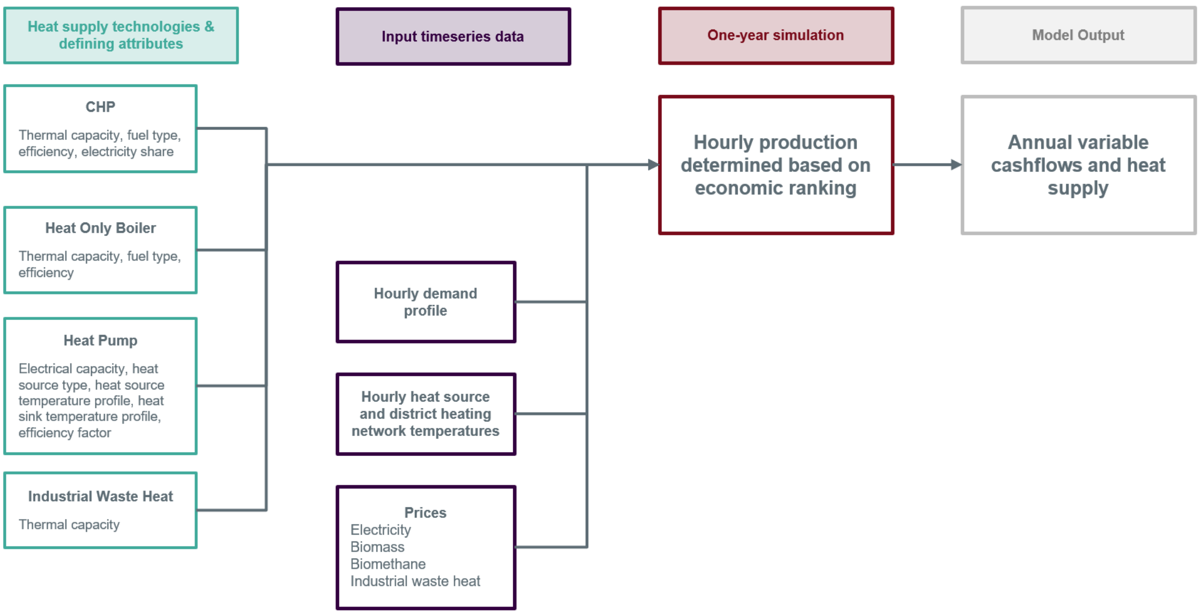

Figure 3.4 Overview of one year TESCA simulation including components and their defining attributes, input timeseries data, and model outputs

Below is a description of each of the components and their defining attributes and methods, as well as of the operation strategy used in the thesis.

CHP

The CHP produces electricity and heat as outputs and can have different fuels as an input (i.e., biomass or biomethane). It is defined by its thermal capacity, efficiency, electricity share, and fuel type. The efficiency is directly connected to the type of fuel input, and is the ratio of the useful energy output to the total energy input:

$$\eta = \frac{E_{out,th} + E_{out,el}}{E_{in}}$$

Where:

η	=	efficiency
$E_{out,th}$	=	thermal energy output [MW]
$E_{out,el}$	=	electrical energy output [MW]
E_{in}	=	energy input from fuel [MW]

Electricity share is the portion of total energetic output that is the form of electricity:

$$\varepsilon = \frac{E_{out,el}}{E_{out,th} + E_{out,el}}$$

Where:

ε	=	electricity share
$E_{out,el}$	=	electrical energy output [MW]
$E_{out,el}$	=	electrical energy output [MW]

Based on these relationships, the methods included for the CHP are: (1) calculation of electric output and thermal output based on a given fuel input, (2) calculation of electric output and fuel input based on a given thermal output, and (3) calculation of thermal output and fuel input based on a given electrical input. Additionally, with fuel and electricity prices as additional input data, the CHP component also has a method included for (4) calculation of the net cost per unit thermal output (sum of cost of fuel needed and profit from electricity output).

The input needed to step the CHP in each timestep is either the fuel input, electrical output, or thermal output in that timestep. These can be equal to zero if the CHP does not operate in the timestep.

HOB

The HOB produces heat as its only output and, like the CHP, can have different fuel sources as an input. It is defined by its thermal capacity, efficiency, and fuel type. As for the CHP, the efficiency depends on the type of fuel and is the ratio of the useful energy output to the total energy input:

$$\eta = \frac{E_{out,th}}{E_{in}}$$

Where:

η	=	efficiency
$E_{out,th}$	=	thermal energy output [MW]
E_{in}	=	energy input from fuel [MW]

Based on this relationship, the methods included are (1) calculation of fuel input based on thermal output and (2) calculation of thermal output based on fuel input. Like the CHP, with additional input data on fuel cost, the HOB has a method included for (3) calculation of the cost per unit thermal output.

Inputs needed to step the HOB in each timestep is either the fuel input or thermal output in that timestep. These can be equal to zero if the HOB does not operate in that timestep.

HP

The HP produces heat as a useful output and has electricity as its input. It extracts heat from a heat source and supplies it to the heat sink. The heat source is at a lower temperature than the heat sink. It is defined by its nominal electric power and efficiency factor. The maximum amount of heat available is dependent on the temperature of the heat source and sink. It is calculated as follow.

First the Carnot COP is calculated. The COP is a ratio of the heat output to the electricity input, with the Carnot COP being the maximum theoretical COP obtainable for a given source and sink temperature.

$$COP_{carnot} = \frac{T_{sink}}{T_{sink} - T_{source}}$$

Where:

COP_{carnot}	=	Carnot COP
T_{sink}	=	heat sink temperature [K]
T_{source}	=	heat source temperature [K]

The real COP is obtained by multiplying the Carnot COP by the HP's efficiency factor:

$$COP = COP_{carnot} \cdot \eta$$

Where:

COP	=	COP
COP_{carnot}	=	Carnot COP
η	=	efficiency factor

Finally, the maximum thermal output can be determined by multiplying the electric capacity by the COP.

$$P_{th,max} = COP \cdot P_{el,max}$$

Where:

COP	=	COP
$P_{th,max}$	=	maximum thermal power output [MW]
$P_{th,max}$	=	electrical capacity [MW]

Similarly, the thermal energy output for a given electricity input can also be obtained by multiplying the electrical energy input by the COP:

$$E_{th} = COP \cdot E_{el}$$

Where:

COP	=	COP
E_{th}	=	thermal output [MWh]
E_{el}	=	electrical input [MWh]

Based on these relationships and data on the source and sink temperatures, the methods included for the HP are: (1) calculation of the Carnot COP, (2) calculation of the COP, (3) calculation of maximum thermal output, (4) calculation of electrical input for a given thermal output, (5) calculation of thermal output for a given electrical input. With additional input data on electricity cost, the HP has a method included for (6) calculation of the cost per unit thermal output.

Inputs needed to step the HP in each timestep are the temperature of the heat source, temperature of the heat sink (the DH network) and a thermal or electric set point. This set point may also be equal to zero if the HP does not operate in that timestep.

Industrial WH

The WH component is intended for modelling high temperature WH that does not require a HP for supplying heat to a DH network. It is defined by its maximum thermal output. This may be a constant value for the entire simulation period or can change over the period analyzed.

With the WH price as an additional input, the method included for the industrial WH is (1) the calculation of the cost per unit thermal output.

The input needed to step the industrial WH is the thermal output in the timestep considered. This may also be equal to zero if the industrial WH is not used in that timestep.

Operation strategy: Economic ranking

The operation strategy defined was an economic ranking. Each timestep, the price per unit thermal output is calculated for each of the components in the system utilizing the component methods and the electricity and fuel prices in that time step. Then the full capacity of the lowest cost source is used until the demand for the timestep being considered is fully met. When using the full capacity of the heat source would lead to supply exceeding demand, only the marginal capacity needed to meet demand is used from that heat source.

3.2.5 LCOH calculation

The annual costs and heat output from the one-year simulation are assumed to be representative for each year of the study period analyzed and combined with investment costs to calculate the LCOH of the system. In the case of a WH source ceasing operation, it is assumed that the WH ceases operation at the start of the year. In this event, the one-year simulation is run again without the WH source. The outputs are assumed to be representative for the remainder of the study period or until another WH source ceases operation and the one-year model is run again.

The LCOH measures the average cost of producing heat over the study period analyzed. It accounts for all costs (CAPEX, OPEX, and the residual value at the end of the study period) and spreads these evenly over the heat produced in the study period analyzed. If the expected lifetime of a heat supply technology is shorter than the study period analyzed, it is assumed that a replacement of the same size is built as soon as the lifetime ends, resulting in new CAPEX costs. The residual value refers to estimated monetary value of each technology at the end of the study period and is accounted for when the expected lifetime of the technology exceeds the study period analyzed. It is estimated as the discounted portion of the initial investment corresponding to the proportion of the remaining useful lifetime at the end of the study period relative to expected lifetime. When a WH source ceases operation, no residual value is accounted for as it is assumed that it is a stranded investment.

Specifically, the residual value is calculated as follows:

$$RV_{T,i} = \frac{\frac{L_i - T}{L_i} \cdot CAPEX_{0,i}}{(1+r)^T}$$

Where:

$RV_{T,i}$	=	residual value of technology i the end of the study period T
L_i	=	expected lifetime of technology i [years]
T	=	study period [years]
$CAPEX_{0,i}$	=	initial investment cost for technology i [€]
r	=	interest rate

The LCOH is calculated as follows:

$$LCOH = \frac{CAPEX_0 + \sum_{t=1}^{T} \frac{OPEX_t + CAPEX_t}{(1+r)^t} - \frac{RV_T}{(1+r)^T}}{\sum_{t=1}^{T} \frac{E_t}{(1+r)^t}}$$

Where:

$LCOH$	=	levelized cost of heat [€/MWh]
$CAPEX_0$	=	initial investment cost [€]
$OPEX_t$	=	operational costs in year t (fixed and variable) [€]
$CAPEX_t$	=	investment costs in year t (occurs if a new heat supply technology is built) [€]
RV_T	$=$	residual value at the end of the study period
E_t	=	heat supplied in year t [MWh]
t	=	year
r	=	interest rate
T	=	study period [years]

Example for single WH drop out scenario:

Figure 3.5 shows an example of how a WH cessation scenario is combined with the one-year simulation to calculate the LCOH for that scenario. The example system consists of a biomass HOB and two WH sources: a datacenter combined with a HP and an industrial WH source. The WH cessation scenario is that WH from the datacenter drops out at the start of year 5 and the WH from the industrial WH source drops out at the start of year 16. The study period is 20 years long lasting from 2050 to 2069.

For years 1 to 4, the one-year simulation is run with the biomass HOB, datacenter HP, and industrial WH, for years 5 to 15, the one-year simulation is run with the biomass HOB and industrial WH, and for years 16 to 20, the one-year simulation is run with only the biomass HOB. The results give the annual heat output and cashflows per technology for each year in the study period. This is combined with investment costs and residual values to calculate the LCOH. This LCOH is then assigned a weight equal to the product of the weight of the energy price scenario and WH cessation scenario being considered.

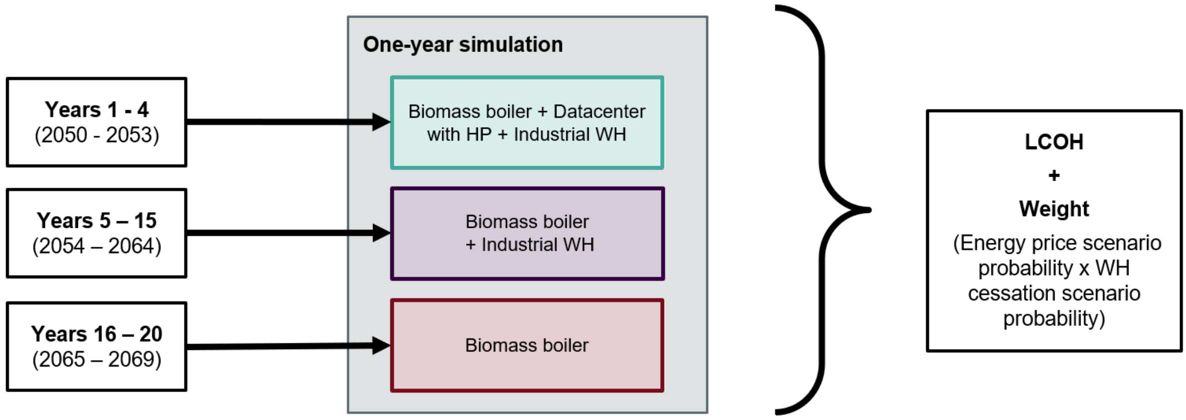

Figure 3.5 Example coupling of a waste heat cessation scenario and the one-year simulation

3.2.6 Result analysis

Once all steps have been processed, a weighted sample of LCOHs is obtained for every system configuration analyzed. To evaluate what these results mean for the techno-economic performance and risk associated with a given system configuration, the mean and standard deviation are calculated. The mean gives an indication of average techno-economic performance. The standard deviation gives an indication of the spread of the distribution and therefore the economic risk associated with that system configuration.

The sample mean is calculated as follows:

$$\mu = \frac{\sum w_i \cdot x_i}{\overline{w} \cdot N}$$

Where:

μ	=	mean of the sample
w_i	=	weight of sample i
x_i	=	LCOH value of sample i
$\overline{w}$	=	average weight
N	=	number of samples

The sample standard deviation is calculated as follows:

$$\sigma = \sqrt{\frac{\sum w_i \cdot (x_i - \mu)^2}{\overline{w} \cdot N}}$$

Where:

σ	$=$	standard deviation of the sample
w_i	$=$	weight of sample i
x_i	$=$	LCOH value of sample i
μ	$=$	mean of the sample
$\overline{w}$	$=$	average weight
N	$=$	number of samples

3.3 General model development

3.3.1 System overview

For the general DH system modeled, four representative AH and WH sources were defined: a low temperature AH source, a medium temperature AH source, a low temperature WH source, and a high temperature WH source.

The **low temperature AH source** has low source side temperatures and must therefore be combined with a HP to obtain heat at the temperature level of the DH network. This is represented by an air source HP, meaning the source side temperatures vary significantly both seasonally and within a single day.

The **medium temperature AH source** refers to an AH source with slightly higher and less volatile temperatures than the low temperature AH source. Examples of such heat sources include ground water or wastewater treatment plant (WWTP) effluent. The source also needs to be combined with a HP to obtain the temperature of the DH network. In the general model it is represented by a WWTP effluent sourced HP.

The **low temperature WH source** refers to WH coming from commercial or industrial processes that is at a higher temperature than the two AH sources, but still requires combination with a HP to supply heat at the temperature of the DH network. In the general model it is represented by WH from the cooling of a datacenter.

The **high temperature WH source** refers to WH coming form an industrial process that is at a high enough temperature to directly supply heat to the DH network without being coupled with a HP. In the general model, it is represented by a generic industrial WH source defined by its thermal capacity.

For both AH sources, there is no risk that the source will cease to be available in the future since sources such as air, ground water or river water will continue to be available in the future. It is also assumed that the availability of AH form WWTP effluent will not change drastically as the cleaning of wastewater will continue to be necessary, and significant changes in the production of wastewater are not expected. However, for the two WH sources there is a fall out possibility if for example the company goes bankrupt, relocates elsewhere, or decarbonizes its processes in such a way that the heat is recovered internally. The properties of the four AH and WH sources are summarized in Table 3.1.

In addition to these sources, the renewable heat supply technologies included were a biomethane CHP, a biomass HOB, and an electric HOB. This is because current European DH systems are largely supplied by CHPs and HOBs [53]. However, the supply continues to be dominated by fossil fuels [11], [53]. In 2017, 25% of the EU-27 DH mix consisted of natural gas, 16 % of hard coal, 5% of lignite (brown coal) and 2% from oil. Biomass also constituted a significant portion of the mix, making up 17% [11]. Thus, the inclusion of a biomethane CHP and biomass and electric HOBs represents current technologies with fully decarbonized fuel sources. Biomethane is a carbon-neutral direct alternative for natural gas, biomass is currently the main renewable fuel supply in DH and expected to continue playing an important role, and an electric HOB represents increased electrification of the heat sector [11], [51]. Furthermore, they have the advantage of being able to ensure security of supply as they do not depend on any external factors in contrast to AH or WH sources. AH or WH sources are dependent on the operation of the heat source. For example, heat may be temporarily unavailable if the WWTP, datacenter or industrial WH source stops operation due to maintenance or another reason. Even air-sourced HPs are dependent on temperature and may be unavailable if air temperatures are too low for the HP to operate.

Table 3.1 Key properties of the representative ambient heat (AH) and waste heat (WH) sources modelled in general model

	Low temperature AH source	Medium temperature AH source	Low temperature WH source	High temperature WH source
Heat source	Air	WWTP effluent	Datacenter WH	Industrial WH
Temperature	10 °C avg*	20 °C avg	40 °C	>100 °C
COP	Low	Medium	High	No HP needed
Annual WH cessation probability	0	0	0.76%	0.76%
Input	Hourly air temperatures	Hourly WWTP effluent temperatures	Constant temperature value	Constant thermal capacity value
CAPEX	High	High	High	Low
OPEX: Electricity for HP	Yes	Yes	Yes	No
OPEX: AH/WH cost	No	No	No	Yes

** An hourly temperature profile is considered*

An overview of the DH system modeled is shown in Figure 3.6.

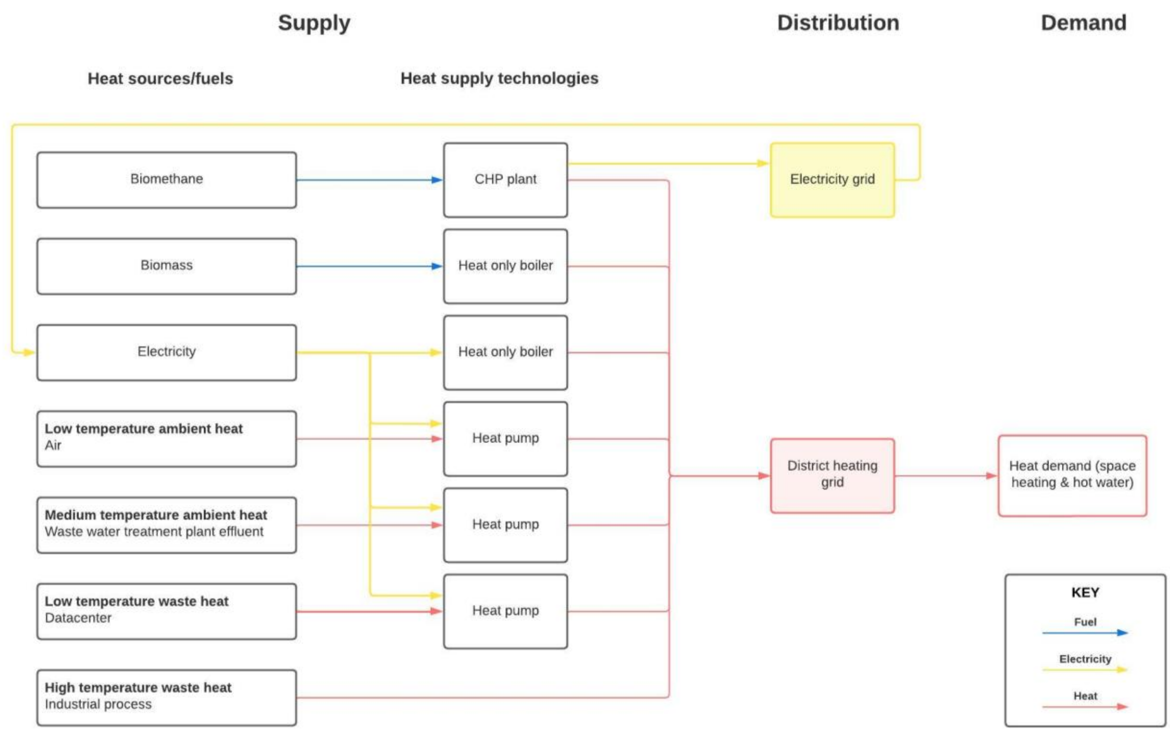

Figure 3.6 General model district heating system overview

3.3.2 Data collection and model parametrization

Technical and economic data for heat supply technologies considered in the general model was obtained from the Danish Energy Agency (DEA)'s catalogue on Technology Data for Generation of Electricity and District Heating [32]. The catalogue provides consistent and current data on a wide range of representative electricity and DH supply technologies. It provides generalized data on the current state of art of the technology as well as estimates for 2030 and 2050. It is based on publicly available, well documented sources and expert knowledge with a focus on European data. The catalogue is intended to provide a basis for energy system analysis and therefore emphasizes consistency and comparability. Thus, utilizing values from the catalogue ensures consistency in the underlying assumptions for the technical and economic data collected, leading to consistency in the general model developed in this thesis. All the technologies modelled except for heat recovery from high temperature industrial WH are included in the DEA catalogue. The specific reference technology used per heat supply technology analyzed in the general model can be found in Table 3.2. For these, the central estimates for 2050 were used. For industrial WH, economic data was obtained from a DH outlook study for 2030 [54].

Table 3.2 Reference technology in the Danish Energy Agency catalogue used per heat supply technology in the general model

Heat supply technology	Reference technology in DEA catalogue
Biomethane CHP	Gas turbine, combined cycle, back pressure, natural gas, medium
Biomass HOB	Wood chips HOB, Medium
Electric HOB	Electric HOB, Large (15 MW)
Air source HP	Compression HP air source (10 MW)
WWTP effluent HP	Compression HP excess heat (10 MW)
Datacenter HP	Compression HP excess heat (10 MW)
Industrial WH	N/A

Specifically, technical data was collected on efficiency and electricity share for the CHP, efficiency and auxiliary electricity consumption for the HOBs, efficiency factors for the HPs and technical lifetime for all technologies. Additionally, economic data was gathered on investment costs (subcategorized into equipment and installation costs) fixed O&M costs, and variable O&M costs other than for fuel or electricity. This data was used as the inputs for defining the heat supply components in the one-year simulation and for the LCOH calculation. Technical and economic lifetime were assumed to be the same. An overview of the technical and economic input values is presented in Table 3.3. All economic values are in real 2022 euros. An interest rate of 5% was assumed.

Table 3.3 Technical and economic input data for heat supply technologies included in the general model (combined heat and power plant (CHP), biomass heat only boiler (HOB), electric HOB, air source heat pump (HP), waste water treatment plant effluent HP, datacenter HP and industrial WH. All economic values are in 2022 euros.

	Heat supply technology						
	CHP	Biomass HOB	Electric HOB	Air HP	WWTP effluent HP	Data-center HP	Industrial WH
Technical parameters							
Efficiency [%]	86%	88%	99%	-	-	-	-
Electricity share [% useful energy output]	61%	-	-	-	-	-	-
Auxiliary electricity consumption [% heat generation]	-	2.2%	0.5%	-	-	-	-
Efficiency factor	-	-	-	0.5*	0.5*	0.5*	-
Lifetime [years]	25	25	25	25	25	25	20
Economic parameters							
Total investment cost [M€/MW$_{th}$, M€/MW$_{el}$ for HP]	2.02	0.53	0.07	3.66	3.84	3.84	0.44
Equipment investment cost [M€/MW$_{th}$, M€/MW$_{el}$ for HP]	1.47	0.40	0.06	2.95	3.14	3.14	-
Installation investment cost [M€/MW$_{th}$, M€/MW$_{el}$ for HP]	0.55	0.13	0.01	0.70	0.70	0.70	-
Fixed O&M costs [€/MW$_{th}$ /a, €/MW$_{el}$/a for HP]	47,653	45,169	1,088	9,223	13,007	13,007	22
Variable O&M cost [€/MWh$_{th}$]	7.3	1.4	0.5	2.0	2.0	2.0	-
Source	[32]	[32]	[32]	[32]	[32]	[32]	[54]

** Average efficiency factor value for large scale HPs (Source: B. Mayr, personal communication, February 29, 2024)*

In addition to the technical and economic input data per heat supply technology, data was collected on DH demand, relevant temperatures, and fuel and electricity prices. Data on hourly DH demand, air temperature, WWTP effluent temperature, and minimum and maximum electricity prices was obtained from an AIT internal dataset based on real Austrian DH case studies. The data for all parameters is based on the same weather year (2012) and thus ensures consistency between the hourly timeseries for heat demand, temperatures, and electricity prices. For simplicity, data on hourly DH demand was scaled to a peak demand of 100 MW. Estimates on the range of biomass and biomethane prices in 2050 were based on expert knowledge.[5] Specifically, biomass prices were estimated to range between 30 and 45 €/MWh and biomethane prices between 80 and 120 €/MWh. The temperature of WH from the datacenter was assumed to be constant throughout the year at 40°C, an average temperature for WH from datacenters [55]. As mentioned previously, the price of industrial WH can be agreed on bilaterally between DH operators and WH operators. Thus, a sensitivity analysis was conducted varying the WH price between 0 and 60 €/MWh in 20 € increments.

[5] G. Resch and S. Reuter, personal communication, March 19, 2024

The temperature in the DH network ranged between 80°C and 100°C and was calculated based on the air temperature. At air temperatures below -12°C, the DH network temperature was at the maximum temperature of 100°C. At air temperatures above 12°C, the DH network was at the minimum temperature of 80°C. For temperatures between -12 and 12 °C the DH network temperature followed a linear relationship between 100°C and 80°C. The calculation of the DH temperature based on air temperature is shown below:

$$T_{DH}(T_{air}) = \begin{cases} T_{DH,max} = 100, & T_{air} \leq -12 \\ T_{DH,min} = 80, & T_{air} \geq 12 \\ -\frac{5}{6}T_{air} + 90, & -12 < T_{air} < 12 \end{cases}$$

Where:

T_{DH}	=	district heating network temperature [°C]
T_{air}	=	air temperature [°C]
$T_{DH,max}$	=	maximum DH network temperature [°C]
$T_{DH,min}$	=	minimum DH network temperature [°C]

A summary of the input data for DH demand, energy prices and temperatures is presented in Table 3.4.

Table 3.4 Summary of the input data used for district heating demand, energy prices, and temperatures for the general model

Data	Fixed/timeseries	Source
Hourly DH demand profile	Timeseries, hourly	AIT internal dataset
Electricity prices	Timeseries, hourly	AIT internal dataset
Biomass prices	Fixed: Minimum: 30 €/MWh Maximum 45 €/MWh	G. Resch and S. Reuter, personal communication, March 19, 2024
Biomethane prices	Fixed: Minimum: 80 €/MWh Maximum 120 €/MWh	G. Resch and S. Reuter, personal communication, March 19, 2024
Industrial WH price	Fixed: 0, 20, 40, 60 €/MWh	Marx et al. 2023 [18]
Air temperature	Timeseries, hourly	AIT internal dataset
WWTP temperature	Timeseries, hourly	AIT internal dataset
Datacenter output temperature	Fixed: 40°C	Pelda et al. 2023 [55]
District heating temperature	Timeseries, hourly	Calculated based on air temperature

3.3.3 System configuration

For defining the system configuration, thermal capacity was considered for the CHP, biomass HOB, electric HOB, and industrial WH. For AH and WH sources with HPs, electric capacity was considered as maximum thermal output will vary depending on the source and DH temperature.

The system configuration was defined in such a way that the peak demand of 100 MW was met by the CHP and HOBs. This is because these technologies can ensure security of supply as they are not dependent on external factors in contrast to AH and WH sources (see 3.3.1). This is referred to as the base configuration. In addition, the system may include the air HP, WWTP effluent HP, datacenter HP, and/or industrial WH as additional heat supply technologies. The combination of AH and WH technologies included in the system is referred to as the AH and WH configuration.

A wide range of possible system configurations were modelled and compared to each other. For the base configuration each heat supply technology (CHP, biomass HOB, and electric HOB) was able to have a capacity of 0, 33.34, or 66.67 MW. All possible combinations that had a total installed capacity of at least 100 MW (the peak demand) were considered. Additionally, the base configuration where peak demand is fully met by the biomass HOB was considered as this is a configuration found in current DH systems. This resulted in a total of 18 possible base configurations. For the AH and WH configuration, each of the four AH and WH sources was able to have a capacity of 0 or the equivalent of 10 MW thermal capacity, amounting to 16 possible combinations. For each base configuration, all 16 possible AH and WH combinations were considered, resulting in a total of 288 configurations analyzed.

The electrical capacity equivalent to 10 MW thermal capacity for each HP was calculated by dividing the 10 MW thermal capacity by the average COP of the HP over the course of the one-year simulation. This is constant across all simulations as the same heat source temperature profile and DH temperature profile is used. Table 3.5 presents the average COP and electrical capacity equivalent of 10 MW thermal capacity for each HP.

Table 3.5 Average coefficient of performance (COP) and electrical capacity equivalent to 10 MW thermal capacity per heat pump (HP) heat source considered in the general model

HP heat source	Average COP	MW_{el} equivalent of 10 MW_{th}
Air	2.52	4.0
WWTP effluent	2.84	3.5
Datacenter	4.12	2.4

A summary of the potential capacity that each of the seven heat supply technologies could have is presented in Table 3.6.

Table 3.6 Potential capacities considered per heat supply technology in the general model

	Potential capacity [MW_{th}, MW_{el} for HP]
Base configuration	
CHP	0, 33.34, 66.67
Biomass HOB	0, 33.34, 66.67, or 100*
Electric HOB	0, 33.34, 66.67
AH and WH configuration	
Air-source HP	0 or 3.97
WWTP effluent HP	0 or 3.52
Data-center HP	0 or 2.43
Industrial WH	0 or 10

* Only considered when the capacity of both the CHP and electric HOB is 0

Each base configuration was given an identification number ranging from 1 to 18 and each AH and WH configuration was given an identification letter ranging from A to P. The identification label for each system configuration was therefore the combination of the number and letter of the respective base configuration and AH and WH configuration. The full list of base configurations and AH and WH configuration is displayed in Table 3.7 and Table 3.8 , respectively.

Table 3.7 Base configurations considered in the general model.

ID	CHP capacity [MW_{th}]	Biomass HOB capacity [MW_{th}]	Electric HOB capacity [MW_{th}]	Total capacity [MW_{th}]
1	0	33.34	66.67	100
2	0	66.67	33.34	100
3	0	66.67	66.67	133
4	33.34	0	66.67	100
5	33.34	33.34	33.34	100
6	33.34	33.34	66.67	133
7	33.34	66.67	0	100
8	33.34	66.67	33.34	133
9	33.34	66.67	66.67	167
10	66.67	0	33.34	100
11	66.67	0	66.67	133
12	66.67	33.34	0	100
13	66.67	33.34	33.34	133
14	66.67	33.34	66.67	167
15	66.67	66.67	0	133
16	66.67	66.67	33.34	167
17	66.67	66.67	66.67	200
18	0	100	0	100

Table 3.8 AH and WH configurations considered in the general model. Equivalent thermal capacity is calculated based on the average COP of each HP heat source: 2.52 for the air HP, 2.84 for the WWTP effluent HP, and 4.12 for the datacenter HP.

ID	Air HP capacity [MW_{el}]	WWTP effluent HP capacity [MW_{el}]	Datacenter HP capacity [MW_{el}]	Industrial WH capacity [MW_{th}]	Total capacity [MW_{th} equivalent]
A	0	0	0	0	0
B	0	0	0	10	10
C	0	0	2.43	0	10
D	0	0	2.43	10	20
E	0	3.52	0	0	10
F	0	3.52	0	10	20
G	0	3.52	2.43	0	20
H	0	3.52	2.43	10	30
I	3.97	0	0	0	10
J	3.97	0	0	10	20
K	3.97	0	2.43	0	20
L	3.97	0	2.43	10	30
M	3.97	3.52	0	0	20
N	3.97	3.52	0	10	30
O	3.97	3.52	2.43	0	30
P	3.97	3.52	2.43	10	40

3.3.4 General model run

For each price lambda considered, the biomethane, biomass and electricity prices for that scenario were calculated as specified in section 3.2.2 with the energy price inputs described in section 3.3.2. The price scenario is assigned a weight equal to the probability of that price lambda occurring as defined by the Beta (2,2) distribution.

. For the general model, the WH providers with a risk of dropping out are the datacenter and industrial WH. A twenty-year study period was considered. Thus, for each WH source, there were twenty-one possible WH cessation scenarios: twenty scenarios for each year the WH could cease operation, and one scenario where it does not stop operating at all. Thus, the total number of possible WH cessation scenarios is 441 if both the datacenter and industrial WH are present in the initial system configuration (21 possibilities for when the datacenter ceases operation x 21 possibilities for when the industrial WH ceases operation), 21 if only one of the two is present in the initial system configuration (21 possibilities for the WH provider present), and 1 if neither is present in the initial system configuration. The annual WH cessation probability for both the datacenter and the industrial WH was estimated to be 0.76%, a proxy based on the annual probability of a company going bankrupt in Austria. Each WH cessation scenario is a assigned a weight equal to the probability of that WH cessation scenario occurring, calculated as outlined in section 3.2.3.

For the one-year simulation, the variable costs accounted for are electricity costs, fuel costs, other O&M costs, and auxiliary electricity costs (for the HOBs). In combination with hourly DH demand, these costs were used as inputs for the economic ranking operation strategy to determine the heat provided by each heat supply technology. The LCOH was calculated considering investment costs, annual variable costs, fixed O&M costs, and residual value at the end of the study period averaged over the total heat supplied by the system. Each LCOH was assigned a weight equivalent to the product of the price scenario weight and the WH cessation scenario weight for that LCOH. The result for each system configuration was a weighted LCOH for each price scenario and each WH cessation scenario.

3.4 CASE STUDY

3.4.1 Case study overview

For the case study, the general model developed was applied to the DH system of a small city in northwestern Poland. This case study was chosen because it is a case study for a project AIT is collaborating on titled HeatMineDH. The project focuses on the mapping of low grade renewable and WH and investment planning for efficient DH networks. The DH network provider of the city is also collaborating on the project, which facilitated data collection and modelling of the DH system.

The city has a population of around 13,000 people and a DH network that covers a large portion of the city. The DH network supplies an annual heat demand of approximately 21.5 gigawatt hours (GWh) and satisfies a peak heat demand of around 10 MW. The current DH network is supplied by two coal fired boilers with a combined capacity of 13.8 MW. Additionally, this year, a natural gas CHP with a capacity of 0.877 MW was installed and started operation in March/April 2024.

Two potential AH and WH sources located near the city which have been identified by the DH network provider are an iron foundry located around two kilometers outside the city and a WWTP located between the iron foundry and the city. In addition, an air source HP was also considered as a potential AH heat supply technology. Like the general model, the case study considered a greenfield scenario in 2050. It was thus assumed that biomass replaces coal as a fuel source for the boilers, and that biomethane replaces natural gas for the CHP. An overview of the system considered is shown in Figure 3.7. A map highlighting the location of the iron foundry and WWTP relative to the city is presented in Figure 3.8.

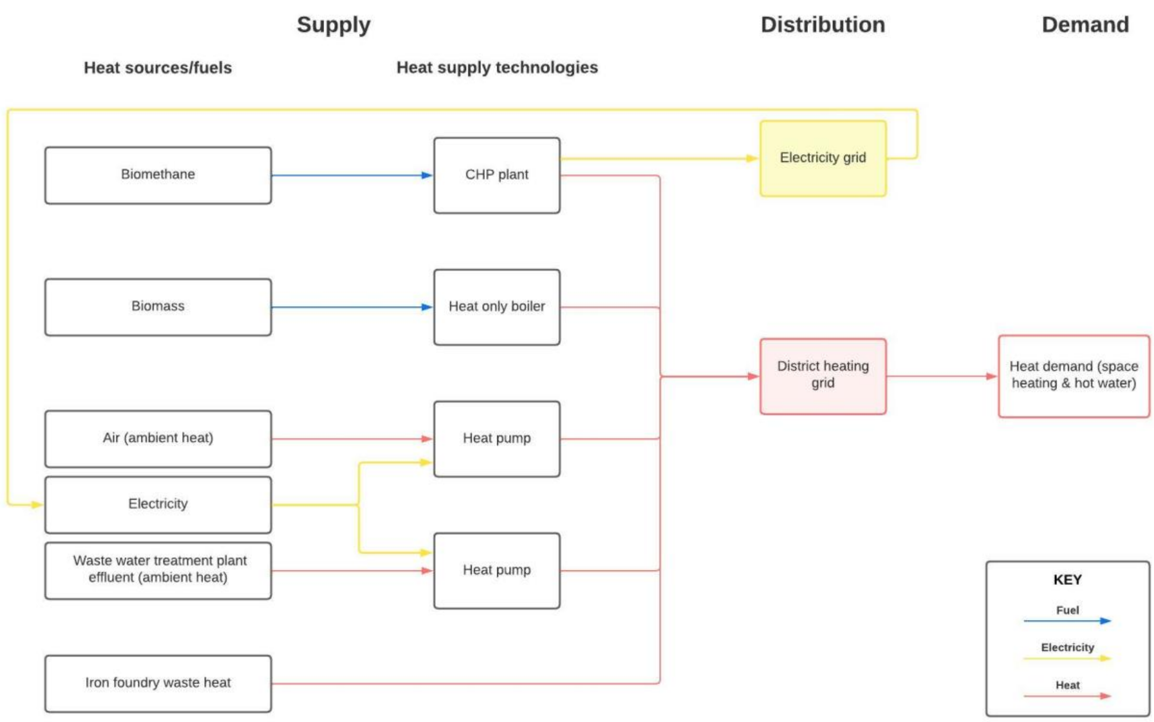

Figure 3.7 Case study district heating system overview

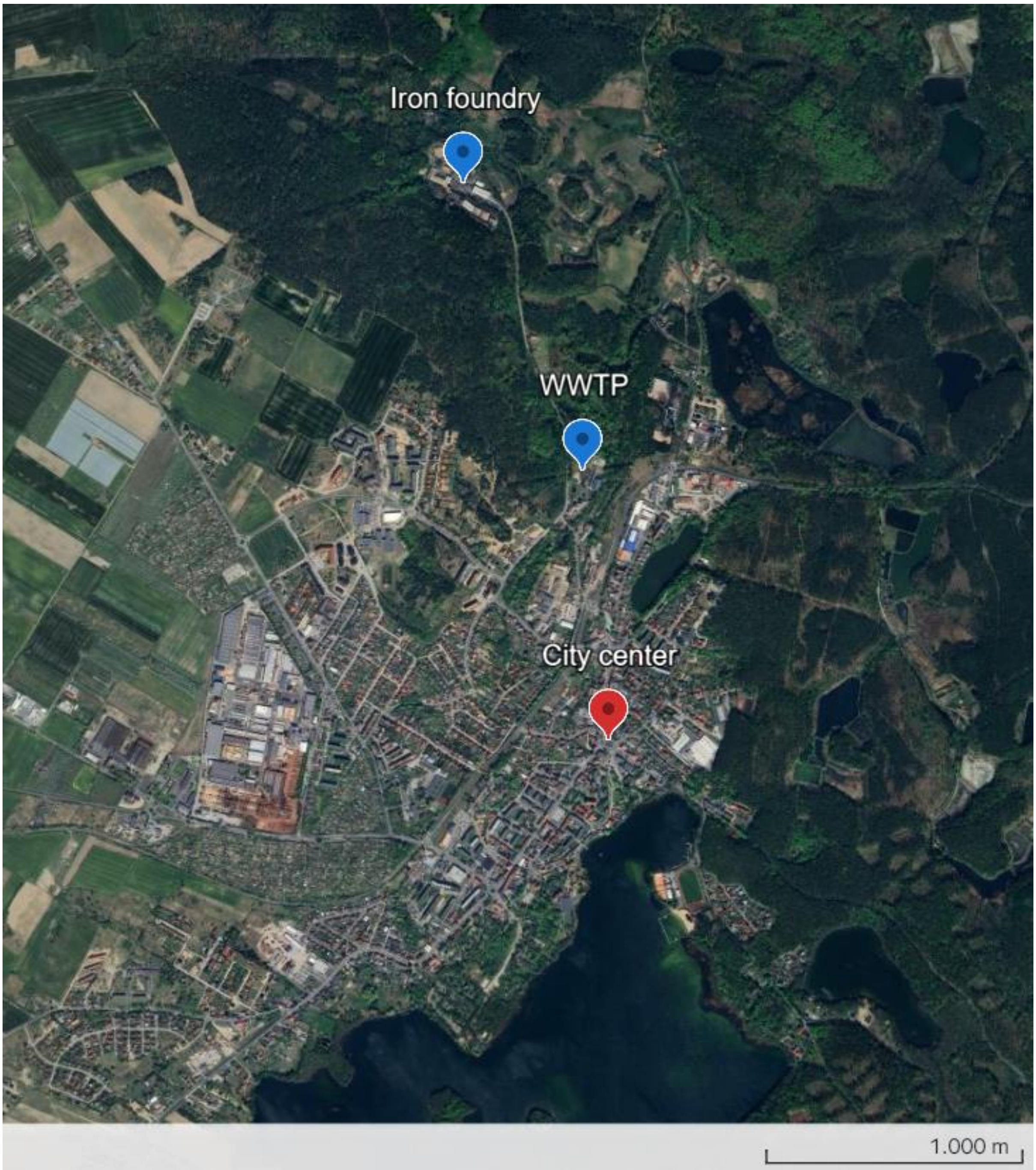

Figure 3.8 Location of the iron foundry and wastewater treatment plant (WWTP) relative to the city center of the case study location (Source: Google Earth [56])

3.4.2 Data collection and model parametrization

For the technical and economic input data per heat supply technology, data was mainly supplied by the DH network operator. No data was available for OPEX and CAPEX for WH from the iron foundry. Thus, economic data was obtained from the DH outlook study used for the general model but for an installation with a capacity of 1 MW rather than 10MW as this is closer to the 1.9 MW capacity estimated for the iron foundry [54]. An overview of the technical and economic input parameters utilized for the case study is presented in Table 3.9. An interest rate of 3.2% was used, based on the assumptions of the DH network operator.

Table 3.9 Technical and economic input data for heat supply technologies included in the case study model (combined heat and power plant (CHP), biomass heat only boiler (HOB), air source heat pump (HP), waste water treatment plant (WWTP) effluent HP, and iron foundry waste heat (WH). All values are in 2022 euros. Source: Case study DH network operator unless otherwise stated

	Heat supply technology				
	Biomass HOB	CHP	Air HP	WWTP effluent HP	Iron foundry WH
Technical parameters					
Efficiency [%]	86%	86.4%	-	-	-
Electricity share [% useful energy output]	-	48%	-	-	-
Efficiency factor	-	-	0.5*	0.5*	-
Lifetime [years]	15	15	15	15	20**
New DH piping length [km]	-	-	-	0.26	1.66
Economic parameters					
CAPEX [M€/MW_{th}, M€/MW_{el} for HP]	0.81	1.50	5.71	5.91	0.61**
OPEX [€/MW_{th}/a, €/MW_{el}/a for HP]	34,949	60,606	285,649	295,442	31**
New DH piping cost [€/m]	-	-	-	1,500***	867***

** Average efficiency factor value for large scale HPs (Source: B. Mayr, personal communication, February 29, 2024)*

*** Source:* [54]

**** Based on assumed piping costs of 750 €/m for natural areas and 1500 €/m for urban areas [Source: R. Schmidt, personal communication, April 15, 2024]. The area between the iron foundry to the WWTP is forested and from the WWTP on to the city it is urban area.*

For DH demand and network temperatures, hourly profiles from 2021 were utilized as a proxy for 2050 as this was the data provided by the network operator. Projected ordered capacity up until 2030 was also provided, thus the hourly DH demand data from 2021 was scaled to the expected ordered capacity in 2030. Specifically, an ordered capacity of 16.2 is expected in 2030, resulting in a peak demand of 11.93 MW. For air temperature, the DH network operator provided daily average temperatures for 2021. To obtain an hourly air temperature profile, data from the integrated surface database (ISD) from the National Oceanic and Atmospheric Administration (NOAA) National Centers for Environmental Information (NCEI) was utilized [57]. There is no weather station for the case study location in the database, so data from the next nearest weather station was used, located around 30 km away from the case study location. There were 119 missing values in the hourly dataset, for which the hourly temperature was assumed to be equal to the average temperature for that day in the case study location. Comparing the daily average temperatures for the cleaned dataset from the weather station and daily average temperatures in the case study location, showed a maximum difference of 2.03 °C and a mean difference of 0.43 °C. This indicates that the hourly air temperature data from the weather station serve as a good approximation for hourly temperatures in case study location. Using 2021 data as a basis for DH demand, DH network temperature, and air temperatures ensures coherences across these hourly profiles and accounts for their interdependencies. For the temperature of the WWTP effluent, monthly average temperatures provided by the DH network operator were used.

For electricity prices, day ahead electricity prices from 2022 were utilized because these were very volatile and can therefore act as a proxy for future prices. The uncertainty range used to estimate minimum and maximum electricity prices was calculated based on historical variation in hourly day-ahead prices using the same approach as Marx et al. used for Austria [18]. Day ahead prices were obtained from the ENTSO-E Transparency Platform [58]. The monthly mean (μ) and standard deviation (σ) of hourly day-ahead prices in Poland were calculated for the period from January 2015 to October 2023. Hourly data was aggregated to monthly data to model variation in electricity prices over longer timeframes. The results of the analysis are presented in Figure 3.9. Over the period studied, the average variation from the mean based on the standard deviation ranged from 0.74 times the mean ((μ-σ)/μ) to 1.26 times the mean ((μ+ σ)/μ). A range of 0.7 to 1.3 was used as a conservative estimate and hourly 2022 day ahead prices were multiplied by these factors to obtain the minimum and maximum electricity price profile for 2050 respectively.

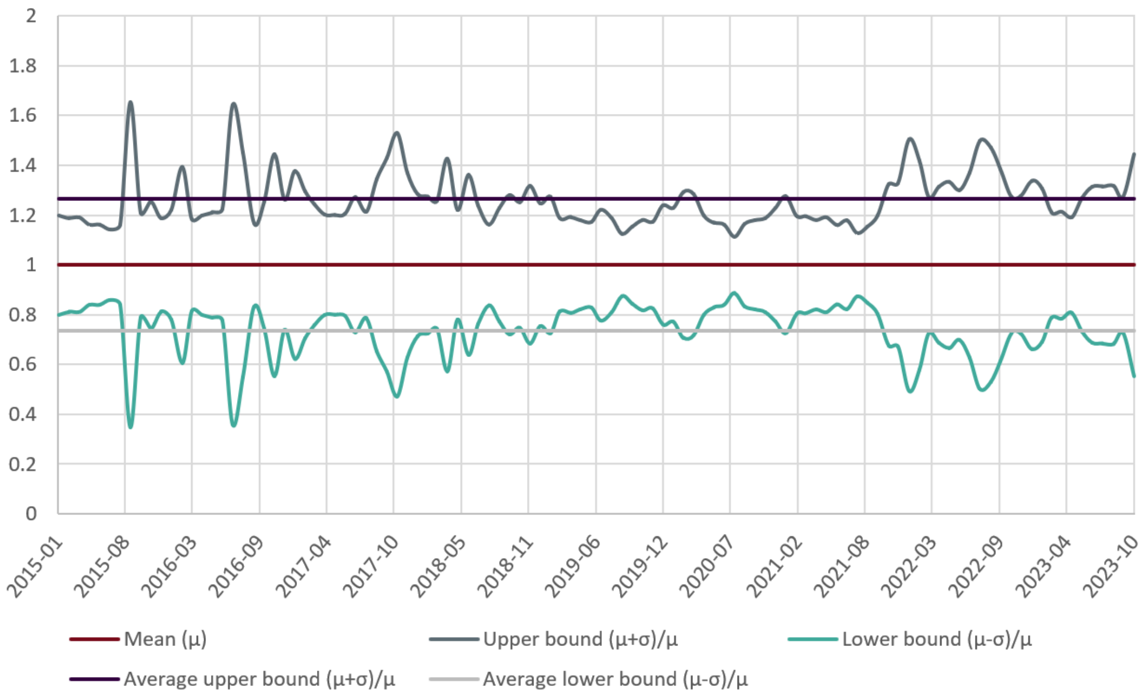

Figure 3.9 Historical variation in day ahead electricity prices in Poland. Upper and lower bounds were estimated based on standard deviation(σ) from the mean(μ).

In 2023, biomass prices in Poland ranged from 20.4 to 23.3 €/MWh. Thus, a minimum to maximum range of 20-35 €/MWh was used as a conservative estimate for 2050. For biomethane prices, the same minimum to maximum range considered in the general model (80 to 120 €/MWh) was utilized as it is assumed there will be a European market for biomethane in the future. As WH prices can be agreed on bilaterally between the WH provider and DH network operator, a sensitivity analysis was conducted for energy prices for WH from the iron foundry. A WH price of 20, 30, and 40 €/MWh was considered. The input data utilized for DH demand, relevant temperatures, and energy prices for the case study is summarized in Table 3.10.

Table 3.10 Summary of the input data used for district heating demand, energy prices, and relevant temperatures for the case study model

Data	Fixed/hourly		Source
Hourly DH demand profile	Hourly	2021 hourly demand scaled to expected ordered capacity in 2030	Case study DH network operator
Air temperature	Hourly	Hourly air temperatures from nearest weather station with missing values filled with daily average from case study location	NOAA NCEI ISD [57], Case study DH network operator
WWTP effluent temperature	Monthly	Estimated monthly average temperature	Case study DH network operator
District heating temperature	Hourly	2021 hourly DH network temperature	Case study DH network operator
Electricity prices	Hourly	2022 hourly day ahead prices as average with historical variation in Polish day-ahead prices used to estimate the uncertainty range used to obtain minimum and maximum prices	ENTSO-E Transparency Platform [58]
Biomass prices	Fixed	Minimum to maximum range of 20-35 €/MWh (conservative estimate based on 2023 biomass prices in Poland)	Case study DH network operator
Biomethane prices	Fixed	Minimum to maximum range of 80-120 €/MWh	G. Resch and S. Reuter, personal communication, March 19, 2024
Industrial WH price	Fixed	0, 10, 20, 30, 40 €/MWh	Sensitivity analysis

3.4.3 System configurations

Two potential decarbonization scenarios identified by the case study DH network operator were utilized as the basis for the system configurations modelled for the case study. These were (1) the use of biomass HOBs and CHP plants and (2) the use of biomass HOBs, CHP plants, and WH from the iron foundry near the city. The CHP that began operating this year is fueled by natural gas. Thus, for the greenfield scenario modelled for 2050, it was assumed that the CHP engines would be fuel by biomethane as this is a carbon neutral, direct substitute for natural gas [51].

To define the system configurations to be analyzed for the case study, these decarbonization scenarios were considered as the two possible base scenarios with capacities per heat supply technology defined by the DH operator and scaled to the ordered capacity in 2030 as an approximation for 2050. Then, for each base scenario, three possible variations were considered which accounted for the inclusion of the potential AH sources identified. Specifically, these variations consisted of the additional installation of an air HP, a WWTP effluent HP, or both an air and WWTP effluent HP. The capacities of the air HP and WWTP HP were defined as the electrical capacity equivalent to 1 MW thermal capacity. This amounted to a total of eight system configurations, displayed in Table 3.11

Table 3.11 System configurations considered for the case study

	Heat supply technology capacity [MW_{th}]					
	Biomass HOB	Biome-thane CHP	Iron foundry WH	Air HP	WWTP effluent HP	Total
Base scenario 1 (B1): Biomass HOB & CHP						
B1	12.31	3.92	-	-	-	16.23
B1+ Air HP	12.31	3.92	-	1	-	17.23*
B1 + WWTP HP	12.31	3.92	-	-	1	17.23*
B1 + Air HP + WWTP HP	12.31	3.92	-	1	1	18.23*
Base scenario 2 (B2): Biomass HOB, CHP, and iron foundry WH						
B2	14.87	1.36	1.9	-	-	18.13**
B2+ Air HP	14.87	1.36	1.9	1	-	19.13**
B2 + WWTP HP	14.87	1.36	1.9	-	1	19.13**
B2 + Air HP + WWTP HP	14.87	1.36	1.9	1	1	20.13**

* 16.23 without air HP or WWTP effluent HP
** 16.23 without iron foundry WH, air HP, or WWTP effluent HP

As for the general model, the electrical capacity equivalent to 1 MW thermal capacity for each HP was calculated by dividing the thermal capacity by the average COP of each heat source over the one-year simulation period. The average COP and electrical capacity for the air source HP and WWTP effluent HP can be found in Table 3.12

Table 3.12 Average coefficient of performance (COP) and electrical capacity equivalent to 1 MW thermal capacity for the air heat pump (HP) and wastewater treatment plant (WWTP) effluent HP in the case study

HP heat source	Average COP	MW_{el} equivalent of 1 MW_{th}
Air	3.10	0.32
WWTP effluent	3.21	0.31

3.4.4 Case study model run

For each system configuration, the case study model was run to obtain a weighted sample of LCOHs. As described in section 3.2.2, for each system configuration, one hundred possible energy price scenarios, represented by the price lambda, were considered. For each price lambda, the biomass, biomethane, and electricity prices were calculated based on the price lambda as specified in section 3.2.2 using the price ranges described in section 3.4.2. The price scenario was assigned a weight equal to the probability of that price lambda occurring as defined by a Beta (2,2) distribution.

For the case study, the only heat source relevant for the WH cessation scenarios is the iron foundry. A twenty-year study period was analyzed, thus there were 21 possible WH cessation scenarios: twenty scenarios for each year the iron foundry could cease operation, and one scenario where it does not cease operation at all. As for the general model, the annual WH cessation probability was estimated by using the probability of a company going bankrupt as proxy. However, this probability was calculated for Poland rather than Austria. Specifically, an average probability of 0.70% was calculated by dividing the annual number of company bankruptcy court orders by the number of companies (non-financial companies with more than 10 employees) in Poland for the period of 2016 to 2022 [59], [60]. Based on this annual WH cessation probability, the probability of each WH cessation scenario occurring was calculated as outlined in section 3.2.3, and assigned as a weight to that WH cessation scenario.

For each system configuration, price lambda, and WH cessation scenario, the one-year simulation was run as needed to obtain annual variable cashflows and heat production per heat supply technology over the 20-year study period analyzed. In the model, the WH from the iron foundry was only available during weekdays as the iron foundry only operates during weekdays. The variable costs considered in the model are electricity costs, and fuel costs. Annual variable cashflows and heat output were combined with fixed O&M costs and investment costs, and residual value to calculate the LCOH for each system configuration, price lambda, and WH cessation scenario (see section 3.2.5). When the expected lifetime of the technology was shorter than the study period, a replacement of the same size was installed, resulting in additional CAPEX costs. Residual values at the end of the study period were accounted for except for the WH from the iron foundry when it ceased operation within the study period. Each LCOH was assigned a weight equal to the product of the weight of the energy price scenario and WH cessation scenario being considered.

3.4.5 Biomass restriction scenarios

The system configurations analyzed for the case study model assume a relatively high share of biomass in the DH system with both B1 and B2 having a relatively large installed capacity for the biomass HOB. Furthermore, in the one-year simulation, an unlimited supply of biomass is assumed as the heat supplied by the biomass HOB in any given timestep is only limited by the installed capacity. Finally, the cost of the biomass is relatively low compared to other heat supply technologies attractive, making it an attractive source for heat.

However, the availability of biomass may be limited in the future. Biomass can be used as a carbon neutral alternative to fossil fuels for a wide range of applications. This includes high value applications that are difficult to decarbonize otherwise such as the production of materials, feedstock for the chemical industry, and production of fuel for aviation and heavy and long-distance transport [61]. Thus, competition with other sectors or within the heating sector may limit the future availability of biomass for DH. Furthermore, it is possible that the use of biomass may be prioritized for use in sectors that are difficult to decarbonize otherwise, which may further limit its availability for heating purposes.

To account for the uncertainty in the future availability of biomass as a fuel source, five scenarios were modelled where the amount of biomass used was restricted. This was achieved by implementing an artificial price increase for biomass during the economic ranking that occurs each timestep. Specifically, the biomass price was multiplied by multiplier (here on referred to as biomass price multiplier). The multiplier was constant throughout the entire one-year simulation. This made using heat from the biomass HOB less attractive compared to other heat supply technologies. The biomass price multiplier was only applied during the economic ranking which determines how much heat is supplied by each technology, no change was made to the actual biomass price. Specifically, the five biomass restriction levels considered were low, medium, high, very high, and maximum, corresponding to a biomass price multiplier of 2, 3, 4, 5 and 10 respectively (see Table 3.13). The biomass price multiplier of 10 represents a maximum restriction level because it results in biomass only being used when it is needed to meet demand.

Table 3.13 Biomass price multiplier for each biomass restriction level considered in the case study

Biomass restriction level	Biomass price multiplier
None (base scenario)	1
Low	2
Medium	3
High	4
Very high	5
Maximum	10

4 RESULTS

The following section presents the results of the analysis, first for the general model and then the case study. Results for the general model are presented from a high-level perspective, examining the key performance indicators (KPIs) chosen (weighted average LCOH and standard deviation) for the various system configurations modelled, and their sensitivity to the industrial WH price. Results for the case study are presented on a general level by looking at the KPIs chosen but also delve deeper into each of the methodological steps and levels of analysis.

4.1 GENERAL MODEL

4.1.1 Main results

Figure 4.1 depicts the weighted average LCOH in €/MWh on the horizontal axis and standard deviation as a percent of the mean LCOH on the vertical axis for each configuration studied in the general model. This allows for a comparison of average cost and economic risk across configurations. The different shapes represent the base configurations, while colors indicate the AH and WH configuration. A pattern is discernable which shows a transition from system configurations with low mean LCOH but high standard deviation (indicating higher economic risk) to system configurations with high mean LCOH but low standard deviation (indicating lower risk). This indicates a tradeoff between average cost and economic risk for DH configurations. Additionally, it is evident that the mean LCOH and standard deviation varies largely across the various system configurations analyzed. Specifically, mean LCOH ranges from 54.88 to 137.00 €/MWh and standard deviation ranges from 0.83 to 9.87 percent of mean LCOH (or 1.00 to 8.83 €/MWh, see Appendix A, Figure A.1 for a graph of LCOH against standard deviation in €/MWh). Thus, despite the high economic risk of technologies with lower LCOH, they often still perform better than the high-cost technologies when the standard deviation is added to the mean LCOH. The average mean LCOH across configurations is 94.79 €/MWh while the average standard deviation is 3.12 % (or 2.68 €/MWh).

The variation in LCOH and standard deviation is also evident across base configurations and AH and WH configurations. However, it appears that the base configuration has a larger impact on performance and economic risk, as data points are clustered together based on base configuration rather than AH and WH configuration. This is to be expected as base configuration technologies makes up a greater portion of installed capacity and heat supply than the additional AH and WH technologies. They therefore have a significant influence on investment and operational costs (and thus, LCOH) but also in the system's response to uncertainty in energy prices. Additionally, in comparing base configurations to each other, it becomes evident that the different AH and WH configurations per base configuration are sometimes clustered together more closely (see for example base configurations 13 and 17) and sometimes more spread apart (see configurations 1 and 4). This indicates that the magnitude of the effect of additional AH and WH heat supply technologies on the mean LCOH and standard deviation varies based on the base configuration.

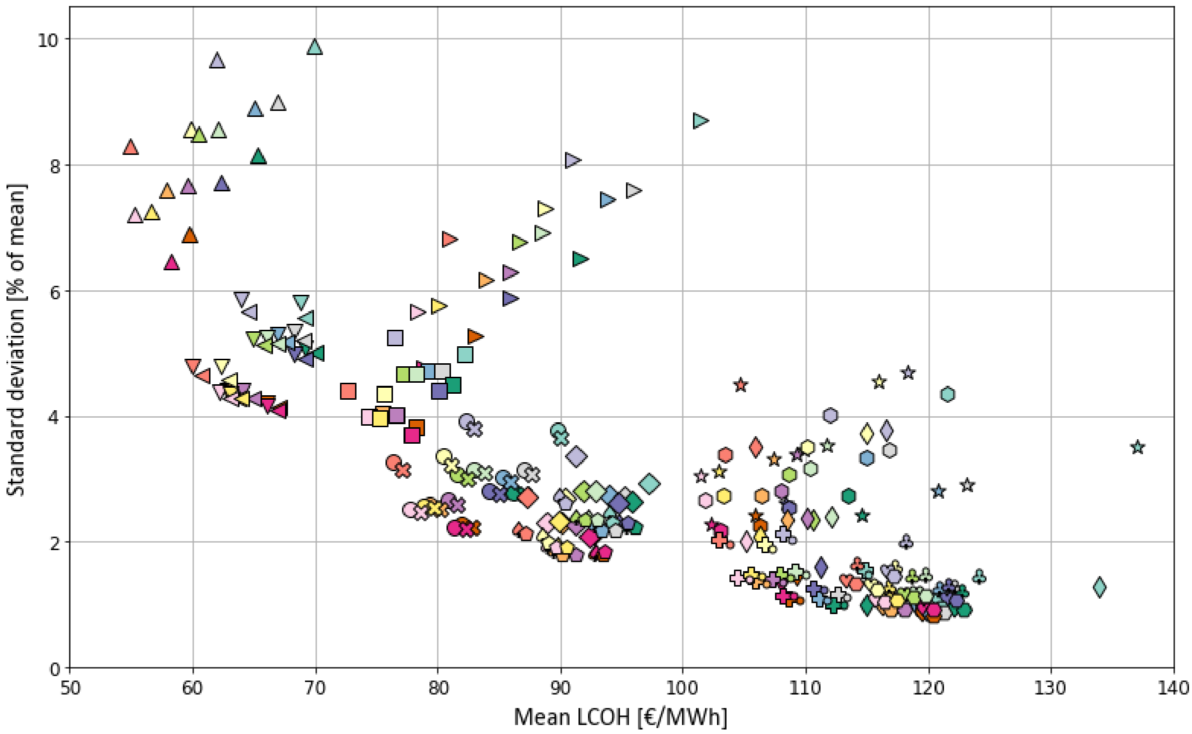

CONFIGURATION LEGEND

Base configuration: CHP, biomass boiler (BMB), electric boiler (ELB) and capacity in MW_{th} (0: ○○○, 33: ●○○, 67: ●●○, or 100: ●●●)

▲ 1: CHP○○○ BMB●○○ ELB●●○	▶ 4: CHP●○○ BMB○○○ ELB●●○	◆ 7: CHP●○○ BMB●●○ ELB○○○	★ 10: CHP●●○ BMB○○○ ELB●○○	✚ 13: CHP●●○ BMB●○○ ELB●○○	♥ 16: CHP●●○ BMB●●○ ELB●○○
▼ 2: CHP○○○ BMB●●○ ELB●○○	● 5: CHP●○○ BMB●○○ ELB●○○	♠ 8: CHP●○○ BMB●●○ ELB●○○	⬢ 11: CHP●●○ BMB○○○ ELB●●○	• 14: CHP●●○ BMB●○○ ELB●●○	⬣ 17: CHP●●○ BMB●●○ ELB●●○
◀ 3: CHP○○○ BMB●●○ ELB●●○	✖ 6: CHP●○○ BMB●○○ ELB●●○	⬟ 9: CHP●○○ BMB●●○ ELB●●○	⧫ 12: CHP●●○ BMB●○○ ELB○○○	♣ 15: CHP●●○ BMB●●○ ELB○○○	■ 18: CHP○○○ BMB●●● ELB○○○

Ambient and waste heat configuration: industrial waste heat (IWH), datacenter heat pump (DHP), wastewater heat pump (WHP), and/or air heat pump (AHP), with 10 MW_{th} capacity if present

A: None	C: DHP	E: WHP	G: WHP, DHP	I: AHP	K: AHP, DHP,	M: AHP, WHP	O: AHP, WHP, DHP
B: IWH	D: DHP, IWH	F: WHP, IWH	H. WHP, DHP, IWH	J: AHP, IWH	L: AHP, DHP, IWH	N: AHP, WHP, IWH	P: AHP, WHP, DHP, IWH

Figure 4.1 Weighted average levelized cost of heat (LCOH) and standard deviation (expressed as a percent of mean LCOH) for each of the configurations analyzed for the general model. The base configuration is indicated by the shape and the ambient and waste heat configuration by the color.

4.1.2 Comparison across configurations

Figure 4.2 and Figure 4.3 present the results from Figure 4.1 with a subplot per base configuration. Figure 4.2 has the same axes across subplots, allowing for comparison of how base configurations perform relative to each other, while Figure 4.3 has varying axes across subplots allowing for comparison of how AH and WH configuration compare to each other across base configurations.[6]

Comparison across base configurations

Looking at Figure 4.2, it is evident that configurations with less technologies and lower installed capacity have a lower mean LCOH but higher standard deviation. These are the configurations found in the top left corner of Figure 4.1. They include base configuration 1-4 which consist of only the biomass HOB and electric HOB or CHP and electric HOB and have an installed capacity exactly equal to peak demand (100 MW). In contrast, configurations with more technologies and a greater installed capacity have higher costs but lower economic risk. These are the configurations in the bottom right corner of Figure 4.1. This includes base configurations 13-17 which have the CHP, biomass HOB, and electric HOB and a total installed capacity ranging between 133 and 200 MW, which significantly exceeds peak demand. Greater installed capacities lead to higher investment costs, which are reflected in a higher mean LCOH. However, the inclusion of more technologies and greater capacities leads to increased flexibility as there is a greater number of options to be chosen from in economic ranking each timestep and the lowest cost heat source can be used, even in timesteps with high demand as installed capacity is greater than peak demand. This results in a reduced standard deviation as the system is more robust in the face of changes in energy prices and WH availability. Especially the combination of a CHP and electric HOB or HPs allow for this as the CHP is profitable and can be used when electricity prices are high while the electric HOB or HPs can be used when electricity prices are low. When this is combined with a biomass HOB, then the biomass HOB can be used when electricity prices are average, and neither the CHP nor electric HOB is particularly cost-effective. The presence of a large biomass HOB also leads to a generally lower standard deviation, likely partly due to the smaller variation in biomass prices across energy price scenarios compared to electricity or biomethane prices.

The capacity of the CHP included in the base configuration also has a significant impact on the mean LCOH. Base configurations with no CHP have a mean LCOH ranging between around 60 and 80 €/MWh (base configurations 1-3 and 18), base configurations with a 33 MW CHP have a mean LCOH ranging between around 80 and 100 €/MWH (base configurations 4-9) and base configurations with a 67 MW CHP have a mean LCOH ranging between around 100 and 120 €/MWh (base configurations 10 to 17). This is due to the relatively high investment cost for the CHP, which results in a significant increase in LCOH. However, when comparing configurations, it is also clear that operational costs also play an important role. For example, the configurations with the highest mean LCOH are configurations 10A and 12A. Configurations 10 A and 12A both have an installed capacity of 100 MW, which is much less than that of other configurations reaching up to 240 MW installed capacity (for example, configuration 17P). Yet, the mean LCOH is still higher for configurations 10A and 12A, indicating that operational costs can also play a significant role in determining the mean LCOH of a system.

[6] See Appendix A, Figure A.2 and Figure A.3 for the results from Figure 4.1 with a subplot per AH and WH configuration with consistent axes and varying axes per subplot, respectively.

In comparing base configurations to each other, it also becomes apparent that some have a greater spread in mean LCOH and standard deviation across AH and WH configurations than others. For example, base configurations 1, 4, and 10- 12 have a large spread while base configurations 7-9 and 13-17 have a lower spread. The base configurations with a higher spread tend to be those with only two technologies, and an installed capacity that exactly meets peak demand. In contrast, base configurations with a low spread, tend to have all three base configuration technologies installed, and an installed capacity greater than peak demand. The inclusion of a biomass HOB also reduces the spread across AH and WH configurations (see for example configurations 4, 6, and 7 which have an increasingly greater biomass HOB installed capacity). For base configurations with a lower spread, the inclusion of an additional AH or WH heat supply technology has a smaller impact on the cost and economic risk than for those with a large spread. As previously mentioned, the inclusion of more technologies and greater installed capacity in the base configuration leads to a greater degree of flexibility on the supply side and ability to make the most out of the least cost heat sources, even in timesteps with high demand. Therefore, the added flexibility offered by HPs by their ability to operate in low electricity price scenarios or the relatively low cost industrial WH has less of an impact on the mean LCOH and standard deviation of systems with all three base configuration technologies and large installed capacities. The presence of a larger biomass HOB also leads to a lower spread since the cost for biomass is relatively less expensive than other heat sources and does not vary throughout the year like electricity prices.

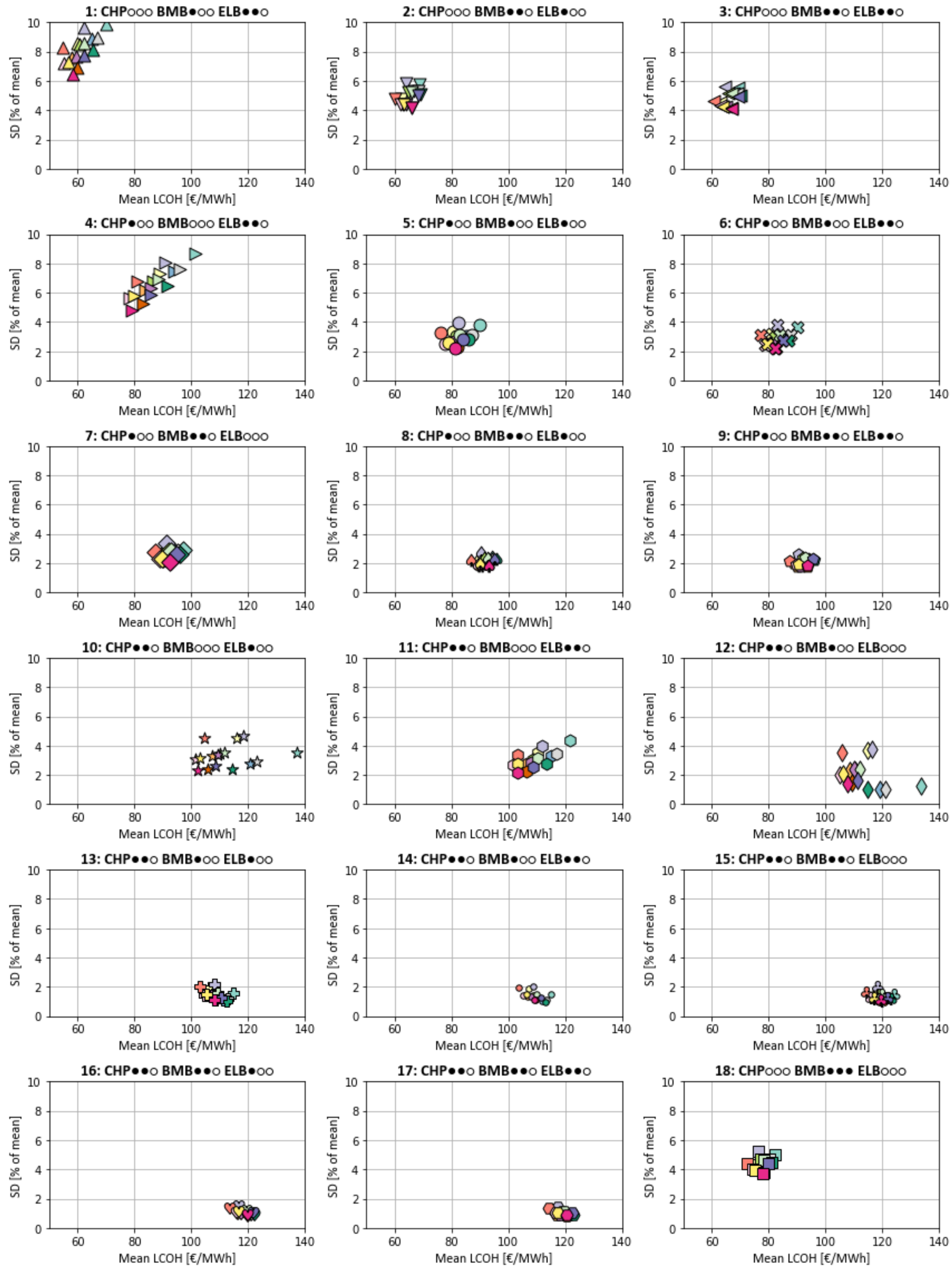

CONFIGURATION LEGEND

Base configuration: CHP, biomass boiler (BMB), electric boiler (ELB) and capacity in MW_{th} (0: ○○○, 33: ●○○, 67: ●●○, or 100: ●●●)

▲ 1: CHP○○○ BMB●○○ ELB●●○ ► 4: CHP●○○ BMB○○○ ELB●●○ ◆ 7: CHP●○○ BMB●●○ ELB○○○ ★ 10: CHP●●○ BMB○○○ ELB●○○ ✚ 13: CHP●●○ BMB●○○ ELB●○○ ♥ 16: CHP●●○ BMB●●○ ELB●○○

▼ 2: CHP○○○ BMB●●○ ELB●○○ ● 5: CHP●○○ BMB●○○ ELB●○○ ♠ 8: CHP●○○ BMB●●○ ELB●○○ ⬢ 11: CHP●●○ BMB○○○ ELB●●○ • 14: CHP●●○ BMB●○○ ELB●●○ ⬣ 17: CHP●●○ BMB●●○ ELB●●○

◄ 3: CHP○○○ BMB●●○ ELB●●○ ✖ 6: CHP●○○ BMB●○○ ELB●●○ ⬟ 9: CHP●○○ BMB●●○ ELB●●○ ⧫ 12: CHP●●○ BMB●○○ ELB○○○ ♣ 15: CHP●●○ BMB●●○ ELB○○○ ■ 18: CHP○○○ BMB●●● ELB○○○

Ambient and waste heat configuration: industrial waste heat (IWH), datacenter heat pump (DHP), wastewater heat pump (WHP), and/or air heat pump (AHP), with 10 MW_{th} capacity if present

A: None C: DHP E: WHP G: WHP, DHP I: AHP K: AHP, DHP, M: AHP, WHP O: AHP, WHP, DHP

B: IWH D: DHP, IWH F: WHP, IWH H. WHP, DHP, IWH J: AHP, IWH L: AHP, DHP, IWH N: AHP, WHP, IWH P: AHP, WHP, DHP, IWH

Figure 4.2 Weighted average levelized cost of heat (LCOH) and standard deviation (expressed as a percent of mean LCOH) for each of the configurations analyzed for the general model. There is one plot per base configuration analyzed, and axes are the same across plots.

Comparison across AH and WH configurations

Looking at Figure 4.3, it is possible to see that the relationship between different AH and WH configurations varies across different base configurations. However, some patterns are discernable.

Across multiple base configurations, the AH and WH configurations with red tones perform better than those with blue tones, having a lower mean LCOH and standard deviation. Specifically, this is evident in base configurations 1-9, 11 and 18, with the difference sometimes being very marked such as in base configurations 2, 3, 8, 9 and 18. The AH and WH configurations with red tones have industrial WH as one of the heat sources while those with blue tones do not. The industrial WH is a relatively low-cost heat supply technology, not only in terms of investment and fixed O&M costs, but also in terms of variable costs. At a price of 20 €/MWh the industrial WH is almost always one of the cheapest heat sources (with an efficiency of 88%, the cost of heat from the biomass HOB ranges from 34.09 to 51.14 €/MWh, and that of the electric HOB and CHP is dependent on electricity prices). This contributes to the lower mean LCOH for sources with industrial WH. Furthermore, the industrial WH price does not vary across energy price scenarios. This may contribute to a decrease in standard deviation relative to configurations without industrial WH as the WH can serve as a stable, low-cost heat source across energy price scenarios. However, the industrial WH is affected by the WH cessation scenarios. Thus, the decrease in standard deviation despite this indicates that the energy price scenarios have a greater influence than the WH cessation scenarios. For other base configurations, namely 10 and 12-17, the AH and WH configurations with red tones have a generally lower mean LCOH but not necessarily a lower standard deviation compared to the AH and WH configurations with blue tones. This indicates that the relatively low cost industrial WH contributes to a lower mean LCOH across all configurations. However, as not all configurations show a lower standard deviation when industrial WH is present, it is evident that the economic risk is also dependent on what other technologies are in the system. Nonetheless, it is important to note that the price set for the industrial WH and the assumption that it remains stable across energy price scenarios has a strong influence on the results of the analysis.

It is also notable that AH and WH configuration A, which has no AH or WH sources, is often one of the AH and WH configurations with the highest mean LCOH. Specifically, it is the most expensive AH and WH configuration across two thirds (12 of the 18) of the base configurations. This indicates that the gains made in variable operational costs due to the inclusion of additional AH and or WH sources, outweighs the added investment cost for those sources. In the remaining third of base configurations, the most expensive AH and WH configuration is configuration M which has the air HP and WWTP HP. In these cases, the added benefits from reduced variable costs does not outweigh the added investment cost for air HP and WWTP HP. These two AH heat sources, have a lower COP than the datacenter HP, which likely contributes to why the added operational benefits do not outweigh the increased investment cost in some base configurations.

In contrast, the AH and WH configuration with the lowest mean LCOH relative to other AH and WH configurations is configuration D, which has datacenter HP and the industrial WH. Specifically, it is the least expensive AH and WH configuration across fourteen of the eighteen base configurations. In the remaining four base configurations, the least expensive AH and WH is configuration H, which has the WWTP HP, datacenter HP, and industrial WH. As previously mentioned, the industrial WH acts as a stable, low-cost heat source across all energy price scenarios, leading to a lower mean LCOH. The datacenter HP has the highest COP of the HPs and is therefore able to offer the greatest amount of heat for the same amount of electricity, and the greatest cost efficiency at low electricity prices. The

WWTP has the second highest COP. Thus, for these sources, the cost gains that are achieved due to their inclusion in the system significantly outweigh the additional investment costs. However, it is important to note that both the datacenter HP and industrial WH are affected by the WH cessation scenarios as there is the possibility that the source is no longer available in the future, for example, due to bankruptcy or relocation. This is sometimes reflected in a relatively higher standard deviation for these configurations such as in configurations 13D, 14D, 16D and 17D.

When comparing the standard deviation of AH and WH configurations with the same base configuration, it is apparent that AH and WH configuration C often has the highest standard deviation. Specifically, it has the highest value in fifteen of the eighteen base configurations. AH and WH configuration C consists of the datacenter HP which has a relatively high COP (an average of 4.12) and can therefore provide heat at very low and competitive prices, especially when electricity prices are low. This can lead to significant variable cost gains compared to the base scenario without AH or WH sources. If an electric HOB is present in the base configuration, the datacenter HP provides much less expensive heat for the same electricity price. While if an electric HOB is not present in the base configuration, it offers even greater price gains as there was previously no technology that offered low-cost heat at low electricity prices. However, the datacenter is subject to the WH cessation scenarios where it is suddenly no longer available. Just as the cost gains are high once a datacenter HP is present, the losses when it is suddenly no longer available are equally as high. This leads to a large variation across WH cessation scenarios. Furthermore, as the datacenter HP is powered by electricity, it is also subject to the impact of variation in electricity prices across energy price scenarios, further increasing the standard deviation. For the remaining three base configurations where AH and WH configuration C does not have the highest standard deviation, configuration A (with no AH or WH sources) has the highest standard deviation. This indicates that in these scenarios. In these scenarios, the lack of flexibility offered by additional AH or WH sources, results in configuration A being more strongly affected by the energy price scenarios, and thus have a higher standard deviation. All base configurations where A has the highest standard deviation (1, 4, and 11) have a 66 MW electric HOB, making the gains from the datacenter HP smaller and reducing the standard deviation of AH and WH configuration C, albeit it is the AH and WH configuration with the second highest standard deviation for all three.

The AH and WH configuration with the lowest standard deviation is slightly more varied across base configurations. AH and WH configuration M has the lowest standard deviation in three base configurations, N in five base configurations, and P in ten base configurations. Configuration M consists of the air HP and WWTP HP. These sources increase the flexibility of the system in the face of fluctuating energy prices as they can be used in low electricity prices, driving the down the standard deviation. Furthermore, they are not affected by WH cessation scenarios, further reducing the variation in the LCOH. AH and WH configuration N has the air HP, WWTP HP, and industrial WH. In addition to the benefits provided by the air and WWTP HP, the industrial WH is a low-cost heat source that offers stability across energy price scenarios as the WH price remains constant, further decreasing the standard deviation. The industrial WH is affected by the WH cessation scenarios, however in these cases the this is outweighed by the benefits it provides in relation to energy price uncertainties and the advantages from the HPs. Finally, AH and WH configuration P has all four AH and WH sources. In these scenarios the added flexibility and low-cost heat provided by the additional inclusion of these sources surmounts the variation in LCOH due to the WH cessation scenarios.

Overall, one can observe that the inclusion of AH and WH sources within a DH system can provide benefits in supplying low-cost heat and flexibility in the face of fluctuating energy prices, reducing both the LCOH and standard deviation in many cases. However, the exact impact of the inclusion of AH and WH sources varies depending on which other heat supply technologies are found in the system.

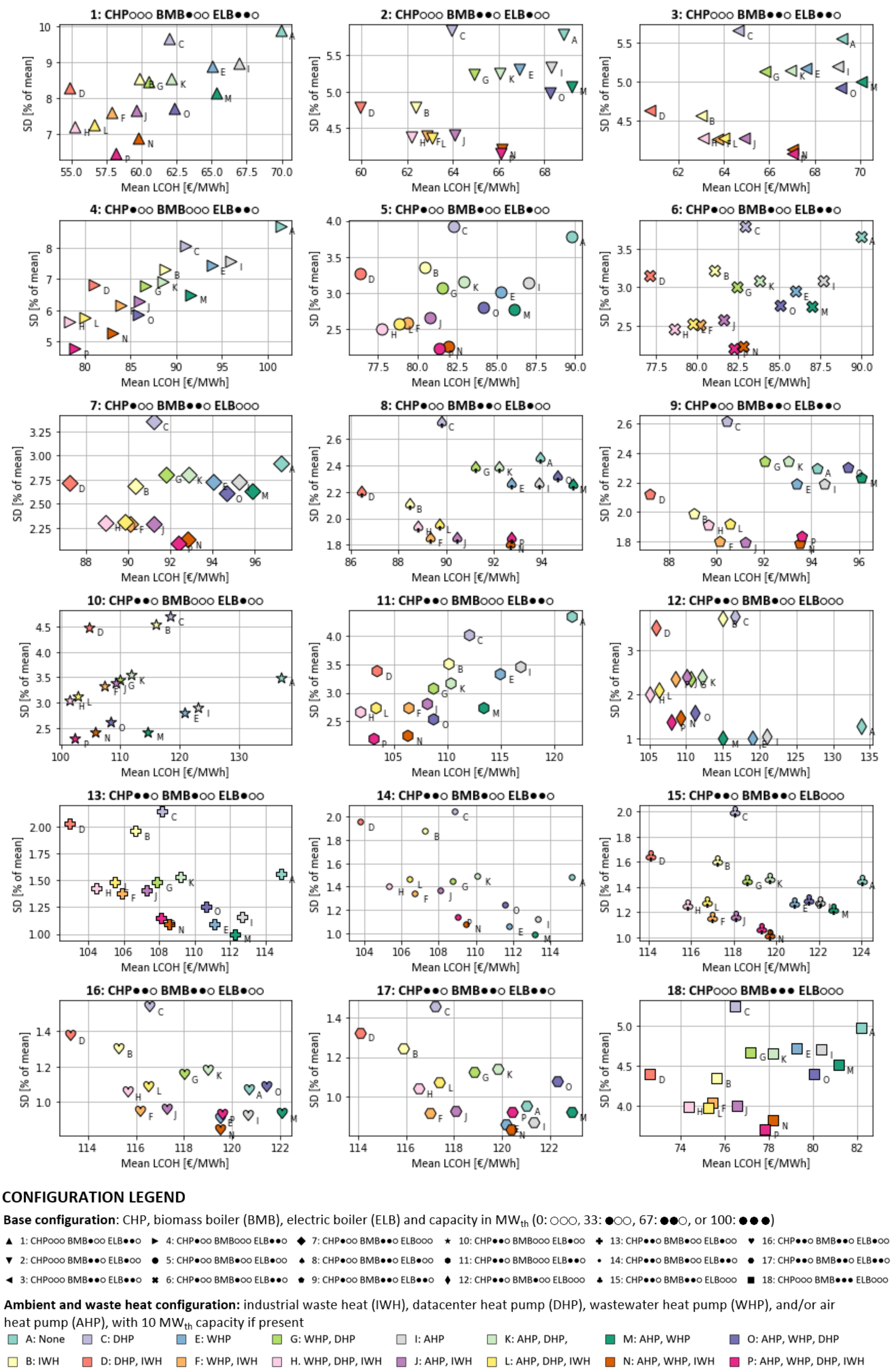

Figure 4.3 Weighted average levelized cost of heat (LCOH) and standard deviation (expressed as a percent of mean LCOH) for each of the configurations analyzed for the general model. There is one plot per base configuration analyzed, and axes vary across plots.

4.1.3 Sensitivity to industrial waste heat price

Sensitivity of mean LCOH to industrial WH price

Figure 4.4 presents the results of the sensitivity analysis of the weighted average LCOH to changes in the industrial WH price, plotted per base configuration.[7] Across all configurations, an increase in the industrial WH price results in a higher mean LCOH. Furthermore, the change in mean LCOH is steeper moving between a WH price of 0 to 40 €/MWh compared to a WH price of 40 to 60 €/MWh. This is likely because up to a price of around 40€/MWh, the industrial WH is consistently one of the cheapest heat sources in the system. Thus, for industrial WH prices up to 40€/MWh, most of the capacity of the WH will be used regardless of the price, and changes in the industrial WH price will directly impact OPEX costs for industrial WH and be reflected in the LCOH. This is also evident in that the change in LCOH when moving from a WH price of 20 to 0 €/MWh leads to a decrease in about 5 €/MWh across all configurations. However, between a price of 40 and 60 €/MWH, other heat sources, such as the biomass HOB, are competitive with the WH, and these will replace some of the heat otherwise supplied by the industrial WH. Therefore, there is a smaller increase in the LCOH despite the same increase in the industrial WH price. This already begins to be apparent at a price of 40 €/MWH, with a greater variation in the LCOH across AH and WH configurations, as systems with more AH and WH sources, and therefore more competition with the industrial WH, having a lower change in LCOH.

Across all base configurations, there is a consistent pattern in which AH and WH configurations are more sensitive to industrial WH prices. The most sensitive configuration is configuration B, followed by D, F; and J (exact order varies), followed by L, H, and N (exact order varies), and finally P. Configuration B consists of only the industrial WH, configurations D, F; and J of the industrial WH and one HP, configurations L, H, and N of the industrial WH and two HPs, and configuraion P has all AH and WH sources. This shows that the more AH and WH technologies are in the system, the less sensitive the mean LCOH is to changes in the industrial WH price either upwards or downwards. This is because a greater number of technologies is able to offer greater flexibility and options for choosing the least cost technology each timestep in the hourly simulation. Thus, the mean LCOH varies less with changes in the industrial WH price.

As for AH and WH configurations, different base configurations have varying sensitivities to changes in industrial WH price. For example, base configuration 1 has a greater variation in mean LCOH across WH prices compared to base configuration 17. Generally, base configurations with more technologies or greater installed capacity have lower variation in mean LCOH. Configurations with a CHP also have lower sensitivities. This once again highlights the added value of having multiple technologies in making the system more flexible on the supply side and robust to changes in industrial WH price.

The variations in sensitivity across configurations, indicates that the configuration of a system is not only important in determining its cost and economic risk but also how it responds to variations in the price of industrial WH. Moreover, it is also evident that the price of industrial WH directly influences the mean LCOH of the system configuration.

[7] See Appendix A, Figure A.4 for a figure showing percent change in LCOH with changes in industrial WH price rather than change in €/MWh as shown in Figure 4.4.

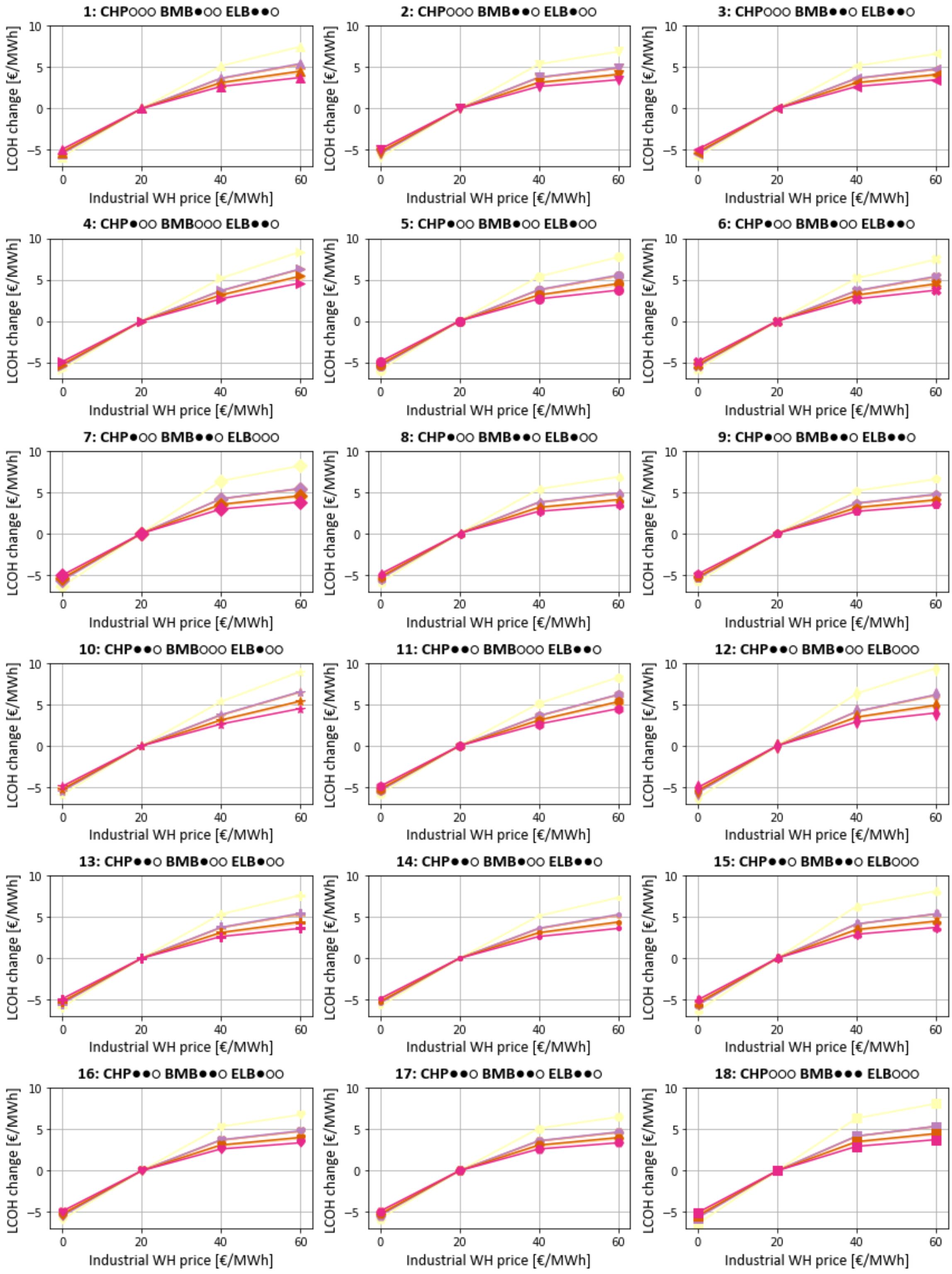

CONFIGURATION LEGEND

Base configuration: CHP, biomass boiler (BMB), electric boiler (ELB) and capacity in MW_{th} (0: ○○○, 33: ●○○, 67: ●●○, or 100: ●●●)

▲ 1: CHP○○○ BMB●○○ ELB●●○ ▶ 4: CHP●○○ BMB○○○ ELB●●○ ◆ 7: CHP●○○ BMB●●○ ELB○○○ ★ 10: CHP●●○ BMB○○○ ELB●○○ ✚ 13: CHP●●○ BMB●○○ ELB●○○ ♥ 16: CHP●●○ BMB●●○ ELB●○○

▼ 2: CHP○○○ BMB●●○ ELB●○○ ● 5: CHP●○○ BMB●○○ ELB●○○ ♠ 8: CHP●○○ BMB●●○ ELB●○○ ⬢ 11: CHP●●○ BMB○○○ ELB●●○ • 14: CHP●●○ BMB●○○ ELB●●○ ● 17: CHP●●○ BMB●●○ ELB●●○

◀ 3: CHP○○○ BMB●●○ ELB●●○ ✖ 6: CHP●○○ BMB●○○ ELB●●○ ⬟ 9: CHP●○○ BMB●●○ ELB●●○ ♦ 12: CHP●●○ BMB●○○ ELB○○○ ♣ 15: CHP●●○ BMB●●○ ELB○○○ ■ 18: CHP○○○ BMB●●● ELB○○○

Ambient and waste heat configuration: industrial waste heat (IWH), datacenter heat pump (DHP), wastewater heat pump (WHP), and/or air heat pump (AHP), with 10 MW_{th} capacity if present

B: IWH D: DHP, IWH F: WHP, IWH H. WHP, DHP, IWH J: AHP, IWH L: AHP, DHP, IWH N: AHP, WHP, IWH P: AHP, WHP, DHP, IWH

Figure 4.4 Sensitivity of the mean levelized cost of heat (LCOH) to variations in industrial waste (WH) prices (expressed as change in mean LCOH relative to the mean LCOH with a WH price of 20 €/MWh), plotted per base configuration.

Sensitivity of standard deviation to industrial WH price

Figure 4.5 presents the sensitivity of the standard deviation in mean LCOH to changes in the industrial WH price, plotted per base configuration. This serves as an indication of the sensitivity of economic risks to industrial WH prices. Unlike for the sensitivity of mean LCOH to changes in industrial WH prices, there is less consistency across configurations.

When comparing configurations to each other, not all follow the same pattern across WH prices. Rather this varies across base configurations and across AH and WH configurations. All configurations have an increase in standard deviation with a decrease in the industrial WH price from 20 to 0 €/MWh. However, changes in the industrial WH price from 20 to 40 or 60 €/MWh has different effects across configurations. Sometimes it results in an increase in standard deviation (see for example plot for base configuration 2), while sometimes it leads to a decrease (see base configuration 11), and sometimes a decrease and then increase (see base configuration 14). Decreases in WH price may lead to increases in standard deviation since scenarios where the WH drops out are relatively more expensive than scenarios where it is present in a scenario where WH is free compared to a scenario where it costs 20 €/MWh. Increases in standard deviation with increases in industrial WH price may be because the WH is used less compared to other sources, and therefore may be affected by variations due to different energy price scenarios. Also, changes in standard deviation are often low moving from and industrial WH price to 20 to 40 €/MWh, especially for configurations with more AH and WH sources, indicating that changes within this price range do not significantly affect how the system performs across energy price and WH cessation scenarios.

In comparing base configurations to each other, it is evident that different configurations have different sensitivity to changes in industrial WH price. The pattern of sensitivity across WH prices varies. For example, for some base configurations the standard deviation is high at a WH price of 0 €/MWh, decreases at WH prices of 20 and 40 €/MWh, and increase again at a price of 60 €/MWh (see base configurations 1 through 9). In contrast other configurations experience a decrease in standard deviation moving from a WH price of 0 to 60 €/MWh (see base configurations 10 and 11). Furthermore, in contrast to average LCOH sensitivity to WH prices, the standard deviation of base configurations with less technologies or lower capacities is generally less sensitive to changes in the WH price. For example, base configuration 1 has lower variation across WH prices than base configuration 14.

When comparing AH and WH configurations to each other, it is apparent they do not follow a consistent pattern in which is more sensitive to changes in industrial WH price like for mean LCOH sensitivity. Rather, this varies across base configurations, and depending on if there is an increase or decrease in the WH price. For example, for base configuration 8 the most sensitive configurations to both a decrease or increase in WH price is AH and WH configuration B. In contrast for base configuration 13, the most sensitive configuration to a decrease in industrial WH price is AH and WH configuration N, while the most sensitive to an increase in industrial WH price are configuration B and F.

Finally, it is relevant to note that standard deviation across all configuration's ranges between -1.72 to 1.32 €/MWh and between -55.89 and 98.36% when expressed a percent change (see Appendix A, Figure A.5 for a figure showing percentage change in standard deviation with changes in WH price). This indicates that variations in the WH price not only have a significant impact on the LCOH as discussed above but also on the economic risk associated with the system. However, the exact effect of changes in industrial WH price on standard deviation, both in terms of magnitude and direction, largely depends on the system configuration being analyzed.

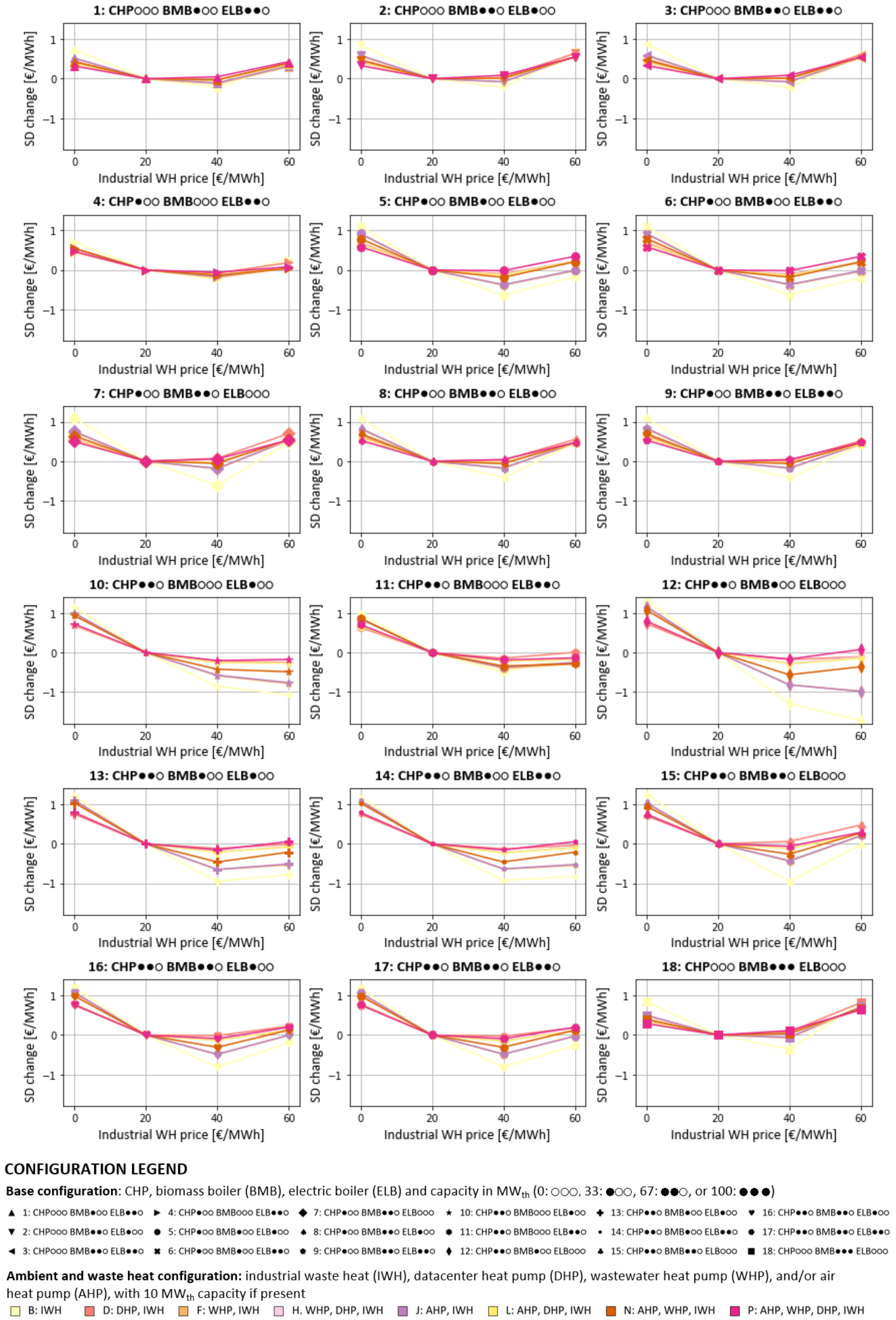

Figure 4.5 Sensitivity of standard deviation (SD) of the mean levelized cost of heat (LCOH) to variations in industrial waste (WH) prices (expressed as change in SD relative to the SD with a WH price of 20 €/MWh), plotted per base configuration.

4.2 Case study

4.2.1 Main results

The weighted average LCOH of the configurations in scenario B1 range from 81.07 to 94.67 €/MWh with a standard deviation of 2.34 to 2.36 €/MWh, those in scenario B2 range from 78.83 to 91.77 €/MWh with a standard deviation of 2.18 to 2.20 €/MWh (Figure 4.6, Table 4.1). The standard deviation across all scenarios is relatively low, ranging between 2.38 and 2.92% of the LCOH, indicating that the economic risk associated with these systems is relatively low. When comparing systems with the same base scenario the addition of a single HP and then both HPs leads to an increase in LCOH but a decrease in standard deviation. This indicates that a greater number of different heat sources in the DH system and the flexibility they offer leads to a reduction in economic risk. Furthermore, though the differences between scenario B1 and B2 are small, each configuration in scenario B2 performs better than its counterpart configuration in scenario B1, having both a lower LCOH and standard deviation. This is largely because the WH from the iron foundry is relatively inexpensive at 20€/MWh, leading to reductions in the mean LCOH. Furthermore, its cost does not vary across price scenarios unlike electricity, biomethane, and biomass prices, resulting in a lower standard deviation. The lower standard deviation of scenario B2 additionally indicates that the uncertainty in future WH availability does not lead to significantly greater economic risk.

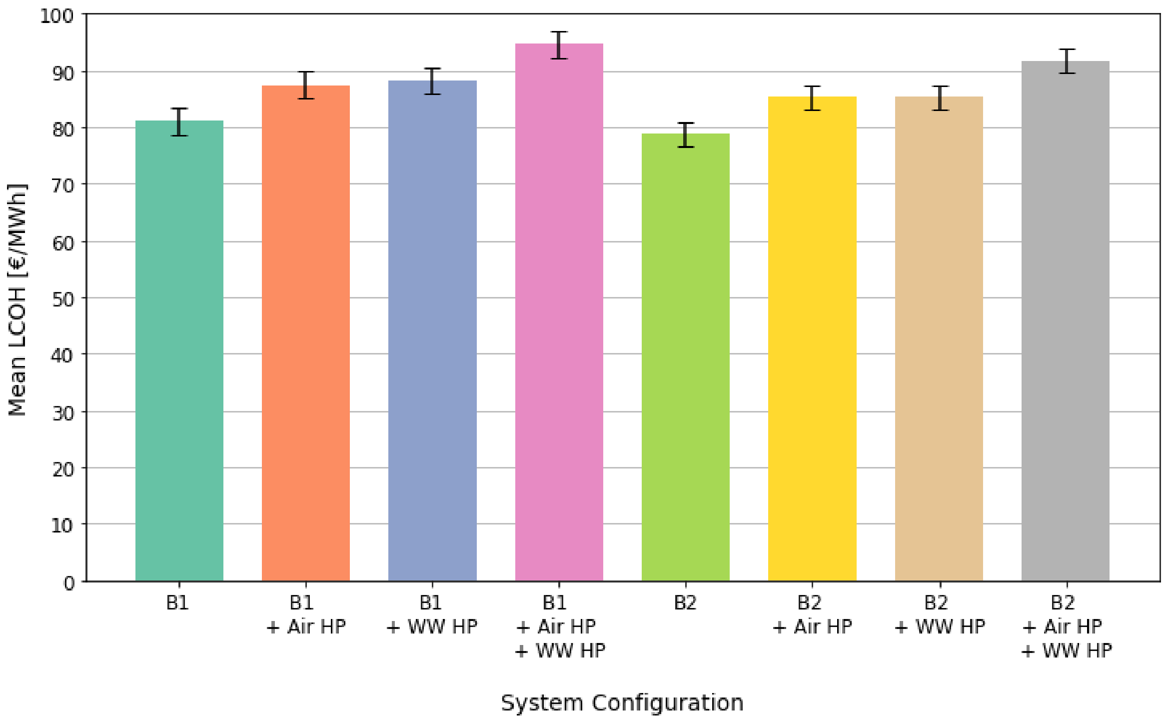

Figure 4.6 Weighted average levelized cost of heat (LCOH) per system configuration in the case study with error bars indicating standard deviation.

Table 4.1 *Weighted average levelized cost of heat (LCOH) and standard deviation (SD) per system configuration in the case study*

	LCOH [€/MWh]	SD [€/MWh]	SD [% of LCOH]
Base scenario 1 (B1): Biomass HOB & CHP			
B1	81.07	2.36	2.92%
B1+ Air HP	87.48	2.35	2.69%
B1 + WWTP HP	88.20	2.35	2.67%
B1 + Air HP + WWTP HP	94.67	2.34	2.47%
Base scenario 2 (B2): Biomass HOB, CHP, and iron foundry WH			
B2	78.83	2.20	2.79%
B2+ Air HP	85.28	2.19	2.56%
B2 + WWTP HP	85.28	2.19	2.56%
B2 + Air HP + WWTP HP	91.77	2.18	2.38%

Figure 4.7 shows the weighted average heat supplied per technology for all system configurations in the case study. The heat production in all configurations is dominated by the biomass HOB, which supplies over 80% of heat in all B1 configurations and over 65% of heat in all B2 configurations. This is due to the large capacity of the biomass HOBs in both B1 and B2, relatively low cost of biomass compared to biomethane and electricity, and the assumed unlimited availability in biomass supply. The CHP can supply heat at a competitive price at high electricity prices due to the revenue from electricity sales. However, this revenue must be large enough to offset the relatively high biomethane prices. Similarly, the HPs supply heat a competitive price when electricity prices are low. Compared to B1 configurations, B2 configurations also have a significant proportion of heat supply (over 20%) from WH from the iron foundry. This is because at a price of 20 €/MWh, the WH from the iron foundry is always less expensive than the biomass HOB, which has an efficiency of 86.4% and therefore a cost ranging from 23.15-40.5 €/MWh across energy price scenarios. In contrast, the CHP has a lower contribution in B2 configurations compared to B1 configurations. This is due to the lower CHP capacity, which is about a third of the CHP capacity in scenario B1, and displacement of CHP heat by the industrial WH.

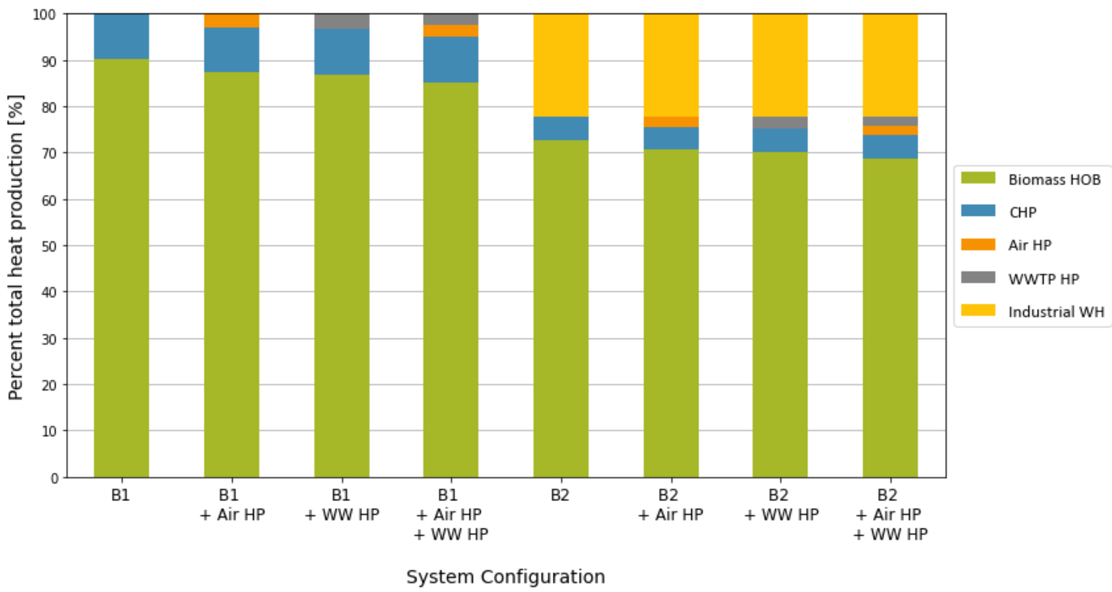

Figure 4.7 Weighted average heat supplied per technology for each system configuration in the case study expressed as the percent of total heat supply

When analyzing the weighted average LCOH of each system configuration broken down into CAPEX and OPEX for each heat supply technology, it is evident that biomass also accounts for the largest share of costs (Figure 4.8). This is to be expected as the biomass HOB is the technology with the largest installed capacity and share of heat production across all configurations. Compared to scenario B1, the biomass HOB CAPEX increases in scenario B2 due to a larger installed capacity, but OPEX decreases as a lower share of heat is supplied by the HOB. For the CHP, OPEX shows the net costs considering electricity revenue as well. The CHP CAPEX and OPEX are smaller in configuration B2 compared to B1, due to a lower CHP capacity and lower production in scenario B2. Furthermore, due to inclusion of WH from the iron foundry in B2, the CHP only operates when its cost is lower than both the biomass HOB and iron foundry WH rather than just the biomass HOB. In scenario B2, the heat provided by the iron foundry comes at a low cost also in terms of CAPEX which is much smaller than for the other heat supply technologies. Interestingly, as HPs are introduced in the B1 or B2 system, the OPEX portion of the LCOH still increases. The variable OPEX of the system decreases as every hour in the one-year simulation the technology with the lowest cost is chosen in the one-year simulation. However, fixed OPEX does not change for the biomass HOB or CHP and is relatively high for the HPs, leading to overall higher OPEX. The CAPEX of the additional HPs also contributes to the higher LCOH in configurations with HPs.

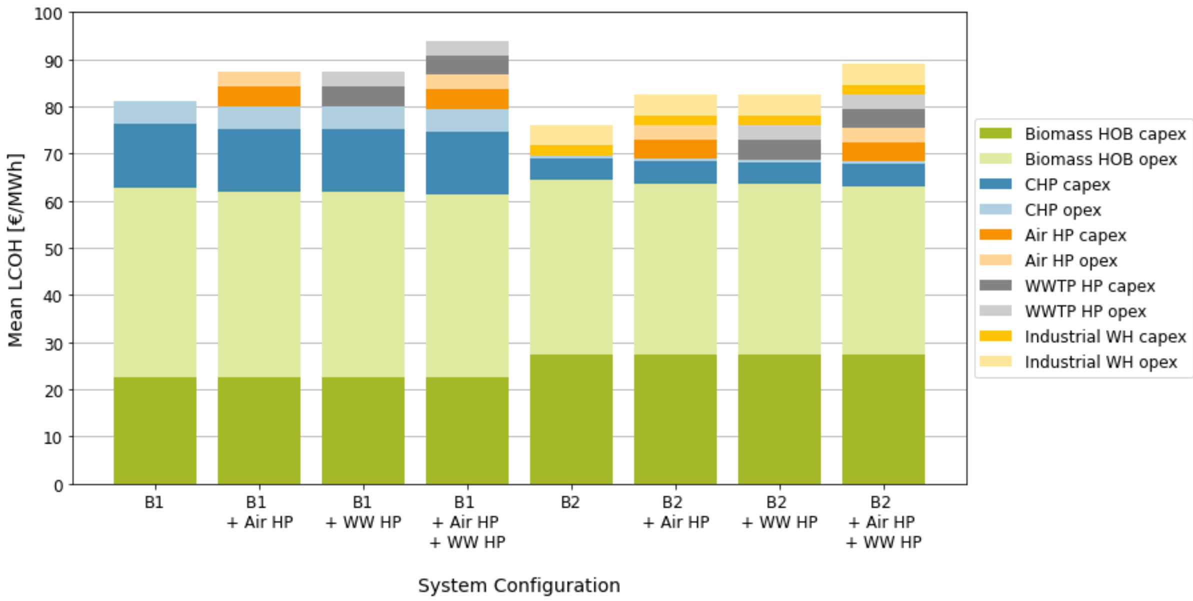

Figure 4.8 Weighted average levelized cost of heat (LCOH) per system configuration in the case study broken down into capital expenditure (CAPEX) and operational expenditures (OPEX) per heat supply technology in the system OPEX costs for the CHP show net cost, accounting for electricity revenues and biomethane cost).

4.2.2 Variation across energy price scenarios

To understand the variation in the techno-economic performance of the DH system configurations studied across energy price scenerios, the heat supply per technology and LCOH was studied across different price lamdas. The plots for system configurations B1 + Air HP + WWTP HP and B2 + Air HP + WWTP HP across eleven price lambdas representing the range of energy price scenaros considered are shown in Figure 4.9. Those for all other system configurations can be found in Appendix B (Figure B.1

and Figure B.2). As energy prices increase, the LCOH increases. This is due to higher OPEX costs as only biomass, biomethane, and electricity prices were varied in energy price scenarions and not investment costs.

For both B1 and B2 systems, heat supply from the biomass HOB decreases as energy prices increase due to higher biomass prices. The higher fuel costs also lead to an overal increase in OPEX from the biomass HOB despite reduced heat production. Similarily, heat production from the both the air and WWTP HPs decreases as electricity prices increase However, as for the biomass HOB, OPEX costs increase despite the reduction in heat output. The decrease of heat production from the HPs is less than that from the biomass HOB since the HPs may still be cost effective in timestpes where electricity prices are low. In contrast, heat production from the CHP increases with the price lambda . This is because with higher electricity prices, electricity revenues increase for the biomethane CHP. This is seen in the reduction in CHP OPEX which shows net costs (biomethane fuel costs minus electricity revenues). For lambda values of 0.905 and 0.995 under the B2 + Air HP + WWTP HP system configuration, CHP OPEX is even negative as a net revenue is achieved. As WH prices are not affected by the energy price scenarios, industrial WH output from the iron foundry and associatated OPEX costs remains relatively constant across price lambdas. Heat output and therefore OPEX increase slightly at first and then reduces as energy prices increase. This is due to the increased attractiveness of operating the CHP due to high electricity revenues. This highlights the importance of the assumption that the industrial WH price is agreed on bilaterally between the WH provider and DH system operator and does not change with energy price scenarios. The stability in WH prices, allows for the WH to continue providing over 20% of the heat supply without OPEX increases despite a higher energy price scenario. It also means the CHP is used in timesteps where it is most favorable economically, when it is cheaper than both the WH and the biomass HOB and not only when it is cheaper than the HOB. This contributes to the lower increase in LCOH as the price lambda increases, as well as to a lower standard deviation associated with the B2 system.

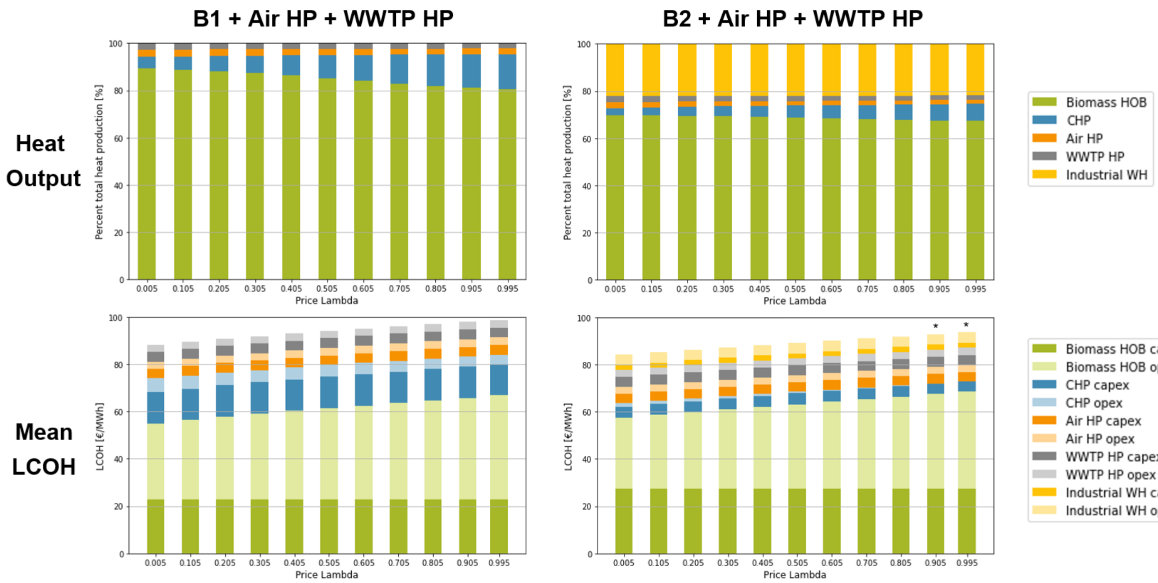

Figure 4.9 Heat output per technology and levelized cost of heat (LCOH) broken down into capital expenditure (CAPEX) and operation expenditure (OPEX) across energy scenarios for system configurations B1 + Air HP + WWTP HP and B2 + Air HP + WWTP HP. The asterisk (*) indicates high price scenarios where the CHP had a net revenue (negative OPEX) which is not shown.

4.2.3 Impact of uncertainty in energy prices and WH availability

Figure 4.10 presents a scatter plot of the price lambda against LCOH and the histogram of weighted LCOH for each energy price scenario and WH cessation scenario modelled for system configurations B1 + Air HP + WWTP HP and B2 + Air HP + WWTP HP. The same plots for all system configurations in the case study can be found in Appendix B (Figure B.3). As also seen in the weighted average LCOH plots above, for both configurations, an increase in the price lambda leads to an increase in LCOH. As the probability of the price lambda is defined by the beta funciton, this pattern is evident in the histogram of LCOH where average LCOH values are more likely than lower or hgiher values. The diagrams for B2 + Air HP + WWTP HP also highlight the impact of the WH cessation scenarios on model outputs. For any given price scenario, scenarios where the WH ceases operation leads to a higher LCOH as it results in a stranded investment and higher operational costs as the relatively low-cost WH is no longer available. This is evident in the vertical spread of the scatter plot as well as the right skewed distribution of the LCOH histogram. However, scenarios where WH ceases operation are less likely to occur than the scenario where WH is availble for the entire study period, indicated by the low frequencey of the upper tail values in the LCOH histogram. The lower standard deviation of LCOH for system configuration B2 + Air HP + WWTP HP compared to system configuration B1 + Air HP + WWTP HP, indicates that the uncertainty in energy prices has a greater impact on economic risk compared to the uncertainty in WH availability. However, as mentioned above, this is also linked to the assumption that the industrial WH price is stable and not affected by energy price scenarios, as well as the low annual WH cessation probability.

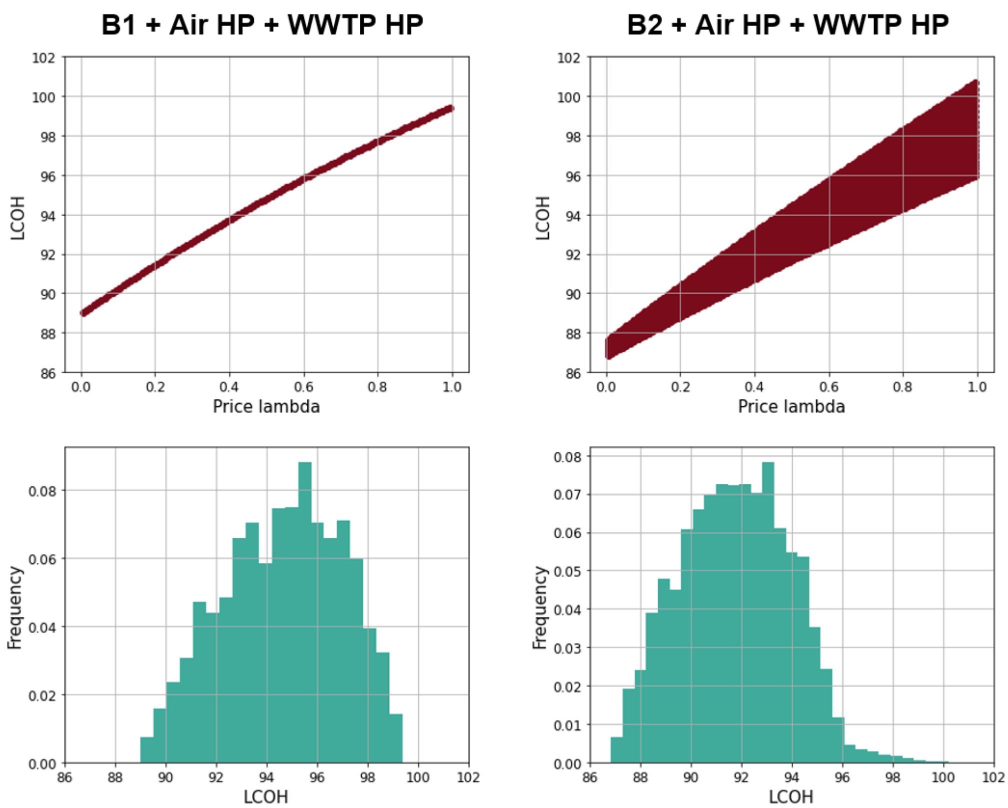

Figure 4.10 Plots showing price lambda vs. LCOH, and histogram of weighted LCOH for scenario B1 + Air HP + WWTP HP and B2 + Air HP + WWTP HP

4.2.4 Hourly heat supply

In analyzing hourly heat supply for an average energy price scenario (price lambda 0.505) across the eight system configurations studied, it is once again evident that the biomass HOB dominates the heat production across all configurations (Figure 4.11). Heat is produced by the CHP in timesteps with high electricity prices due to the revenues from electricity sales. This occurs mainly over the summer and in the fall. WH from the iron foundry is almost always used whenever it is available, with the pattern of availability only during weekdays clearly visible on the chart. The only period where industrial WH is not used is during the summer when production from the CHP is more cost effective and demand for heat is relatively low, so it is not necessary to use both sources. The air and WWTP HPs are used sporadically throughout the year whenever electricity prices are low, making heat production from the HPs economically attractive.

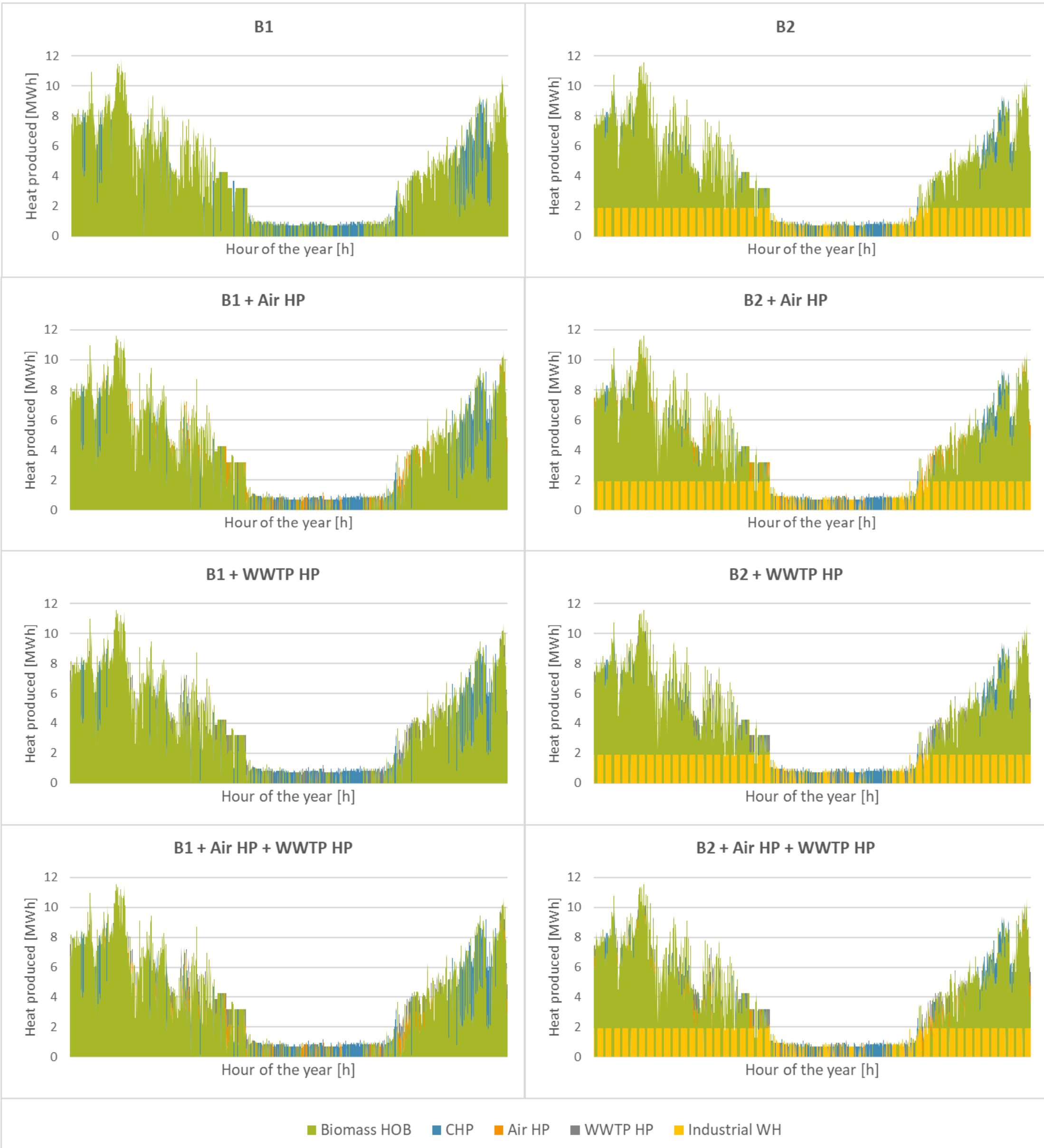

Figure 4.11 Hourly production for the eight system configurations studied for the case study under an average price scenario (price lambda of 0.505) and no waste heat cessation for the iron foundry

4.2.5 Sensitivity to iron foundry waste heat price

Results from the sensitivity analysis of LCOH to changes in the price of WH from the iron foundry are shown in Figure 4.12. As the price of industrial WH increases, so does the LCOH as it leads to a higher OPEX costs from the industrial WH. For WH prices between 0 and 30 €/MWh, an equal increase in WH price results in the same increase in the weighted average LCOH. However, the increase is weighted average LCOH is smaller when WH pries increase from 30 to 40 €/MWh. This is because at a price between 0-30 €/MWh the WH is still one of the cheapest sources in the system, so an increase in WH price leads to an LCOH increase that is directly linked to an increase in WH OPEX costs. However, at a price at 40 €/MWh, heat from the biomass HOB is less expensive than the WH in most energy price scenarios and will be used instead. Therefore, the LCOH is less affected by the increase in WH price. The slope of the increase in LCOH is greatest for system B2, then B2 with a single HP (air or WWTP), and finally for a system with both HPs. This highlights the benefit of having multiple technologies in the system which create flexibility in prices and make the DH system more robust to changes.

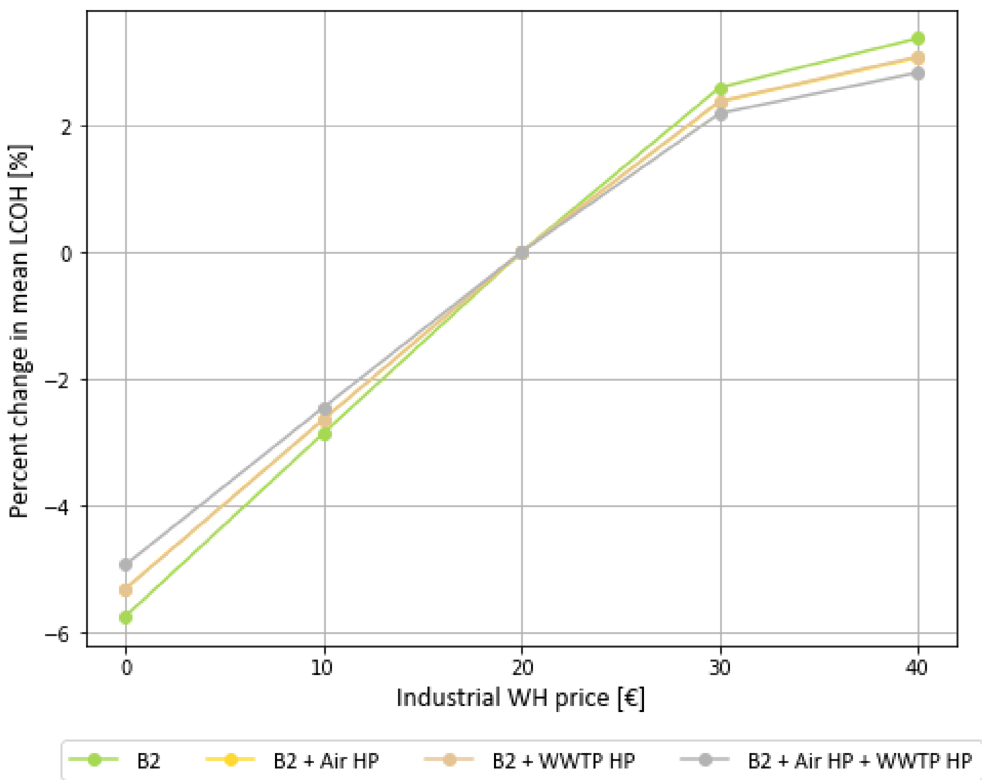

Figure 4.12 Sensitivity of weighted average levelized cost of heat (LCOH) to variations in the iron foundry industrial WH price across system configuration with industrial WH in the case study, expressed as percent change in LCOH relative to the scenario where the WH costs 20 €/MWh. The values for the B2+Air HP are very similar to those of B2+WWTP and therefore not visible on the graph.

In contrast, the standard deviation in LCOH increases with both a reduction and an increase in the price of WH. Moreover, the change in standard deviation across WH prices is nearly identical across the four configurations with industrial WH. When WH prices decrease, standard deviation likely increases because scenarios where the WH ceases operation are now more expensive relative to scenarios where the WH is present. At higher WH prices, standard deviation probably increases since the WH price is competitive with heat from the biomass HOB and other heat sources, and therefore the LCOH varies more with changes in energy prices across the energy price scenarios studied.

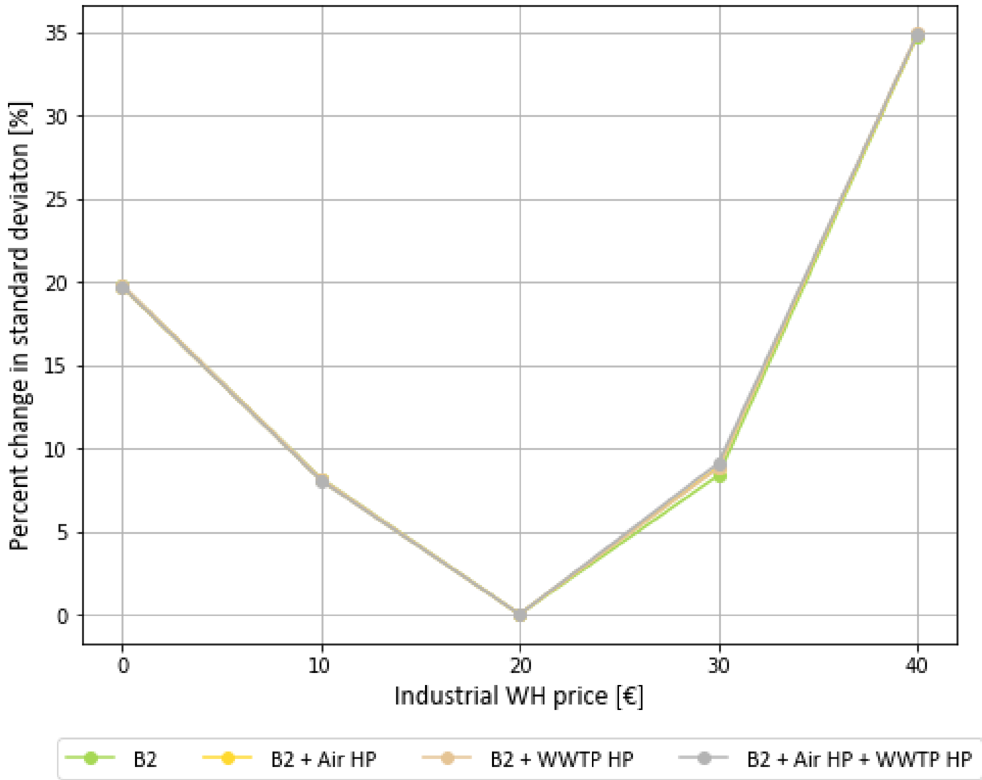

Figure 4.13 Sensitivity of standard deviation in weighted average levelized cost of heat (LCOH) to variations in the iron foundry industrial WH price across system configuration with industrial WH in the case study, expressed as percent change in standard deviation relative to the scenario where the WH costs 20 €/MWh

4.2.6 Impact of biomass restriction

Figure 4.14 and Figure 4.15 show the hourly heat production per technology for system configurations B1 + Air HP + WWTP HP and B2 + Air HP + WWTP HP for the base scenario with no biomass restriction and the five biomass restriction levels considered (low, medium, high, very high, and maximum) under an average price scenario (price lambda of 0.505). Hourly heat production graphs for all system configurations and biomass restriction levels can be found in Appendix B (Figure B.4-B.8). As to be expected, the higher the biomass restriction level, the greater the role of technologies other than the biomass HOB in the system. At the low biomass restriction level, the HPs and CHP are not used simultaneously but rather at alternative times depending on their profitability. The CHP is used when electricity prices and therefore electricity revenues are high, and the HPs are used when electricity prices are low. However, from the medium biomass restriction level onwards the CHP and HPs sometime operate simultaneously as both perform better in the economic ranking compared to the biomass HOB with the artificial price increase. Under the maximum restriction scenario, where the biomass HOB is only used when it is needed to meet demand, the biomass HOB is mainly used in winter months where demand is high. The amount of industrial WH used in the system is B2 + Air HP + WWTP

HP is the only quantity that stays relatively constant, as this technology was already more competitive than biomass in the base scenario and being used to nearly its full capacity (except in times where very low or very high electricity prices made the CHP or HP more competitive and demand was low enough to where the iron foundry WH was not needed to meet demand). Of heat production from sources other than WH from the iron foundry in system B2 + Air HP + WWTP HP, heat from the biomass HOB occupies a relatively larger share than in system B1 + Air HP + WWTP HP. This is because the capacity of the CHP in B2 configurations is only around a third as large as its capacity in B1 configurations. Thus, the amount of heat from the biomass HOB needed to meet demand is relatively larger.

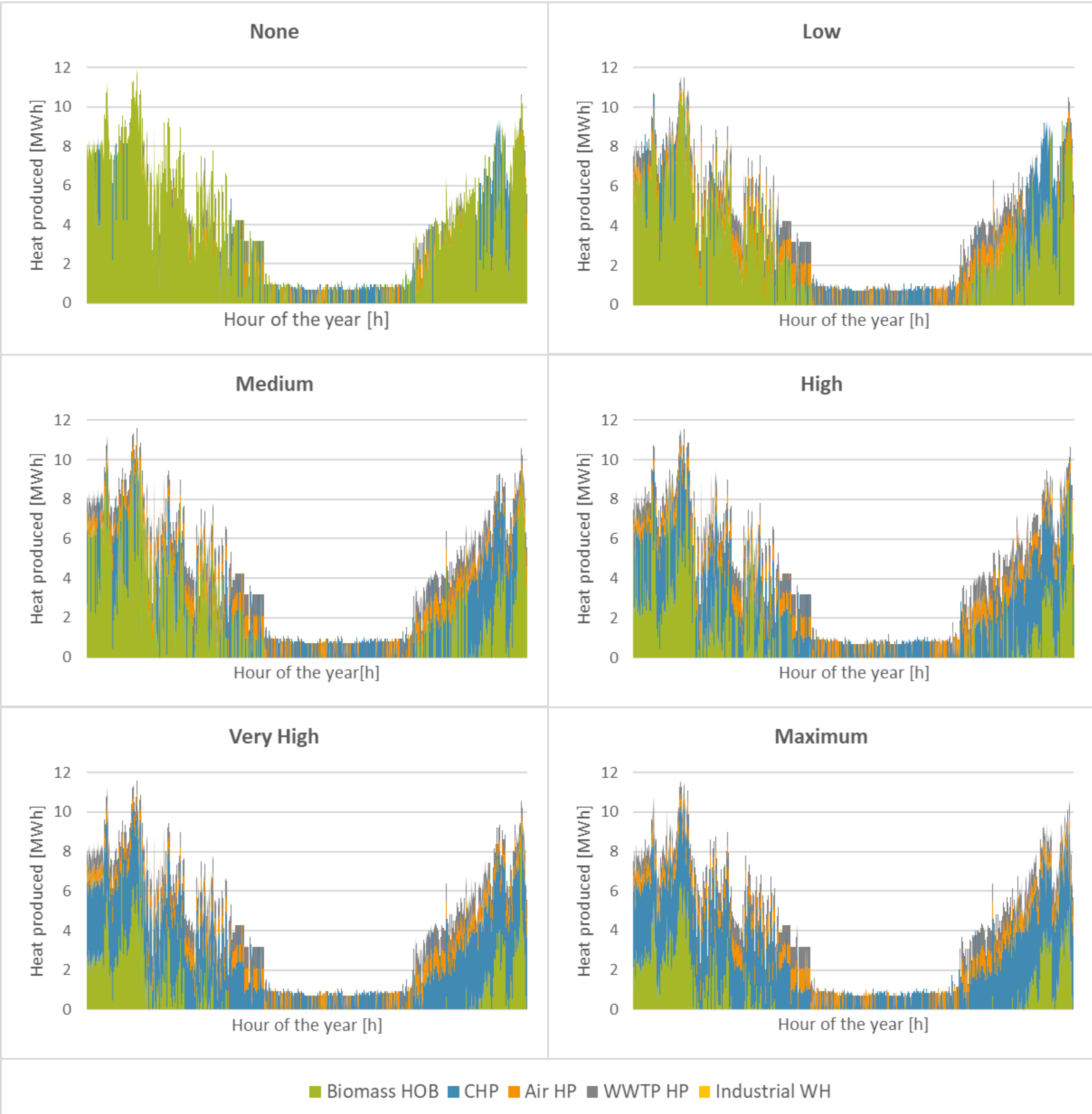

Figure 4.14 Hourly heat production per technology for system configuration B1 + Air HP + WWTP HP in an average price scenario (price lambda of 0.505) under the base scenario with no biomass restriction and the five biomass restriction levels studied: low, medium, high, very high, and maximum.

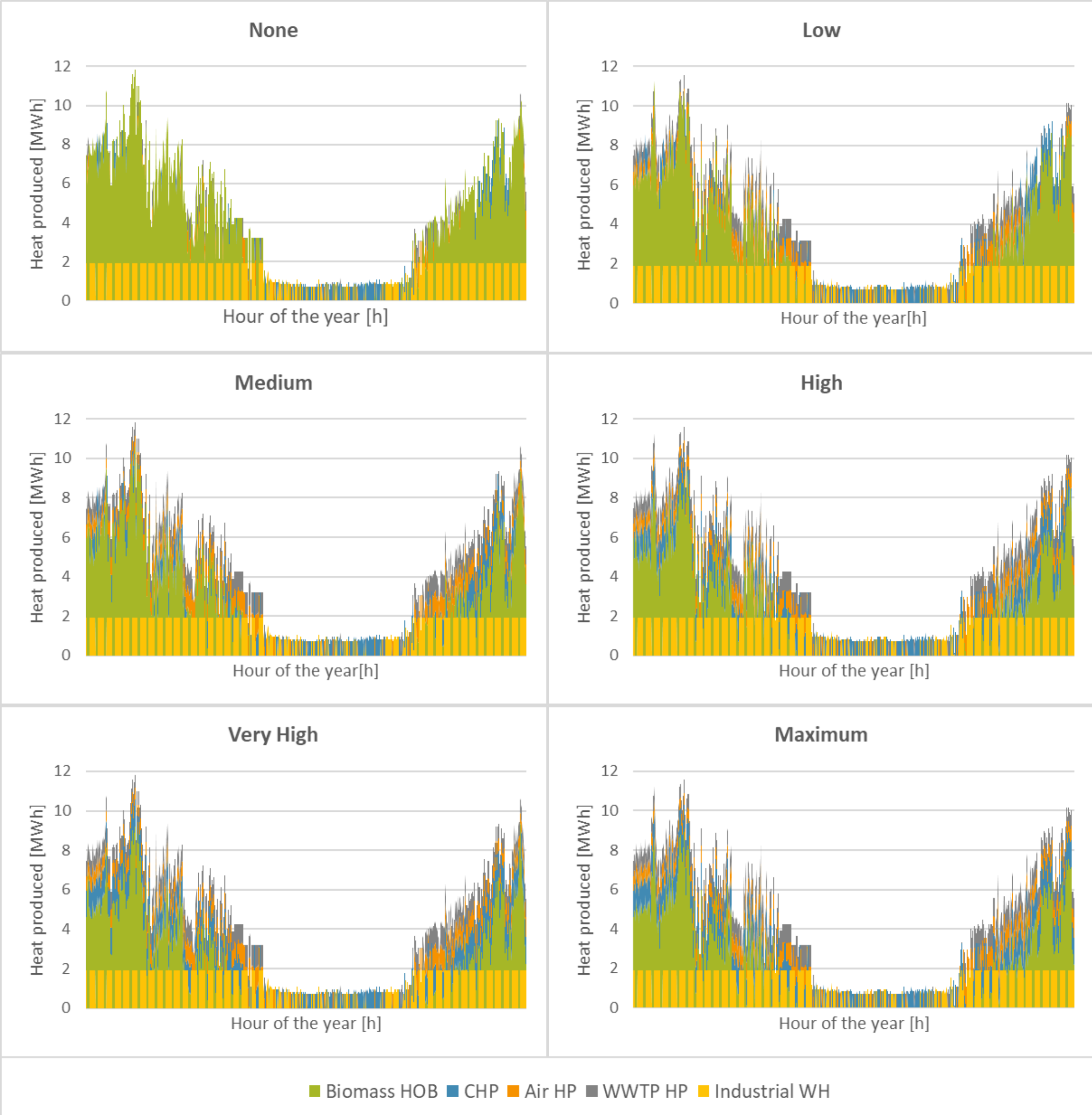

Figure 4.15 Hourly heat production per technology for system configuration B1 + Air HP + WWTP HP in an average price scenario (price lambda of 0.505) and no waste heat cessation for the iron foundry under the base scenario with no biomass restriction and the five biomass restriction levels studied: low, medium, high, very high, and maximum.

To further understand the effect of biomass restrictions on LCOH, the share of heat production from the biomass HOB for each configuration and biomass restriction level was calculated and compared to the mean LCOH of that system (Figure 4.16[8]). As the biomass share decreases, the mean LCOH of the system increases. This is because the relatively low-cost biomass is no longer available and instead relatively more expensive technologies need to be used (such as the CHP and HPs). At the maximum biomass restriction level, the biomass HOB share reaches a minimum, which is the minimum amount

[8] See Appendix B, Figure B.9 for the same figure plotting biomass share against mean LCOH but with error bars showing standard deviation in mean LCOH.

of biomass needed to always meet demand. This minimum is defined based on the capacities of the technologies in the system. For B2 configurations, this minimum share is higher as the CHP capacity is smaller and the biomass HOB capacity is larger than for B1 configurations. When comparing configurations to each other, it becomes evident that as the biomass share decreases, configurations with HPs become more competitive. For example, for configurations in scenario B1, configurations with one HP (B1 + Air HP and B2 + WWTP HP) become more attractive than a configuration without a HP (B1) at a biomass HOB share of around 65%. The configuration with both HPs (B1 + Air Hp + WWTP HP) becomes more attractive than a configuration without HP at a biomass HOB share of around 52% and then a configuration with one HP at a biomass HOB share of around 45%. Configurations under scenario B2 follow a similar pattern. This shows the benefit that a system configuration with more technologies under uncertainty in future developments, in this case the future development of biomass availability.

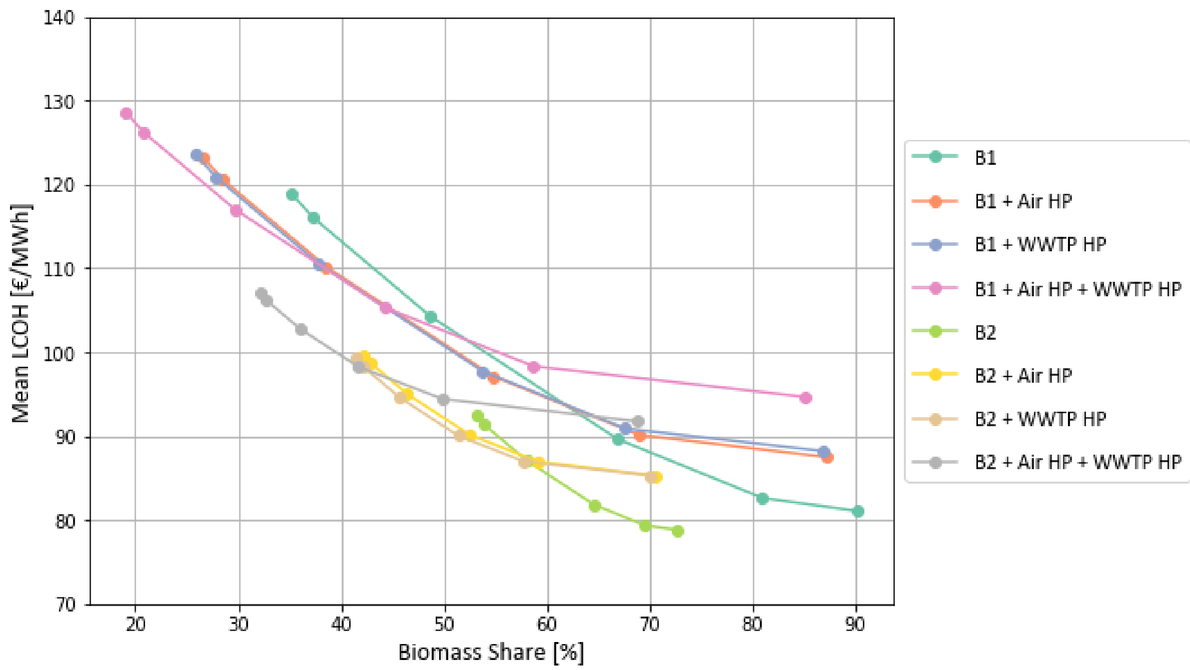

Figure 4.16 Mean levelized cost of heat (LCOH) compared to the share of heat production from the biomass HOB as a percent of total heat production across the eight configurations studied for the case study. Each of the points modelled per system configuration represents a biomass restriction level (none, low, medium, high, very high, and maximum when moving from high biomass share to low biomass share).

5 DISCUSSION

5.1 SYNTHESIS OF KEY FINDINGS

In comparing the results from the general model and case study, it is possible to discern commonalities across key research outcomes:

1. Techno-economic performance is strongly influenced by the system configuration.

Both in the general mode and case study, it is apparent that the system configuration plays a key role in determining the average cost and economic risk of the modelled DH systems. This is not only evident in the wide variation in mean LCOH and standard deviation across system configurations, but also in their varied response to changes in WH prices and biomass availability.

In the general model, the least expensive configuration has a 60% lower mean LCOH relative to the most expensive configuration (with an absolute reduction of 82.12 €/MWh from an LCOH of 137.00 to 54.88 €/MWh). Similarly, the configuration with the lowest economic risk has an 89% lower standard deviation than the configuration with the highest risk (with an absolute reduction of 7.83 €/MWh moving from a standard deviation of 8.83 to 1.00 €/MWh). This highlights the magnitude of the influence of system configuration on both average cost and economic risk.

This is also evident in the case study, albeit at a lower magnitude in part due to the lower variation across system configurations modelled in the case study. The least expensive configuration has a 17% lower mean LCOH relative to the most expensive configuration (with an absolute reduction of 15.84 €/MWh from an LCOH of 94.67 to 78.83 €/MWh. Similarly, the configuration with the lowest economic risk has an 8% lower standard deviation than the configuration with the highest risk (with an absolute reduction of 0.18 €/MWh moving from a standard deviation of 2.36 to 2.18 €/MWh)

2. There is a tradeoff between average cost and economic risk.

Especially in the general model, a tradeoff exists between minimizing average system costs and minimizing system risks. Here, a clear pattern emerges which transitions from system configurations with a low mean LCOH and high standard deviation to configurations with high mean LCOH and low standard deviation. It is also evident in the case study: in both B1 and B2 configurations, as more HPs are added to the system, mean LCOH increases but standard deviation decreases. The configurations with high costs and low risks are generally those with more technologies and greater installed capacity. It is notable that configurations with low cost and high risk may still perform better than the those with high cost and low risk even when the economic risk is accounted for. For example, in the case study, the worst case LCOH for configuration B1 which has low cost and high risk (calculated as mean LCOH plus the standard deviation: 81.07 + 2.36 = 83.43 €/MWh) is still lower than the best case LCOH for configuration B1 + Air HP + WWTP HP which has high cost and lower risk (calculated as mean LCOH minus the standard deviation: 94.67 - 2.34 = 92.33 €/MWh).

3. Industrial WH is beneficial to the techno-economic performance of DH systems.

Under the assumptions made, the inclusion of an industrial WH source in the DH system leads to a reduction in cost and often also a reduction in economic risk. In comparing AH and WH configurations across base configurations in the general model, configurations with industrial WH almost always had a lower cost than configurations without, and in over half the base configurations, also a lower standard deviation, with the difference being very marked in some cases. In the case study, all base scenario 2 configurations, which have WH from the iron foundry, have a lower LCOH and standard deviation compared to their counterpart configuration under base scenario 1. This is because the industrial WH serves as a stable, low-cost heat source across energy price scenarios. The reduction in standard deviation despite the presence of industrial WH and the associated uncertainty in its future availability, also indicates that the WH cessation scenarios have a smaller influence compared to energy price scenarios.

4. Assumptions related to modelling of industrial WH are important.

The above-mentioned benefits of industrial WH in DH systems are largely connected to the assumptions made concerning industrial WH. Specifically, these are: the relatively low industrial WH price, the lack of variation in the price of industrial WH across energy price scenarios, and the relatively low annual WH cessation probability. The relatively low cost and stability across energy price scenarios contribute to both the lower mean LCOH and standard deviation, while the low WH cessation probability contributes to the low standard deviation. Thus, it is important to recognize the implications of these assumptions and their weight in influencing the model outcomes.

This was considered through the sensitivity analyses concerning industrial WH prices, which indicated that the WH price directly influences LCOH and standard deviation. Specifically, the sensitivity analysis of LCOH to WH price in the general model and case study present the same patterns:

- An increase in WH price leads to an increase in mean LCOH,
- The increase in mean LCOH is initially steeper for the same change in WH price due to increased OPEX of the industrial WH, but then flattens out due to competition with other heat sources at higher prices and the replacement of WH with cheaper alternatives, reducing the impact of increased WH OPEX costs, and
- Systems with a greater number of HPs are less sensitive to WH prices.

In relation to standard deviation, the sensitivity analysis in both the general model and case study indicated that a reduction in industrial WH price relative to the base price of 20 €/MWh increased standard deviation. However, the effects of an increase in industrial WH price varied.

5. High abundance and low prices of biomass reduce average costs.

In both the general model and case study, it is evident that the assumed unlimited availability of biomass (only limited by the capacity of the biomass HOBs) and relatively low biomass prices (ranging from 30-45 €/MWh and 20-35 €/MWh in the general model and case study respectively) led to lower average costs for the DH systems. In the general model, base configurations with only the biomass HOB and electric HOB (base configurations 1-3) or only a biomass HOB (base configuration 18) have the lowest mean LCOHs across all system configurations studied. In the case study, there is a heavy reliance on biomass across all configurations, with the biomass HOB supplying over 80% of heat in all B1 configurations and over 65% of heat in all B2 configurations. This is due to the large capacity of biomass HOB, assumed unlimited fuel availability, and relatively low fuel cost. Moreover, when looking at the biomass restriction scenarios, as biomass use increase, mean LCOH decreases for all configurations analyzed. This highlights how the assumed high abundance and low cost of biomass leads to lower average costs.

6. Increased supply side flexibility reduces economic risks.

Greater supply side flexibility though a larger and more diversified heat source portfolio leads to increased robustness of the DH system in the face of future uncertainties, not only in relation to energy prices and WH availability, but also WH prices and biomass availability. This is evident in the general model as:

- Base configurations with more technologies and/or greater installed capacities have lower standard deviation and lower variation across AH and WH configurations,
- Configurations with more HPs are less sensitive to changes in WH price, and
- The AH and WH configurations with lowest standard deviation across most base configurations is AH and WH configuration P which has all AH and WH sources.

The benefits of supply side flexibility are evident in the case study in that:

- Inclusion of HPs or industrial WH lead to a reduction in standard deviation,
- B2 configurations with more HPs are less sensitive to changes in WH price, and
- As biomass restriction increases, systems with more HPs become competitive and have a lower mean LCOH.

7. AH and WH supply technologies generally lead to lower economic risk.

The presence of AH and WH sources in the system configuration results in lower standard deviation. In the case study, B2 configurations (with industrial WH) have a lower standard deviation than B1 configurations (with no industrial WH). Furthermore, within the B1 or B2 scenario, standard deviation is lower the more HPs are in the system. In the general model, configurations with AH and/or WH sources generally have lower standard deviation compared to configuration A, which has no AH or WH sources. However, this is not always the case as the base configurations are also influential and the effect of including additional AH and WH sources in the DH system varies across base configurations. Additionally, AH and WH configuration C, which consists of the datacenter HP, has a notably high standard deviation across base configurations.

There are also differences that become apparent when comparing the results of the general model and case study which are noteworthy:

8. Input data strongly influences results.

The input data for energy prices, CAPEX and OPEX varied between the general model and case study and had a direct impact on the results. For example, configurations with additional HPs in the case study even saw an increase in operational costs due to high fixed OPEX costs. Similarly, the range for biomass prices was lower in the case study (20-35 €/MWh) compared to in the general model (30-45 €/MWh) making the biomass HOB the dominant heat source in the general model. Furthermore, electricity prices were different in the two models, both in terms of absolute values but also the annual profiles (e.g., the general model has high prices in winter while the case study has high prices in summer). This directly influenced the profitability and therefore operating hours of the CHPs and HPs, and thus had a significant influence on model outcomes.

9. Inclusion of HPs does not always reduce costs.

Although industrial WH led to cost reductions in both the general model and case study, the effect of AH with HPs on the mean LCOH varied. While in the general model, the inclusion of HPs in the system generally resulted in a reduction in mean LCOH, in the case study, the inclusion of an additional HP always led to an increase in mean LCOH. In the case study, there was even an increase in OPEX costs with the addition of HPs due to high fixed operational costs. However, it is notable that in the general model, in the five base configurations where AH and WH configuration A (no AH or WH) is not the most expensive, the AH and WH configurations that are more expensive are AH and WH configurations M (air HP and WWTP HP), O (air HP, WWTP HP, and datacenter HP), and occasionally I (air HP). This shows that across some base configurations in the general model, AH and WH configurations with HPs were also more expensive. This indicates that the effect is dependent on what other technologies are in the system. Furthermore, it is important to note that HP operation and performance depends on the electricity price and heat demand profile model inputs. This is also an influential factor for the difference in HP performance between the general model and case study.

10. HP COP strongly influences average cost.

Results of the general model indicate that the HP COP has a strong influence on average cost. For each base configuration, when comparing AH and WH configurations I (Air HP), E (WWTP HP) and C (Datacenter HP), which have progressively higher average COPs, the mean LCOH decreases with increasing COP. Specifically, the average COP of the air HP, WWTP HP, and Datacenter HP was 2.52, 2.84, and 4.12, respectively. The same pattern is also seen when comparing AH and WH configurations J (Air HP and industrial WH), F (WWTP HP and industrial WH) and I (Datacenter HP and industrial WH). This is to be expected as a higher COP means the HP can provide more heat for the same amount of electricity (same cost). However, in the case study, very little to no variation is seen in the mean LCOH of system configurations with the air HP compared to that of those with the WWTP HP. This is probably related to the low variation in average COP across the two HPs in the case study (with an average COP of 3.10 and 3.21 for the air HP and WWTP HP respectively), as well as the influence of OPEX and CAPEX data which was similar for the two HPs in the case study. Additionally, the variation in electricity price profiles between the general model and case study also has an influence on the cost of the HPs.

11. Datacenter HP leads to high economic risk.

Another difference between results is that in the general model, AH and WH configuration C (datacenter HP), often has one of the highest standard deviations when comparing AH and WH configurations across base configurations. In contrast, in the case study, the additional inclusion of all AH or WH sources analyzed (air HP, WWTP HP, and iron foundry WH) all led to a reduction in standard deviation compared to a system with no AH or WH sources. However, the datacenter HP is a unique source as it is impacted both by the WH cessation scenarios and energy price scenarios. Furthermore, it has a high COP and can therefore offer relatively cheap heat at low electricity prices compared to a system without it.

12. Impact of additional AH and WH sources varies with system configuration.

Additionally, in the general model, there was a variation in the effect of AH and WH configurations on the mean LCOH and standard deviation across base configurations. However, in the case study, the HP variations on the two base scenarios analyzed had a similar effect both on mean LCOH and standard deviation. However, this is largely due to a much larger quantity and variety of system configurations analyzed in the general model. In the case study, the two base scenarios were similar in that both included of a large biomass HOB and CHP. Furthermore, it is important to note that in the case study, base scenario 2 already included industrial WH as one of the heat sources in the system configuration, and only the addition of HPs (AH) was varied equally across the two scenarios. Thus, the variation across base configurations in the general model and base scenarios in the case study are not necessarily directly comparable.

5.2 Results in the context of literature

This thesis provides a techno-economic analysis of the employment of AH and WH as heat sources for DH networks. It compares various types of AH and WH sources and the performance of decarbonized DH systems with and without them. Furthermore, it accounts for the economic risk arising from uncertainty in the future development of energy prices and WH availability. It is unique relative to other studies in that it focuses specifically on AH and WH, analyzes these sources on a general level, and quantifies the economic risk of DH systems with AH and WH. While the focus of this analysis is different from other studies, it is important to consider the results in the context of existing literature on the techno-economic performance of AH and WH sources, either individually or as part of a DH system, or uncertainties and economic risk within DH systems. This section provides this contextual analysis.

In conducting this comparison, it becomes evident that there are various points of agreement between the key findings of this work and existing literature:

Both the general model and case study indicate that the DH system configuration has a strong influence on average cost and economic risk. The **importance of the DH system configuration** is supported by the results of the various studies which also compare different technology combinations and find that techno-economic performance varies across them. For example, Kontu et al. found varying average heat production costs across DH systems with HPs depending on the DH network size and the other technologies found in the system [4]. As another example, Yang et al. compared the LCOH of a DH system supplied by a ground source HP, natural gas boiler, biomass boiler, or electric boiler with and without thermal storage, and found the LCOH was dependent on the system configuration [20].

The **tradeoff between average cost and economic risk** found in the results of this work, is mirrored in the results of Kienzle et al. [42]. Specifically, they found that the inclusion of storage, DSM or both in an energy hub led to increased investment costs but also reduced the economic risk (measured as percent standard deviation in the system's present value).

Additionally, the **cost effectiveness of WH** as a heat source for DH systems, is widely present in techno-economic analyses on WH. Bühler et al., Pakere et al., Morandin et al., and Su et al. all found WH sources in DH systems to be profitable [5], [6], [22], [23]. Pakere even found a lower LCOH for systems with WH compared to the reference scenario without, just like in the results of the case study and general model for configurations with industrial WH. Similarly, Morandin found WH from the petrochemical sector to be profitable even with an assumed decrease in availability due to greater internal heat recovery, just as configurations with industrial WH were profitable despite the WH cessation scenarios modelled in this work. However, Spirito et al., found that DH systems with steelwork WH had higher investment costs due to the investment in the HPs that needed to be coupled to the steelwork [21].

The **benefits of increased supply side flexibility** for having DH systems that are resilient to uncertainties in the future development of key factors, indicated by the results of both the general model and case study, is also widely reported in the literature. Fitó et al.'s results showed that a centralized DH heating system with various supply sources was more robust to changes in heating demand, HP COPs, and carbon constraints compared to a decentralized individual heat system with decentralized PV and HPs [3]. Similarly, Marx et al. found that an interregional DH network was more robust compared to an individual heating system(evidenced in a lower spread in LCOH). This was because the DH network could make use of different technologies in the face of varying electricity prices depending on which was the most cost effective [18]. Maribu and Fleten argue that CHPs are attractive heat sources because of their ability to respond to high electricity prices [27]. This is directly evident in comparing heat production share across energy price scenarios in the case study (see section 4.2.2). As energy prices increase, the operation of the CHP increases and, in some scenarios, it even makes a net revenue due to high electricity prices. In addition, studies have shown that supply side flexibility in DH systems is not only beneficial for the heating system but also the electricity system. Both Fambri et al. and Østergaard et al. find that through coupling the electricity and heat sectors, HPs can bring additional flexibility to the electricity grid and increase renewable energy integration, which will be increasingly relevant with a greater number of intermittent renewable electricity sources in the future [7], [9].

The **importance of energy prices and input data**, highlighted by differences between the general model and case study, as well as the greater weight of energy price scenarios compared to WH cessation scenarios in influencing standard deviation, is also reflected in the findings of Zhang et al. [35]. Specifically, they found that the performance of DH systems was most sensitive to changes in heat demand and electricity prices while that of individual heating systems was most sensitive to equipment efficiency and investment costs. The importance of electricity prices for DH systems links to the energy price scenarios and maximum and minimum electricity price profiles included in the models, while that of efficiency and investment costs to input data on technical and economic parameters.

Studies on the integration of HPs in DH networks found that the **COP plays a key role in determining operation and costs associated with HPs**. In analyzing the performance of drinking water, WWTP and sea water HPs in Copenhagen's DH network, Bach et al. found that lower COPs led to higher operational costs and reduced operation [8]. Furthermore, Fitó et al. found that alongside heating demand, HP COP was one of the two parameters with the greatest effect on total cost of the heating systems analyzed [3]. This is also seen in the general model since for each base configuration, AH and WH configurations with just an air HP, WWTP HP, or datacenter HP (which have a progressively higher average COP) have a progressively lower mean LCOH. The same pattern is evident for AH and WH configurations with industrial WH and just an air HP, WWTP HP, or datacenter HP.

The **variation in economic attractiveness of system configurations with HPs**, found in comparing the general model and case study, as well as comparing different AH and WH configurations within the general model, is reflected in the lack of consensus on the profitability of HPs in existing literature. For example, while Fambri et al. found that groundwater-based HPs in Turin's DH network not only help balance the electricity distribution network but are profitable even without any incentives for flexibility, Østergaard et al. found that a DH system with seawater HPs and storage increased renewable energy integration but were less profitable compared to a biomass based DH system [7], [9]. Kontu et al.'s results indicate that HPs are more profitable in small DH systems with just a HOB than in medium- to large-scale DH systems with HOBs and CHPs [4]. This variation in profitability depending on system configuration and size is also seen in the wide variation in mean LCOH across configurations in the general model. Furthermore, Kontu et al. found that HPs reduce variable costs in all configurations studied. This is reflected in the general model, where AH and WH configurations with HPs often have a lower mean LCOH relative to a system with no AH or WH, indicating that reductions in OPEX associated with the HPs outweigh the additional CAPEX costs. However, the case study indicated higher average costs for systems with HPs.

Finally, regardless of exactly which input parameters or technologies were varied, studies with a focus on uncertainty modelling, agree that **uncertainty modelling allows for the inclusion of more information and knowledge, as well as the quantification and consideration of economic risks** associated with heating technologies and systems (see section 2.2). Furthermore, the failure to account for uncertainty can lead to an overestimation of potential cost savings[29]. The importance and value of uncertainty modeling is also apparent in the results of this thesis as LCOH varies across energy scenarios and WH cessation scenarios. This demonstrates that these parameters have an impact on the techno-economic performance of DH systems and that the uncertainty associated with their future development leads to an economic risk. Moreover, the magnitude of this risk, measured through the standard deviation, varies widely across configurations in the general model and not accounting for them may lead to an underestimation of mean LCOH. It is therefore important to take these uncertainties into account in designing resilient DH decarbonization strategies.

There are also instances where the results of the study do not agree with those within the literature:

Firstly, there were differences in the perceived **relationship between HPs and industrial WH**. Yuan et al. argued that there is a tradeoff between HPs and industrial WH because HPs support renewable energy integration in the electricity grid but have high costs while industrial WH does not lead to greater renewable energy integration but has lower costs [17]. Although, this study did not consider renewable integration as a KPI, results from the general model do not show a tradeoff between HPs and industrial WH in terms of cost. Rather, a mix of the two leads to a decrease mean LCOH. This is evident that AH and WH configurations with both industrial WH and HPs always perform better than AH and WH configuration A which has no AH or WH. However, in the case study industrial WH reduces mean LCOH while HPs increase mean LCOH. Nonetheless, results from both the general model and cased study indicate a reduction in economic risk is associated with the combination of both heat sources, with AH and WH configuration P (air HP, WWTP HP, datacenter HP and industrial WH) often having the lowest standard deviation across base configurations in the general model, and the system with the iron foundry WH, air HP and WWTP HP having the lowest standard deviation in the case study.

Secondly, results regarding the **economic risk associated with a datacenter HP** in DH systems varied from those of Volodina et al. Specifically, they found that a DH system with a datacenter HP was more robust than a system with a CHP or a CHP and datacenter HP [44]. In contrast, results from the general model indicate that AH and WH configuration C (datacenter HP) often has the highest standard deviation across base configurations. However, while Volodina et al. considered uncertainty in energy prices and heat demand, this work considers uncertainty in energy prices and WH availability. The uncertainty in the datacenter's future availability increases the economic risk associated with it, which is not reflected in Volodina et al.'s model.

5.3 Limitations

This section discusses limitations identified regarding this thesis. First limitations pertaining to the input data are considered, followed by those related to the model, and finally, other general limitations are addressed.

5.3.1 Input Data

General model

Regarding the input data for the general model, technical and economic input data for the heat supply technologies considered was mainly sourced from the DEA's catalogue on Technology Data for Generation of Electricity and District Heating. This ensured consistency across assumptions for the technologies. However, the DEA data is often based on DH networks with an 80°C supply and 40°C return temperature while the supply temperature of the DH network modeled in the general model ranged between 80-100°C. Furthermore, the DEA catalogue only has data on HPs with air, excess heat (cooling water cooled from 25 to 15°C), and seawater. Therefore, data on an excess heat HP was used as a proxy for the WWTP HP and datacenter HP. This means that variations in investment, fixed O&M, and other variable O&M costs that arise from sourcing heat from a WWTP compared to a datacenter, are not reflected in the model. Furthermore, the DEA catalogue did not have data on heat recovery from industrial WH. This means data was collected from a different source which may result in differences in underlying assumptions. Furthermore, investment costs for the industrial WH were not split between equipment and installation costs and there was no value given for additional variable O&M costs.

Case study

Regarding input data for the case study, projections of hourly profiles for heating demand, air temperatures, and DH temperatures for 2050 were not available. Rather, 2021 values were used since the DH network operator provided hourly demand and DH network temperatures for this year and using air temperature values for the same year reflected the correlation between air temperature and heat demand. However, this does not reflect changes in air temperatures and heat demand that will occur due to climate change. Moreover, since only daily air temperature averages were available for the case study location, hourly data from a nearby town was used. Similarly, only estimated monthly averages for the WWTP effluent temperature were available, which leads to a less accurate depiction of the WWTP HP. Additionally, since projections for electricity prices in 2050 were also not available, 2022 hourly day ahead electricity prices were used. Although this can serve as a proxy for future electricity prices for electricity networks with a high share of intermittent renewable energy prices due to the large variation in electricity prices in 2022, it may not be the most accurate estimate. Furthermore, the correlations between electricity prices and weather are not reflected in the model, as it is a different year than the air temperature data.

WH cessation probability

Finally, for both the general model and the case study, the probability of WH ceasing to be available is not directly measurable. Therefore, the probability that a company goes bankrupt each year was calculated based on historical data and used as a proxy. However, this does not account for variations across sectors and may not accurately reflect the probability of WH cessation scenarios occurring.

5.3.2 Model

Limited number of technologies and configurations

A key conclusion from this work is that technical and economic performance is strongly influenced by the system configuration. Thus, one of the main model limitations is that only a limited number of configurations and technologies were considered. The inclusion of additional technologies and system configurations would provide even further insight into the average cost and economic risks associated with the incorporation of AH and WH sources in DH systems, as well as key patterns and influential factors. Especially the inclusion of large scale seasonal thermal storage would be interesting because it greatly increases the flexibility of the DH system and can help optimize the use of AH and WH sources and maximize the benefits they provide. For example, HPs could be used to charge the storage over the summer when electricity prices are low due to high solar energy production, and the stored heat could be used in the winter months with high heating demand. Furthermore, the impact of including additional renewable heat supply technologies such as geothermal or solar thermal energy would also be relevant to consider. Additionally, the model did not include a biomethane boiler and the electricity share of the CHP was fixed. This resulted in limitations since in timesteps with low electricity prices but high heat demand, the CHP still had to operate to meet demand, even if producing electricity was unprofitable. Consequently, the CHP plant incurred losses from selling electricity at low prices. In such situations, it would be advantageous to have a biomethane boiler so that the biomethane can be used solely to produce heat and no losses are made from electricity production.

Simple representation of technologies

Another limitation of the model is the simple representation of technologies. This was necessary to minimize the model runtime and enable the risk assessment through modelling of all WH cessation scenarios for all energy price scenarios. However, it also limited the accuracy of the model. For example, technology ramp up and ramp down rates, as well as minimum runtime or downtime were not modelled, even though these are important considerations for the operation of heat supply technologies in DH networks. Furthermore, the electricity share of the CHP was fixed, which limited the CHP's optimal operation as explained previously. Also, the maximum power output from HPs was calculated based on the HPs electric capacity and COP from temperature differences between the heat source and the DH network supply temperature, not on the flow rate of water through the HP.

Additionally, the general model included representative AH and WH technologies modelled on a general level. This is a strength of this work as a techno-economic analysis focusing on AH and WH supply sources for DH on a general level was lacking in the literature. However, it is also a limitation since it would also be interesting to understand and compare the performance of a wide variety of different AH and WH sources on a specific level (e.g., including additional, specific AH and WH sources like river water or ground sourced HPs or WH from supermarkets and subway tunnels).

Industrial WH

There were also multiple limitations in the way industrial WH and its future availability was modelled. Temporal changes in industrial WH availability were not considered in the general model (it was assumed that the full capacity was always available) and only considered to a limited extent for the case study (only available during the weekdays). This means the temporal mismatch between industrial WH supply and heat demand was not accounted for, which impacts the profitability of the industrial WH source [22], [23]. Additionally, in modelling uncertainty in future WH availability, variation across sectors was not accounted for. In reality, the WH cessation probability will vary across sectors. For example, smaller, less established businesses have a higher chance of going bankrupt than large, established companies. Furthermore, in the WH cessation scenarios, the WH was either fully present or not. Partial reductions in WH availability or changes in temperature were not considered. However, this may be the case if industries increase internal heat recovery, increase efficiency, or decarbonize their processes in such a way that WH temperatures are reduced [6], [50], [55].

Electricity grid

Another limitation is that the electricity grid is not included in the model. This is especially relevant when considering large increases in electric heating (e.g., through electric HOBs and HPs) as this increases electricity demand and can puts a significant burden on the electricity grid. Yang et al. highlight this in their study as they found that electric heating more than doubled the electricity demand in the case study they considered (Harbin, China) [20].

Simulation not optimization

Another source of limitations in the model is that it was based on simulations rather than optimization. The use of simulations provided insight into the techno-economic performance of AH and WH as DH heat sources considering economic risk arising from the uncertainty in the future development of energy prices and WH availability. It was chosen due to its computational performance allowing for the uncertainty analysis across energy price scenarios and WH cessation scenarios. However, it also led to some limitations.

The use of simulations meant that system configurations were determined as inputs for the model. The different configurations could then be compared to each other by looking at mean LCOH and standard deviation as indicators of techno-economic performance and patterns across AH and WH configurations and base configurations could be discerned. However, an optimization model would allow for the calculation of the optimal system configuration to minimize costs and/or economic risks.

Furthermore, in the one-year simulation, the model steps through hourly timesteps and determines the optimal technology operation in each timestep based on the economic ranking for each timestep. It does not have an overview of the entire period that is modelled. This meant that it was difficult to implement an absolute restriction on the total biomass quantity used, as biomass would have been used as usual up until the timestep where the available biomass supply was depleted. This would result in an optimal use of biomass up until the point where the supply was depleted but a non-optimal use of biomass considering the entire duration of the one-year simulation. For this reason, the biomass restriction was implemented through an artificial price increase in the economic ranking process. However, as an optimization model would optimize over the entire study period, it would be possible to implement such an annual restriction on total biomass quantity and obtain its optimal use throughout the entire study period.

Optimization over longer time frames (such as one year) is also important for the modelling of the optimal operation of a large-scale seasonal storage. Seasonal storage was not included as one of the technologies modelled in this thesis but would be relevant to consider in future analyses.

Representativeness of the one-year model

In the model, the one-year simulation is assumed to be representative for the duration of the twenty-year study period. Thus, for each year in the study period, the same hourly profile for heating demand, temperatures, and electricity prices is used. Similarly, fixed prices for biomass, biomethane, and industrial WH in the one-year model are constant over the duration of the study period. This fails to account for variations from year to year, or general trends that may emerge over a longer period.

5.3.3 Other

Consideration of additional uncertainty sources

Another limitation of this study is that uncertainty sources other than uncertainty in energy prices and WH availability were not considered. This includes for example changes in air temperatures due to climate changes which would not only impact heating demand in DH networks but also AH availability for air HPs. Another possible source of uncertainty is changes in DH demand due to retrofitting of buildings or changes in investment costs for heating technologies.

Consideration of environmental impacts

Additionally, this study did consider the environmental impacts of the configurations analyzed. This is relevant to fully understand the potential of AH and WH to contributing to the decarbonization of DH networks. For example, especially for electric heating sources, the electricity mix strongly influences their potential CO_2 savings [20].

Mean LCOH and standard deviation as KPIs

Finally, average cost was measured through mean LCOH and economic risk through standard deviation across energy price and WH cessation scenarios. These KPIs measure the central tendency and magnitude of the variation in LCOH due to uncertainty in future energy prices and WH availability. The right-skewed distributions caused by the WH cessation scenarios, are reflected in that the higher LCOH of scenarios where WH ceases operation led to a higher mean and standard deviation. However, to better understand the spread of LCOH across scenarios, additional measures could be used. For instance, the median value or interquartile range can provide insight to where most of the datapoints lie as these measures are less affected by extreme values. Moreover, to better understand the worst-case scenario high LCOH values caused by WH cessation, other measures of risk such as value at risk or conditional value of risk could be used.

5.4 Future outlook

Many of the limitations identified in section 5.3 are factors that were not accounted for in the model, all of which present opportunities for further research. This includes the modelling of additional technologies (i.e., large scale seasonal thermal storage, geothermal energy, or cooling technologies) and system configurations (i.e., systems with greater share of AH and WH), as well as the more detailed modelling of heat supply technologies that are included (i.e., considering necessary ramp up and ramp down times, or more detailed modelling of investment costs which are largely case-specific). Also, further research on the effect of restricted biomass availability would be highly relevant since competition across sectors or potential prioritization for higher value applications makes the availability and cost of biomass for heating purposes highly uncertain in the future. Furthermore, it would also be interesting to consider different operation strategies other than economic ranking.

This thesis considered uncertainty in future energy prices and WH availability. Future research could look further into these two factors, for example at the range considered for energy prices, the volatility of electricity prices, and the assumption that energy prices are correlated with each other. It could also consider changes in WH availability across sectors in terms of quantity and quality. Additionally, further analysis of the definition of the probabilities associated with the energy price scenarios and WH cessation scenarios could be carried out. The consideration of other uncertainty sources would also be relevant such as uncertainties in investment costs, variations in heat demand and air temperature due to climate change, reductions in DH supply temperatures, or variations in heat demand due to retrofitting of existing buildings.

Furthermore, since the way industrial WH was modelled was key in determining the performance of system configurations with industrial WH, the modelling of industrial WH is also a potential area for future research. This includes greater detail in the temporal availability of WH to reflect the temporal mismatch between heat demand and industrial WH availability, which impacts the effectiveness of industrial WH as a DH heat source [22], [23]. It also includes the further analysis of how WH availability may change in the future, considering the effect of industry decarbonization on WH production, different WH cessation probabilities (across sectors and overall), partial reductions in availability, or future changes in WH quality (i.e., temperature). Finally, the independence of the price of industrial WH to changes in energy price scenarios may also be an area of further investigation.

An additional possibility for future research is the replication of the study on a closer timescale or modelling of decarbonization pathways from now up to 2050, accounting for intermediate decarbonization targets (e.g., 80% by 2040) and existing assets. Also, the consideration of the environmental impacts of different system configurations is relevant for understanding the potential of different strategies for contributing to decarbonization of the heating sector. The application of the model developed in this thesis to additional case studies would also be interesting for understanding the techno-economic performance and economic risk associated with decarbonization plans for real DH networks. Additional research could also be done in comparing DH systems with AH and WH sources to individual heating systems or considering the impacts of demand side flexibility in addition to supply side flexibility.

Finally, an important area for future research is the use of optimization rather than simulation. A similar study utilizing optimization would allow for:

- A further understanding of which system configurations and operation strategies are optimal for minimizing costs and/or economic risk, considering both investment and operational costs,
- Modelling of the optimal allocation of limited fuels for heat production from CHP plants or HOBs using biomethane or biomass as a fuel source, and
- Understanding and modelling of the optimal operation of large-scale seasonal thermal storage to support the integration of AH and WH in DH networks.

Understanding optimal operation of technologies with limited fuel availability over the study period or of a seasonal storage is difficult to do through simulation as an overview over the entire study period is needed to determine the optimal timesteps for using biomass fueled heat sources or thermal storage. Nonetheless this is key due to the high uncertainty regarding biomass availability and cost in the future, as well as the large potential of thermal energy storage to increase the flexibility of heat systems and make the most of varying supply sources. This makes optimization a key focus for future research.

5.5 INSIGHTS AND RECOMMENDATIONS FOR STAKEHOLDERS

The results of this thesis highlight that the implementation of renewable heat supply technologies, such as AH and WH, in DH systems is subject to economic risks. These risks stem from increased coupling with energy markets and the associated uncertainty in future energy prices, as well as the reliance on WH sources with uncertain future availability. However, they also have the potential for contributing to the resilient decarbonization of DH systems and possibly to reduced costs. Therefore, the findings of this work are relevant for a wide range of stakeholders: not only the DH network operators, but also end users relying on DH, companies and industries producing WH, and governments that aim to support the decarbonization of the heating sector.

DH network operators

For DH network operators, a key research outcome is that uncertainties in the development of key factors lead to economic risks that impact the techno-economic performance of the DH system. Furthermore, the DH system configuration strongly influences the techno-economic performance and magnitude of economic risk associated with the DH system. Thus, in planning the decarbonization of their DH network, the careful consideration of different heat supply technologies and system configurations accounting for uncertainty is highly beneficial. To do so, a methodology or model such as the one developed in this thesis can serve as a useful tool. Furthermore, results indicate that AH and WH sources are attractive heat sources as they can lead to reduced average costs and economic risk. Also, a diversified portfolio and increased supply side flexibility can increase resilience to future uncertainties. However, exact results are largely dependent on the system configuration as well as input data, therefore it is advisable to conduct an analysis specific to the DH network in question.

DH end-users

End-users can benefit from the realization of DH networks that are resilient in the face of uncertainties, as it can ultimately lead to improved security and affordability of heat supply.

WH providers

For companies and industries producing WH, this study highlights the potential for collaborations with DH networks. As evidenced by the results, a fixed WH price that is stable across energy price scenarios provides significant benefits for the DH network operators, evidenced in the lower mean LCOH and standard deviation for configurations with WH. This shows companies and industries producing WH that their WH can be sold as a valuable product and act as an additional source of revenue rather than being dissipated in the environment. However, as the sensitivity analysis to WH prices indicated, the WH must be offered at a competitive price for it to be attractive to DH network operators. Furthermore, potential WH cessation has an impact on costs and economic risk and may deter DH operators from considering WH as a heat source. Thus, offering a guarantee of continued supply (to the extent possible) may increase the attractiveness of WH for DH network operators.

Governments

Finally, for governments that aim to advance the transition to decarbonized DH systems, it is evident that to successfully realize the transition, it is necessary to tackle the risks arising from uncertainty in future energy prices and waste heat availability. Therefore, policy tools should be set in place to:

1. **Increase awareness and consideration of risks.** Policy should ensure that there is awareness that these risks exist and that these risks are considered in the planning of future DH system. This could be implemented for example by requiring DH companies to make a decarbonization plan that considers and accounts for economic risks arising from uncertainties in the future development of key factors.
2. **Support risk management**. With the acknowledgment that these risks exist, policy tools should be set in place that support risk management. For example, the French government established a guarantee fund for geothermal operations to support risk management for deep geothermal drilling. The fund is co-financed by the government and project beneficiaries. It provides financial compensation to the beneficiaries in the event of a failure in either the quality or quantity of the geothermal resource [62], [63]. By sharing the financial burden of potential losses, a fund such as this once encourages investments in renewable energy sources despite the risks associated with it. A similar fund could be set up for DH companies using WH sources, to reduce the risk posed by potential WH cessation.
3. **Support DH system diversification.** Results indicated that system diversification and increased supply side flexibility leads to greater robustness of DH systems. However, due to the tradeoff between cost and risk, these options are often more expensive. Thus, offering support for system diversification could be a beneficial in reducing economic risks associated with DH systems.
4. **Limit reliance on biomass.** As the case study highlighted, the assumption that biomass will be available for DH at a low cost, can make biomass fueled heat supply technologies appear as attractive low-cost and low-risk heat sources. However, due to competition with other sectors and prioritization for higher value applications, there is uncertainty in the cost and availability of biomass for DH in the future. Therefore, policy measures should limit reliance of biomass in DH networks. For example, German regulations limit the contribution of biomass to a maximum of 25% of annual heat supply in new DH networks extending over 50 km, effective as of January 1, 2024 [64].

6 Conclusion

The heating sector makes up a large portion of final energy demand and is heavily reliant on fossil fuels. Therefore, its decarbonization is incredibly relevant for achieving climate neutrality and mitigating the negative effects of climate change. DH networks have a strong potential to contribute to this, since they enable the implementation of sustainable heating solutions on a large scale and the use of heat sources that are difficult to integrate on a small scale. This includes AH and WH, which are heat sources with large, untapped potential. However, a comprehensive analysis of the technical and economic performance of DH systems with AH and WH was missing in existing literature. Furthermore, AH and WH sources are subject to economic risks arising from uncertainty surrounding the future development of key factors, such as energy prices and WH availability, but a quantification of these risks was also missing from the literature. Accordingly, this thesis evaluated the technical and economic performance of AH and WH sources employed for the resilient decarbonization of DH networks considering economic risks due to uncertainty in future energy prices and WH availability.

This was achieved by developing a model to simulate DH systems with and without AH and WH sources and evaluate their LCOH in the context of a general model and a case study application for a small city in northwestern Poland. For each system configuration analyzed, the DH system was simulated for all possible WH cessation scenarios for each of the one hundred energy price scenarios considered. Each LCOH was assigned a weight based on the probability of the WH cessation scenario and energy price scenario occurring. The mean LCOH and standard deviation across the results for each system configuration were used to measure the central tendency and magnitude of the variation in LCOH due to uncertainty in future energy prices and WH availability. This provided an indication of average cost and associated economic risk across the configurations analyzed.

A main conclusion is that the DH system configuration plays a key role in determining the average cost and economic risk of the DH system. Furthermore, results indicated that a tradeoff exists between minimizing average cost and minimizing economic risk. The presence of industrial WH proved to be beneficial to the techno-economic performance of DH systems, leading to reduced mean LCOH and often also a reduction in standard deviation. However, this is largely due to the assumptions concerning the modelling of industrial WH. Namely: the relatively low industrial WH price, the lack of variation in the price of industrial WH across energy price scenarios, and the relatively low annual WH cessation probability. Results also evidence that increased supply side flexibility, through a greater variety and installed capacity of heat supply sources, leads to reduced economic risk in the face of future uncertainties. The inclusion of AH and WH sources also generally led to reduced economic risk both in the general model and case study. However, it is important to note that results are directly influenced by the input data for the model.

Key directions for future research are the consideration of a greater variety of heat supply technologies and DH system configurations, as well as increased detail in the representation of the technologies and DH system in the model. Additionally, further research into other uncertainties in the future development of key factors can further the understanding of economic risks that arise from these uncertainties and the resilience of DH systems in the face of them. Another relevant direction for future research is the use of optimization rather than simulation, allowing for the identification optimal configurations to minimize costs and/or economic risks, as well as modelling the optimal operation of large scale seasonal thermal storage and biomass-based heat supply technologies under restricted fuel availability.

The principal insight for stakeholders in planning the resilient decarbonization of DH systems is the importance of the careful consideration of different heat supply technologies and DH system configurations, accounting for uncertainty surrounding future developments in key factors like energy prices and WH availability. The model developed in this thesis exemplifies an effective tool for such analyses and offers valuable insight into key patterns that emerge when incorporating AH and WH in DH systems. However, as outcomes largely depend on the system configuration and input data for the model, it is important to conduct an analysis specific to the DH system in question.

7 REFERENCES

[1] "European climate law." Accessed: Nov. 08, 2023. [Online]. Available: https://climate.ec.europa.eu/eu-action/european-climate-law_en#:~:text=The%20European%20Climate%20Law%20writes%20into%20law%20the,least%2055%25%20by%202030%2C%20compared%20to%201990%20levels.

[2] M. Sporleder, M. Rath, and M. Ragwitz, "Design optimization of district heating systems: A review," *Front. Energy Res.*, vol. 10, p. 971912, Oct. 2022, doi: 10.3389/fenrg.2022.971912.

[3] J. Fitó, M. Vallée, A. Ruby, and E. Cuisinier, "Robustness of district heating versus electricity-driven energy system at district level: A multi-objective optimization study," *Smart Energy*, vol. 6, p. 100073, May 2022, doi: 10.1016/j.segy.2022.100073.

[4] K. Kontu, S. Rinne, and S. Junnila, "Introducing modern heat pumps to existing district heating systems – Global lessons from viable decarbonizing of district heating in Finland," *Energy*, vol. 166, pp. 862–870, Jan. 2019, doi: 10.1016/j.energy.2018.10.077.

[5] Y. Su, P. Hiltunen, S. Syri, and D. Khatiwada, "Decarbonization strategies of Helsinki metropolitan area district heat companies," *Renew. Sustain. Energy Rev.*, vol. 160, p. 112274, May 2022, doi: 10.1016/j.rser.2022.112274.

[6] M. Morandin, R. Hackl, and S. Harvey, "Economic feasibility of district heating delivery from industrial excess heat: A case study of a Swedish petrochemical cluster," *Energy*, vol. 65, pp. 209–220, Feb. 2014, doi: 10.1016/j.energy.2013.11.064.

[7] P. A. Østergaard, J. Jantzen, H. M. Marczinkowski, and M. Kristensen, "Business and socioeconomic assessment of introducing heat pumps with heat storage in small-scale district heating systems," *Renew. Energy*, vol. 139, pp. 904–914, Aug. 2019, doi: 10.1016/j.renene.2019.02.140.

[8] B. Bach, J. Werling, T. Ommen, M. Münster, J. M. Morales, and B. Elmegaard, "Integration of large-scale heat pumps in the district heating systems of Greater Copenhagen," *Energy*, vol. 107, pp. 321–334, Jul. 2016, doi: 10.1016/j.energy.2016.04.029.

[9] G. Fambri, A. Mazza, E. Guelpa, V. Verda, and M. Badami, "Power-to-heat plants in district heating and electricity distribution systems: A techno-economic analysis," *Energy Convers. Manag.*, vol. 276, p. 116543, Jan. 2023, doi: 10.1016/j.enconman.2022.116543.

[10] R.-R. Schmidt and B. Leitner, "A collection of SWOT factors (strength, weaknesses, opportunities and threats) for hybrid energy networks," *Energy Rep.*, vol. 7, pp. 55–61, Oct. 2021, doi: 10.1016/j.egyr.2021.09.040.

[11] European Commission. Directorate General for Energy., E Think., TU Wien., Fraunhofer ISI., Öko Institut e.V., and Viegand Maagoe., *Renewable space heating under the revised Renewable Energy Directive: ENER/C1/2018 494 : final report.* LU: Publications Office, 2022. Accessed: Mar. 24, 2024. [Online]. Available: https://data.europa.eu/doi/10.2833/525486

[12] M. Gonzalez-Salazar *et al.*, "Evaluation of Energy Transition Pathways to Phase out Coal for District Heating in Berlin," *Energies*, vol. 13, no. 23, p. 6394, Dec. 2020, doi: 10.3390/en13236394.

[13] A. Lake, B. Rezaie, and S. Beyerlein, "Review of district heating and cooling systems for a sustainable future," *Renew. Sustain. Energy Rev.*, vol. 67, pp. 417–425, Jan. 2017, doi: 10.1016/j.rser.2016.09.061.

[14] "Ambient heat." May 06, 2020. Accessed: Nov. 17, 2020. [Online]. Available: https://www.bfe.admin.ch/bfe/en/home/supply/energy-efficiency/ambient-heat.html

[15] H. Jouhara, N. Khordehgah, S. Almahmoud, B. Delpech, A. Chauhan, and S. A. Tassou, "Waste heat recovery technologies and applications," *Therm. Sci. Eng. Prog.*, vol. 6, pp. 268–289, Jun. 2018, doi: 10.1016/j.tsep.2018.04.017.

[16] S. Nielsen, K. Hansen, R. Lund, and D. Moreno, "Unconventional Excess Heat Sources for District Heating in a National Energy System Context," *Energies*, vol. 13, no. 19, p. 5068, Sep. 2020, doi: 10.3390/en13195068.

[17] M. Yuan, J. Z. Thellufsen, P. Sorknæs, H. Lund, and Y. Liang, “District heating in 100% renewable energy systems: Combining industrial excess heat and heat pumps,” *Energy Convers. Manag.*, vol. 244, p. 114527, Sep. 2021, doi: 10.1016/j.enconman.2021.114527.
[18] N. Marx, R. Blakcori, T. Forster, K. Maggauer, and S. Ralf-Roman, “Risk assessment in district heating: Evaluating the economic risks of inter-regional heat transfer networks with regards to uncertainties of energy prices and waste heat availability using Monte Carlo simulations,” *Smart Energy*, vol. 12, p. 100119, Nov. 2023, doi: 10.1016/j.segy.2023.100119.
[19] M. H. Abokersh, M. Vallès, K. Saikia, L. F. Cabeza, and D. Boer, “Techno-economic analysis of control strategies for heat pumps integrated into solar district heating systems,” *J. Energy Storage*, vol. 42, p. 103011, Oct. 2021, doi: 10.1016/j.est.2021.103011.
[20] T. Yang, W. Liu, and G. J. Kramer, “Integrated assessment on the implementation of sustainable heat technologies in the built environment in Harbin, China,” *Energy Convers. Manag.*, vol. 279, p. 116764, Mar. 2023, doi: 10.1016/j.enconman.2023.116764.
[21] G. Spirito, A. Dénarié, V. F. Cirillo, F. Casella, J. Famiglietti, and M. Motta, “Energy mapping and district heating as effective tools to decarbonize a city: Analysis of a case study in Northern Italy,” *Energy Rep.*, vol. 7, pp. 254–262, Oct. 2021, doi: 10.1016/j.egyr.2021.08.147.
[22] I. Pakere, M. Feofilovs, K. Lepiksaar, V. Vītoliņš, and D. Blumberga, “Multi-source district heating system full decarbonization strategies: Technical, economic, and environmental assessment,” *Energy*, p. 129296, Oct. 2023, doi: 10.1016/j.energy.2023.129296.
[23] F. Bühler, S. Petrović, F. M. Holm, K. Karlsson, and B. Elmegaard, “Spatiotemporal and economic analysis of industrial excess heat as a resource for district heating,” *Energy*, vol. 151, pp. 715–728, May 2018, doi: 10.1016/j.energy.2018.03.059.
[24] K. Specht, H. Kondziella, T. Bruckner, and F. Scheller, “Scenarios for the decarbonization of district heating: the case of Leipzig,” in *2023 19th International Conference on the European Energy Market (EEM)*, Lappeenranta, Finland: IEEE, Jun. 2023, pp. 1–11. doi: 10.1109/EEM58374.2023.10161822.
[25] F. Al-Mansour and M. Kožuh, “Risk analysis for CHP decision making within the conditions of an open electricity market,” *Energy*, vol. 32, no. 10, pp. 1905–1916, Oct. 2007, doi: 10.1016/j.energy.2007.03.009.
[26] G. Di Lorenzo, P. Pilidis, J. Witton, and D. Probert, “Monte-Carlo simulation of investment integrity and value for power-plants with carbon-capture,” *Appl. Energy*, vol. 98, pp. 467–478, Oct. 2012, doi: 10.1016/j.apenergy.2012.04.010.
[27] K. M. Maribu and S.-E. Fleten, “Combined Heat and Power in Commercial Buildings: Investment and Risk Analysis,” *Energy J.*, vol. 29, no. 2, Apr. 2008, doi: 10.5547/ISSN0195-6574-EJ-Vol29-No2-7.
[28] M. Momen, M. Shirinbakhsh, A. Baniassadi, and A. Behbahani-nia, “Application of Monte Carlo method in economic optimization of cogeneration systems – Case study of the CGAM system,” *Appl. Therm. Eng.*, vol. 104, pp. 34–41, Jul. 2016, doi: 10.1016/j.applthermaleng.2016.04.149.
[29] L. Urbanucci and D. Testi, “Optimal integrated sizing and operation of a CHP system with Monte Carlo risk analysis for long-term uncertainty in energy demands,” *Energy Convers. Manag.*, vol. 157, pp. 307–316, Feb. 2018, doi: 10.1016/j.enconman.2017.12.008.
[30] T. Verschelde and W. D’haeseleer, “Methodology for a global sensitivity analysis with machine learning on an energy system planning model in the context of thermal networks,” *Energy*, vol. 232, p. 120987, Oct. 2021, doi: 10.1016/j.energy.2021.120987.
[31] D. Connolly *et al.*, “Heat Roadmap Europe: Combining district heating with heat savings to decarbonise the EU energy system,” *Energy Policy*, vol. 65, pp. 475–489, Feb. 2014, doi: 10.1016/j.enpol.2013.10.035.
[32] DEA, “Technology Data - Energy plants for electricity and district heating generation Version number: 0014.” Danish Energy Agency, Feb. 2024. Accessed: Mar. 24, 2024. [Online]. Available: https://ens.dk/en/our-services/projections-and-models/technology-data/technology-data-generation-electricity-and

[33] N. Lamaison, S. Collette, M. Vallée, and R. Bavière, “Storage influence in a combined biomass and power-to-heat district heating production plant,” *Energy*, vol. 186, p. 115714, Nov. 2019, doi: 10.1016/j.energy.2019.07.044.
[34] A. Ioannou, A. Angus, and F. Brennan, “Risk-based methods for sustainable energy system planning: A review,” *Renew. Sustain. Energy Rev.*, vol. 74, pp. 602–615, Jul. 2017, doi: 10.1016/j.rser.2017.02.082.
[35] Y. Zhang, P. Johansson, and A. S. Kalagasidis, “Roadmaps for heating and cooling system transitions seen through uncertainty and sensitivity analysis,” *Energy Convers. Manag.*, vol. 292, p. 117422, Sep. 2023, doi: 10.1016/j.enconman.2023.117422.
[36] Ł. Bartela, A. Skorek-Osikowska, and J. Kotowicz, “An analysis of the investment risk related to the integration of a supercritical coal-fired combined heat and power plant with an absorption installation for CO 2 separation,” *Appl. Energy*, vol. 156, pp. 423–435, Oct. 2015, doi: 10.1016/j.apenergy.2015.07.045.
[37] M. Swing Gustafsson, J. Myhren, and E. Dotzauer, “Life Cycle Cost of Heat Supply to Areas with Detached Houses—A Comparison of District Heating and Heat Pumps from an Energy System Perspective,” *Energies*, vol. 11, no. 12, p. 3266, Nov. 2018, doi: 10.3390/en11123266.
[38] A. Rentizelas, G. Tziralis, and K. Kirytopoulos, “Incorporating uncertainty in optimal investment decisions,” *World Rev. Entrep. Manag. Sustain. Dev.*, vol. 3, no. 3/4, p. 273, 2007, doi: 10.1504/WREMSD.2007.014046.
[39] U. Arnold and Ö. Yildiz, “Economic risk analysis of decentralized renewable energy infrastructures – A Monte Carlo Simulation approach,” *Renew. Energy*, vol. 77, pp. 227–239, May 2015, doi: 10.1016/j.renene.2014.11.059.
[40] J. Laakso, “Using mixed integer linear programming with stochastic models for monte carlo investment analysis in the district heating sector,” Master thesis, Aalto University, Espoo, 2019. Accessed: Nov. 08, 2023. [Online]. Available: https://aaltodoc.aalto.fi/bitstream/handle/123456789/42698/master_Laakso_Juhana_2020.pdf?sequence=1
[41] M. Pärssinen, M. Wahlroos, J. Manner, and S. Syri, “Waste heat from data centers: An investment analysis,” *Sustain. Cities Soc.*, vol. 44, pp. 428–444, Jan. 2019, doi: 10.1016/j.scs.2018.10.023.
[42] F. Kienzle, P. Ahcin, and G. Andersson, “Valuing Investments in Multi-Energy Conversion, Storage, and Demand-Side Management Systems Under Uncertainty,” *IEEE Trans. Sustain. Energy*, vol. 2, no. 2, pp. 194–202, Apr. 2011, doi: 10.1109/TSTE.2011.2106228.
[43] F. Kienzle and G. Andersson, “Valuing investments in multi-energy generation plants under uncertainty: A real options analysis,” presented at the IAEE European Conference, 2009.
[44] V. Volodina, E. Wheatcroft, and H. Wynn, “Comparing district heating options under uncertainty using stochastic ordering,” 2020, doi: 10.48550/ARXIV.2003.04170.
[45] I. Postnikov and E. Mednikova, “A reliability analysis of fuel supply for district heating systems based on statistical test method,” *Energy Rep.*, vol. 8, pp. 304–311, Nov. 2022, doi: 10.1016/j.egyr.2022.08.020.
[46] M. Valinčius, I. Žutautaitė, G. Dundulis, S. Rimkevičius, R. Janulionis, and R. Bakas, “Integrated assessment of failure probability of the district heating network,” *Reliab. Eng. Syst. Saf.*, vol. 133, pp. 314–322, Jan. 2015, doi: 10.1016/j.ress.2014.09.022.
[47] L. F. Fuentes-Cortés, J. E. Santibañez-Aguilar, and J. M. Ponce-Ortega, “Optimal design of residential cogeneration systems under uncertainty,” *Comput. Chem. Eng.*, vol. 88, pp. 86–102, May 2016, doi: 10.1016/j.compchemeng.2016.02.008.
[48] K. Lygnerud and S. Werner, “Risk assessment of industrial excess heat recovery in district heating systems,” *Energy*, vol. 151, pp. 430–441, May 2018, doi: 10.1016/j.energy.2018.03.047.
[49] J. Pelda, F. Stelter, and S. Holler, “Potential of integrating industrial waste heat and solar thermal energy into district heating networks in Germany,” *Energy*, vol. 203, p. 117812, Jul. 2020, doi: 10.1016/j.energy.2020.117812.

[50] P. Manz, T. Fleiter, and W. Eichhammer, "The effect of low-carbon processes on industrial excess heat potentials for district heating in the EU: A GIS-based analysis," *Smart Energy*, vol. 10, p. 100103, May 2023, doi: 10.1016/j.segy.2023.100103.

[51] P. Sulewski, W. Ignaciuk, M. Szymańska, and A. Wąs, "Development of the Biomethane Market in Europe," *Energies*, vol. 16, no. 4, p. 2001, Feb. 2023, doi: 10.3390/en16042001.

[52] J. Kaeller and K. Maggauer, "TESCA Simulation framework: Techno-economic system and component analysis," presented at the EES-IES Seminar Series, Apr. 13, 2023.

[53] S. Werner, "International review of district heating and cooling," *Energy*, vol. 137, pp. 617–631, Oct. 2017, doi: 10.1016/j.energy.2017.04.045.

[54] N. Thamling *et al.*, "Perspektive der Fernwärme." Hamburg Institut & Prognos im Auftrag des AFGW, Nov. 2020. Accessed: Mar. 24, 2024. [Online]. Available: https://www.hamburg-institut.com/wp-content/uploads/2021/06/AGFW_Perspektive_der_Fernwaerme_2030_final.pdf

[55] J. Pelda *et al.*, "Advanced algorithm for spatial identification, evaluation of temporal availability and economic assessment of waste heat sources and their local representation," IEA DHC/CHP, 2023. [Online]. Available: https://www.iea-dhc.org/the-research/annexes/annex-xiii/annex-xiii-project-02

[56] Google LLC, "Google Earth." 2023. Accessed: Apr. 16, 2024. [Online]. Available: https://earth.google.com/web/@53.02283102,15.37738881,108.27644782a,33515.89746513d,35y,0h,0t,0r

[57] NOAA National Centers for Environmental Information, "Global Hourly - Integrated Surface Database (ISD)." 2001. Accessed: Apr. 07, 2024. [Online]. Available: https://www.ncei.noaa.gov/access/search/data-search/global-hourly?bbox=52.801,15.168,52.661,15.308&pageNum=1

[58] "ENTSO-E transparency platform." Accessed: Apr. 11, 2024. [Online]. Available: https://transparency.entsoe.eu/

[59] A. Sas, "Annual number of company bankruptcy court orders in Poland from 2013 to 2023." Statista, Mar. 08, 2024. Accessed: Apr. 09, 2024. [Online]. Available: https://www.statista.com/statistics/1369277/poland-bankruptcy-court-orders/

[60] A. Sas, "Number of enterprises in Poland from 2016 to 2022." Statista, Feb. 06, 2024. Accessed: Apr. 04, 2024. [Online]. Available: https://www.statista.com/statistics/1448945/poland-number-of-companies/

[61] Sociaal economische raad (SER), "Biomass in the balance - A sustainability framework for high value use of bio-based raw materials," Jul. 2020. Accessed: May 12, 2024. [Online]. Available: https://www.ser.nl/-/media/ser/downloads/engels/2020/biomass-in-the-balance.pdf

[62] C. Boissavy, "The successful geothermal risk mitigation system in France from 1980 to 2015," *European Geologist*, vol. 43, May 2017, Accessed: May 30, 2024. [Online]. Available: https://eurogeologists.eu/european-geologist-journal-43-boissavy-the-successful-geothermal-risk-mitigation-system-in-france-from-1980-to-2015/

[63] Représentation en France, "Aides d'État : la Commission autorise un régime d'aides français de 195,6 millions € mettant en place un fonds de garantie pour les opérations de géothermie profonde." Jul. 24, 2023.

[64] *Gesetz für die Wärmeplanung und zur Dekarbonisierung der Wärmenetze, Bundesgesetzblatt Jahrgang 2023 Teil 1, Nr. 394*. 2023. Accessed: May 30, 2024. [Online]. Available: https://www.bmwsb.bund.de/SharedDocs/gesetzgebungsverfahren/Webs/BMWSB/DE/Downloads/waermeplanung/wpg-bgbl.pdf?__blob=publicationFile&v=2

APPENDIX A: GENERAL MODEL ADDITIONAL FIGURES

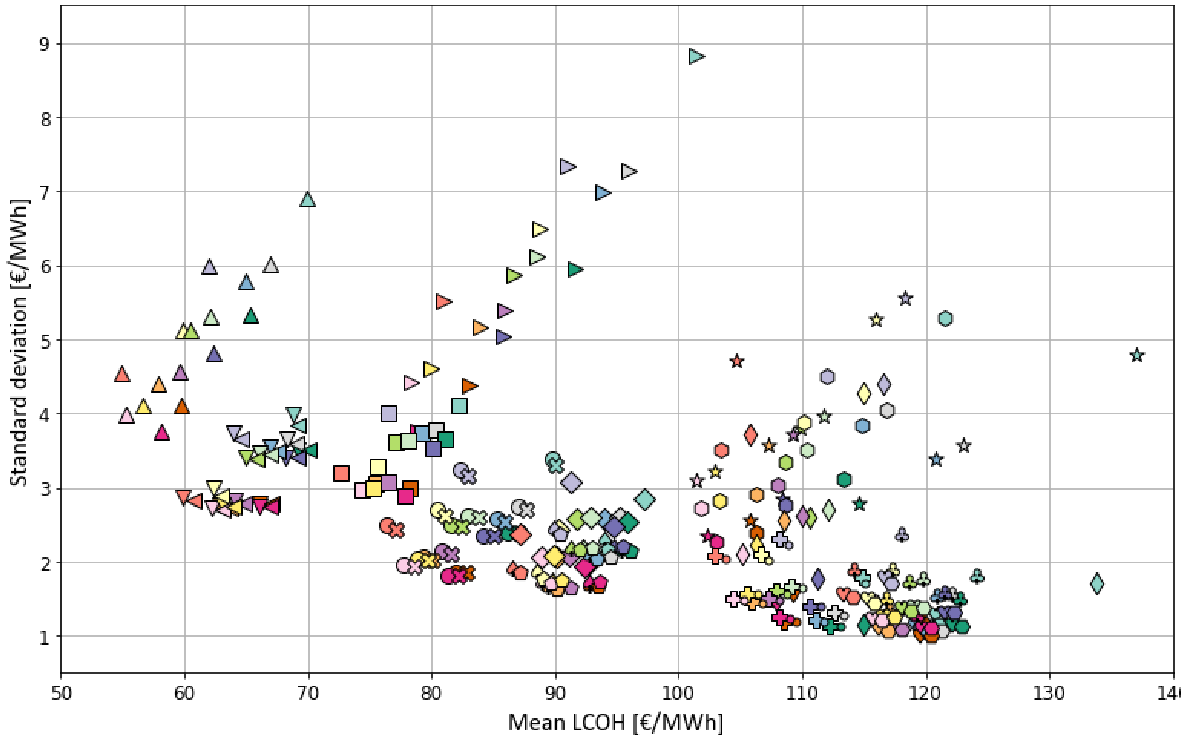

CONFIGURATION LEGEND

Base configuration: CHP, biomass boiler (BMB), electric boiler (ELB) and capacity in MW_{th} (0: ○○○, 33: ●○○, 67: ●●○, or 100: ●●●)

▲ 1: CHP○○○ BMB●○○ ELB●●○	► 4: CHP●○○ BMB○○○ ELB●●○	◆ 7: CHP●○○ BMB●●○ ELB○○○	★ 10: CHP●●○ BMB○○○ ELB●○○	✚ 13: CHP●●○ BMB●○○ ELB●○○	♥ 16: CHP●●○ BMB●●○ ELB●○○
▼ 2: CHP○○○ BMB●●○ ELB●○○	● 5: CHP●○○ BMB●○○ ELB●○○	♠ 8: CHP●○○ BMB●●○ ELB●○○	⬢ 11: CHP●●○ BMB○○○ ELB●●○	• 14: CHP●●○ BMB●○○ ELB●●○	⬣ 17: CHP●●○ BMB●●○ ELB●●○
◄ 3: CHP○○○ BMB●●○ ELB●●○	✖ 6: CHP●○○ BMB●○○ ELB●●○	⬟ 9: CHP●○○ BMB●●○ ELB●●○	♦ 12: CHP●●○ BMB●○○ ELB○○○	♣ 15: CHP●●○ BMB●●○ ELB○○○	■ 18: CHP○○○ BMB●●● ELB○○○

Ambient and waste heat configuration: industrial waste heat (IWH), datacenter heat pump (DHP), wastewater heat pump (WHP), and/or air heat pump (AHP), with 10 MW_{th} capacity if present

A: None	C: DHP	E: WHP	G: WHP, DHP	I: AHP	K: AHP, DHP,	M: AHP, WHP	O: AHP, WHP, DHP
B: IWH	D: DHP, IWH	F: WHP, IWH	H. WHP, DHP, IWH	J: AHP, IWH	L: AHP, DHP, IWH	N: AHP, WHP, IWH	P: AHP, WHP, DHP, IWH

Figure A.1 Weighted average levelized cost of heat (LCOH) and standard deviation for each of the configurations analyzed for the general model. The base configuration is indicated by the shape and the ambient and waste heat configuration by the color.

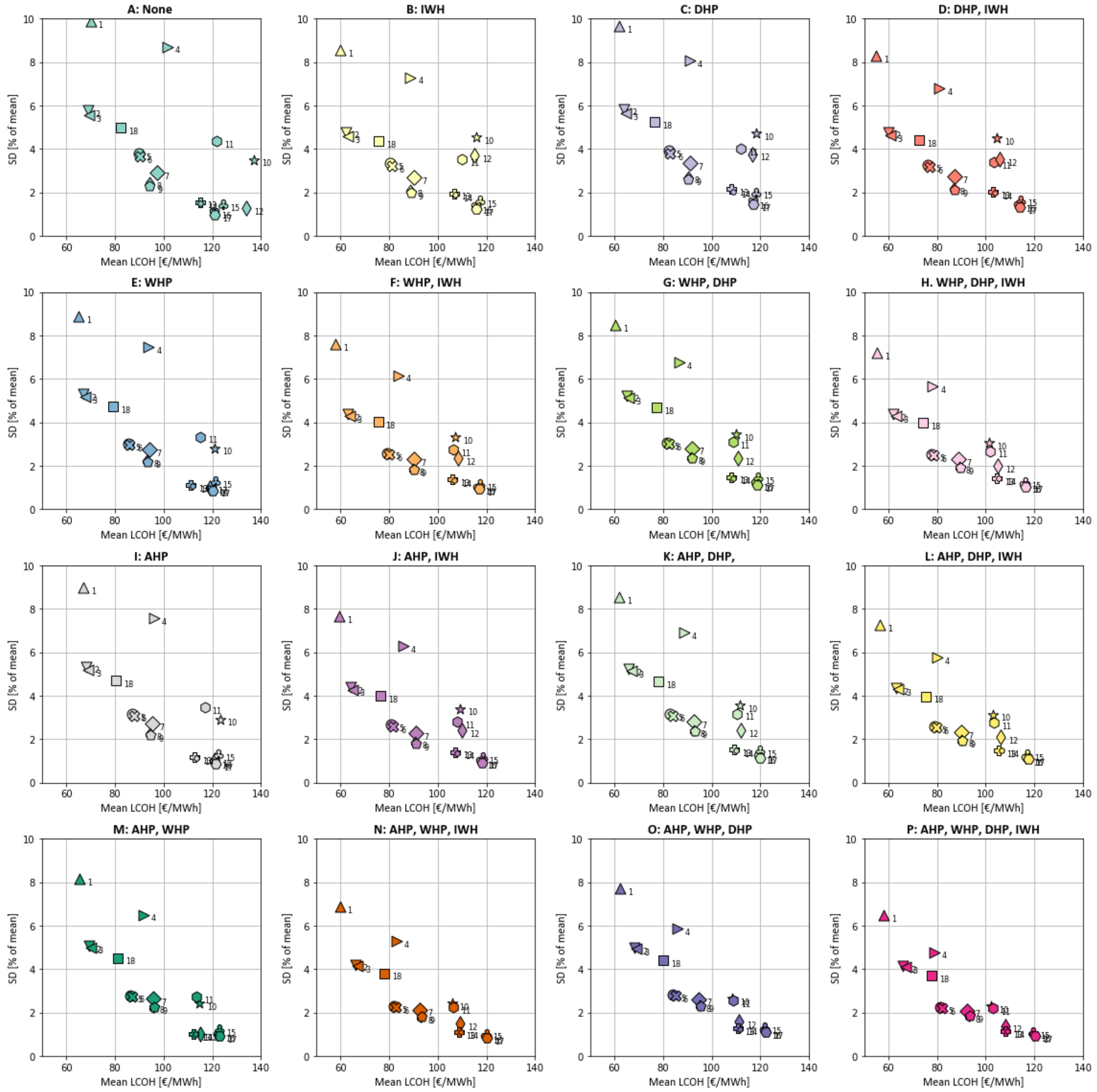

CONFIGURATION LEGEND

Base configuration: CHP, biomass boiler (BMB), electric boiler (ELB) and capacity in MW_{th} (0: ○○○, 33: ●○○, 67: ●●○, or 100: ●●●)

▲ 1: CHP○○○ BMB●○○ ELB●●○ ▶ 4: CHP●○○ BMB○○○ ELB●●○ ◆ 7: CHP●○○ BMB●●○ ELB○○○ ★ 10: CHP●●○ BMB○○○ ELB●○○ ✚ 13: CHP●●○ BMB●○○ ELB●○○ ♥ 16: CHP●●○ BMB●●○ ELB●○○

▼ 2: CHP○○○ BMB●●○ ELB●○○ ● 5: CHP●○○ BMB●○○ ELB●○○ ♠ 8: CHP●○○ BMB●●○ ELB●○○ ⬢ 11: CHP●●○ BMB○○○ ELB●●○ • 14: CHP●●○ BMB●○○ ELB●●○ ⬣ 17: CHP●●○ BMB●●○ ELB●●○

◀ 3: CHP○○○ BMB●●○ ELB●●○ ✖ 6: CHP●○○ BMB●○○ ELB●●○ ⬟ 9: CHP●○○ BMB●●○ ELB●●○ ⧫ 12: CHP●●○ BMB●○○ ELB○○○ ♣ 15: CHP●●○ BMB●●○ ELB○○○ ■ 18: CHP○○○ BMB●●● ELB○○○

Ambient and waste heat configuration: industrial waste heat (IWH), datacenter heat pump (DHP), wastewater heat pump (WHP), and/or air heat pump (AHP), with 10 MW_{th} capacity if present

A: None, C: DHP, E: WHP, G: WHP, DHP, I: AHP, K: AHP, DHP, M: AHP, WHP, O: AHP, WHP, DHP

B: IWH, D: DHP, IWH, F: WHP, IWH, H. WHP, DHP, IWH, J: AHP, IWH, L: AHP, DHP, IWH, N: AHP, WHP, IWH, P: AHP, WHP, DHP, IWH

*Figure A.2 Weighted average levelized cost of heat (LCOH) and standard deviation (expressed as a percent of mean LCOH) for each of the configurations analyzed for the general model. There is **one plot per ambient heat and waste heat configuration** analyzed, and **same axes** across plots.*

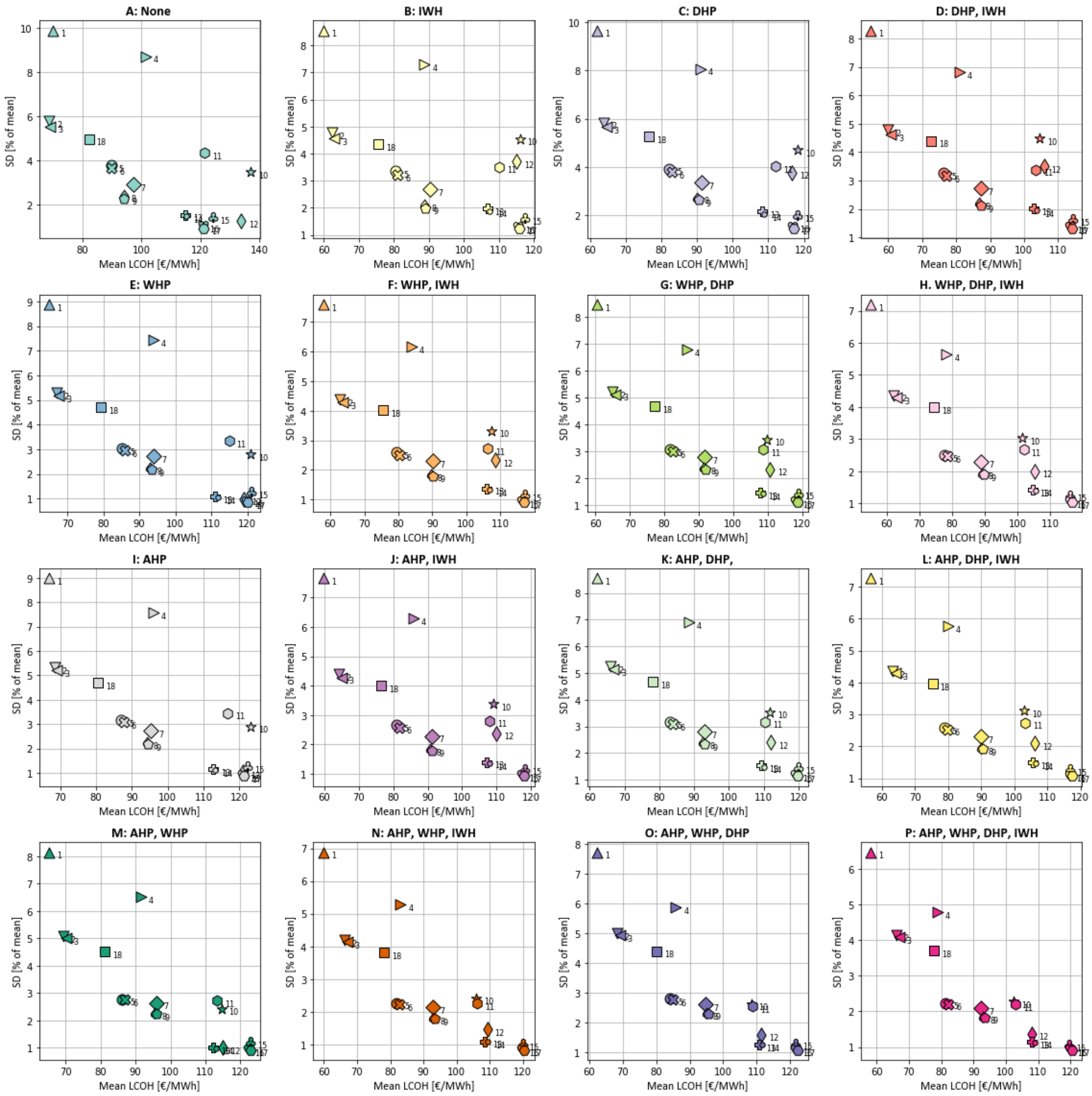

CONFIGURATION LEGEND

Base configuration: CHP, biomass boiler (BMB), electric boiler (ELB) and capacity in MW_{th} (0: ○○○, 33: ●○○, 67: ●●○, or 100: ●●●)

▲ 1: CHP○○○ BMB●○○ ELB●●○ ► 4: CHP●○○ BMB○○○ ELB●●○ ◆ 7: CHP●○○ BMB●●○ ELB○○○ ★ 10: CHP●●○ BMB○○○ ELB●○○ ✚ 13: CHP●●○ BMB●○○ ELB●○○ ♥ 16: CHP●●○ BMB●●○ ELB●○○

▼ 2: CHP○○○ BMB●●○ ELB●○○ ● 5: CHP●○○ BMB●○○ ELB●○○ ♠ 8: CHP●○○ BMB●●○ ELB●○○ ⬢ 11: CHP●●○ BMB○○○ ELB●●○ • 14: CHP●●○ BMB●○○ ELB●●○ ⬣ 17: CHP●●○ BMB●●○ ELB●●○

◄ 3: CHP○○○ BMB●●○ ELB●●○ ✖ 6: CHP●○○ BMB●○○ ELB●●○ ⬟ 9: CHP●○○ BMB●●○ ELB●●○ ⧫ 12: CHP●●○ BMB●○○ ELB○○○ ♣ 15: CHP●●○ BMB●●○ ELB○○○ ■ 18: CHP○○○ BMB●●● ELB○○○

Ambient and waste heat configuration: industrial waste heat (IWH), datacenter heat pump (DHP), wastewater heat pump (WHP), and/or air heat pump (AHP), with 10 MW_{th} capacity if present

A: None C: DHP E: WHP G: WHP, DHP I: AHP K: AHP, DHP, M: AHP, WHP O: AHP, WHP, DHP

B: IWH D: DHP, IWH F: WHP, IWH H. WHP, DHP, IWH J: AHP, IWH L: AHP, DHP, IWH N: AHP, WHP, IWH P: AHP, WHP, DHP, IWH

*Figure A.3 Weighted average levelized cost of heat (LCOH) and standard deviation (expressed as a percent of mean LCOH) for each of the configurations analyzed for the general model. There is **one plot per ambient heat and waste heat configuration** analyzed, and **different axes** across plots.*

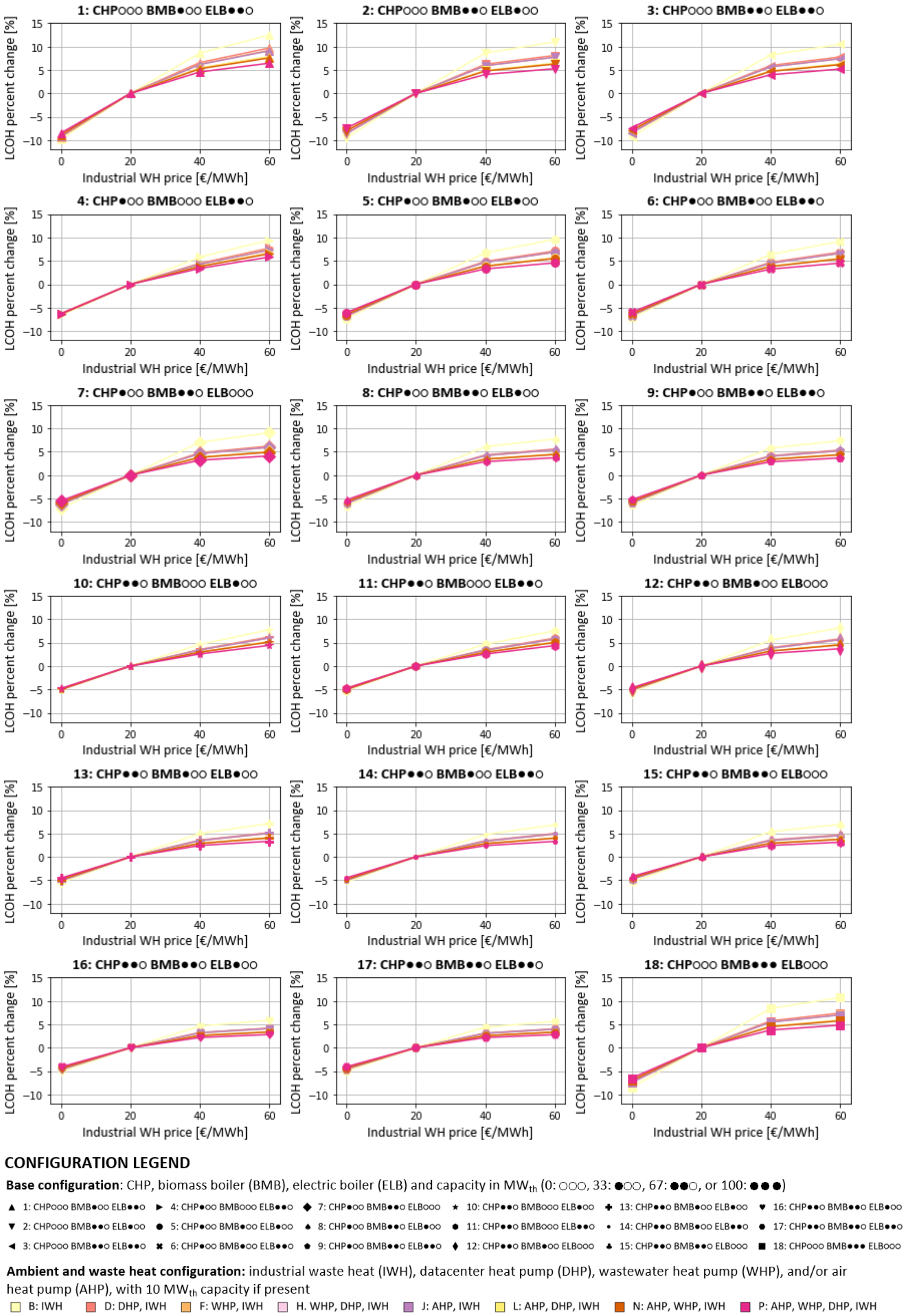

Figure A.4 Sensitivity of the mean levelized cost of heat (LCOH) to variations in industrial waste (WH) prices (expressed as percent change in SD relative to the SD with a WH price of 20 €/MWh), plotted per base configuration.

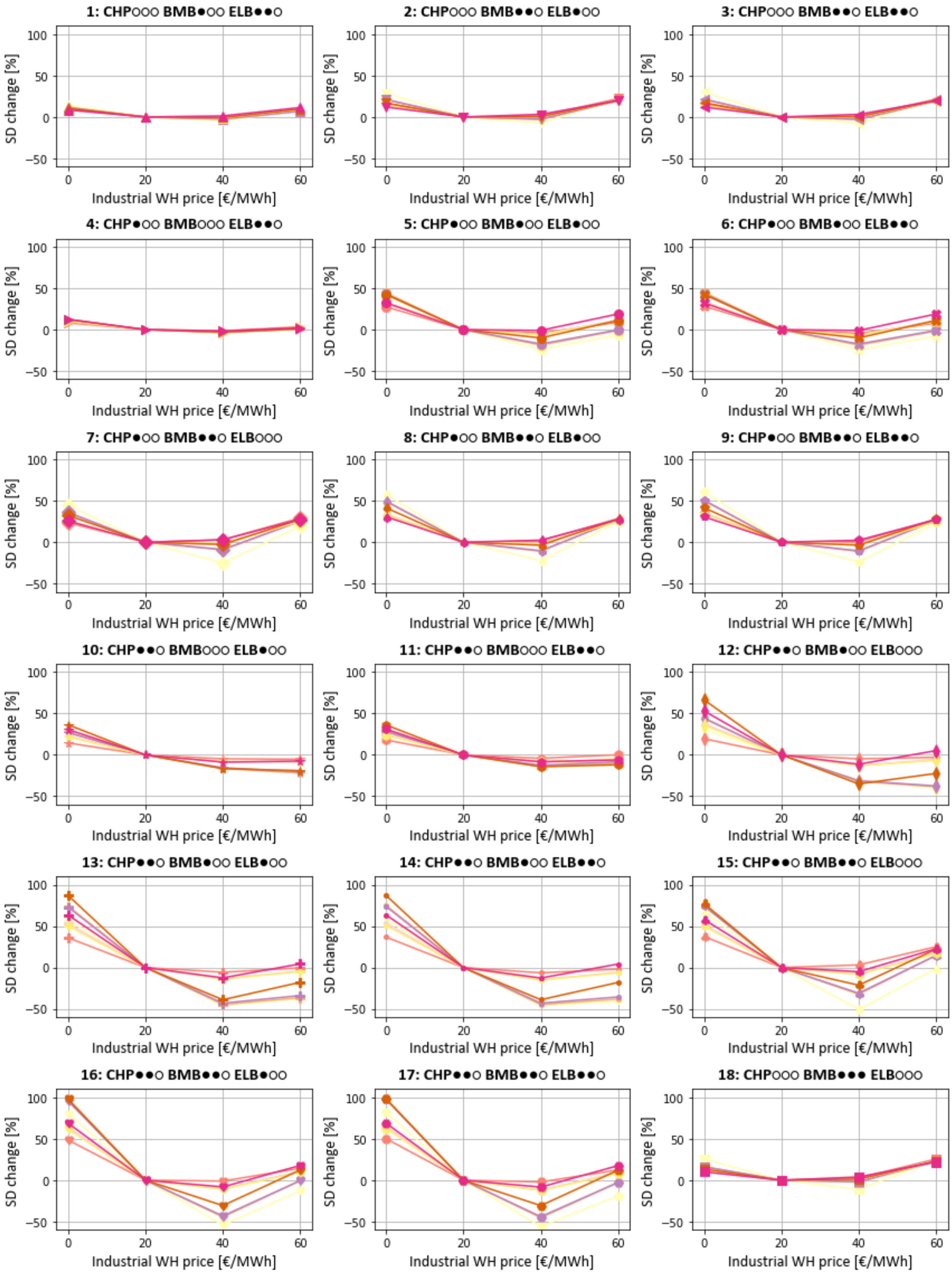

CONFIGURATION LEGEND

Base configuration: CHP, biomass boiler (BMB), electric boiler (ELB) and capacity in MW_{th} (0: ○○○, 33: ●○○, 67: ●●○, or 100: ●●●)

▲ 1: CHP○○○ BMB●○○ ELB●●○ ► 4: CHP●○○ BMB○○○ ELB●●○ ◆ 7: CHP●○○ BMB●●○ ELB○○○ ★ 10: CHP●●○ BMB○○○ ELB●○○ ✚ 13: CHP●●○ BMB●○○ ELB●○○ ♥ 16: CHP●●○ BMB●●○ ELB●○○

▼ 2: CHP○○○ BMB●●○ ELB●○○ ● 5: CHP●○○ BMB●○○ ELB●○○ ♠ 8: CHP●○○ BMB●●○ ELB●○○ ⬢ 11: CHP●●○ BMB○○○ ELB●●○ • 14: CHP●●○ BMB●○○ ELB●●○ ● 17: CHP●●○ BMB●●○ ELB●●○

◄ 3: CHP○○○ BMB●●○ ELB●●○ ✖ 6: CHP●○○ BMB●○○ ELB●●○ ⬟ 9: CHP●○○ BMB●●○ ELB●●○ ⧫ 12: CHP●●○ BMB●○○ ELB○○○ ♣ 15: CHP●●○ BMB●●○ ELB○○○ ■ 18: CHP○○○ BMB●●● ELB○○○

Ambient and waste heat configuration: industrial waste heat (IWH), datacenter heat pump (DHP), wastewater heat pump (WHP), and/or air heat pump (AHP), with 10 MW_{th} capacity if present

B: IWH D: DHP, IWH F: WHP, IWH H. WHP, DHP, IWH J: AHP, IWH L: AHP, DHP, IWH N: AHP, WHP, IWH P: AHP, WHP, DHP, IWH

Figure A.5 Sensitivity of standard deviation (SD) of the mean levelized cost of heat (LCOH) to variations in industrial waste (WH) prices (expressed as percent change in SD relative to the SD with a WH price of 20 €/MWh), plotted per base configuration.

Appendix B: Case study model additional figures

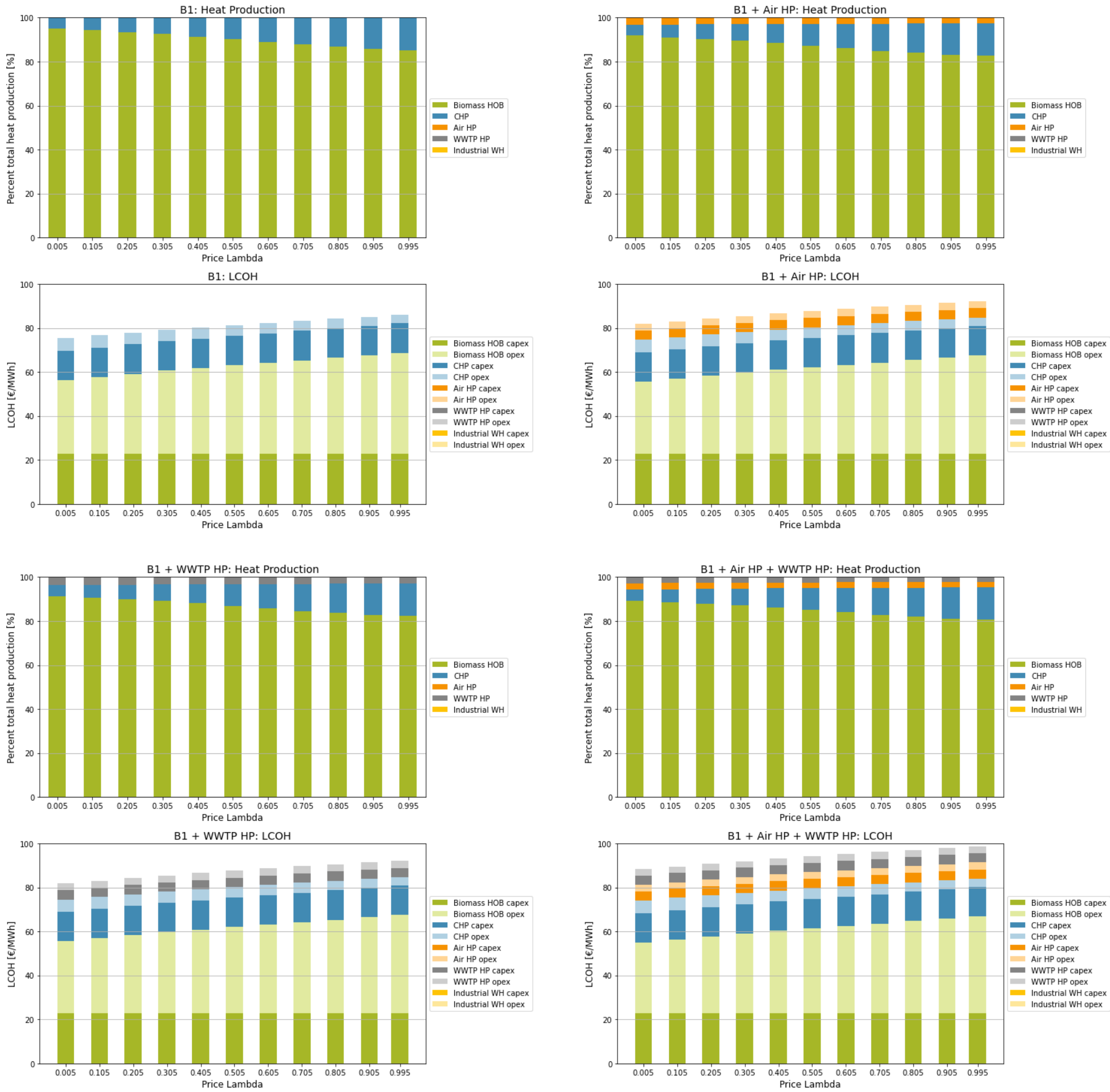

Figure B.1 Heat output per technology and levelized cost of heat (LCOH) broken down into capital expenditure (CAPEX) and operation expenditure (OPEX) across energy scenarios for system configurations in scenario B1.

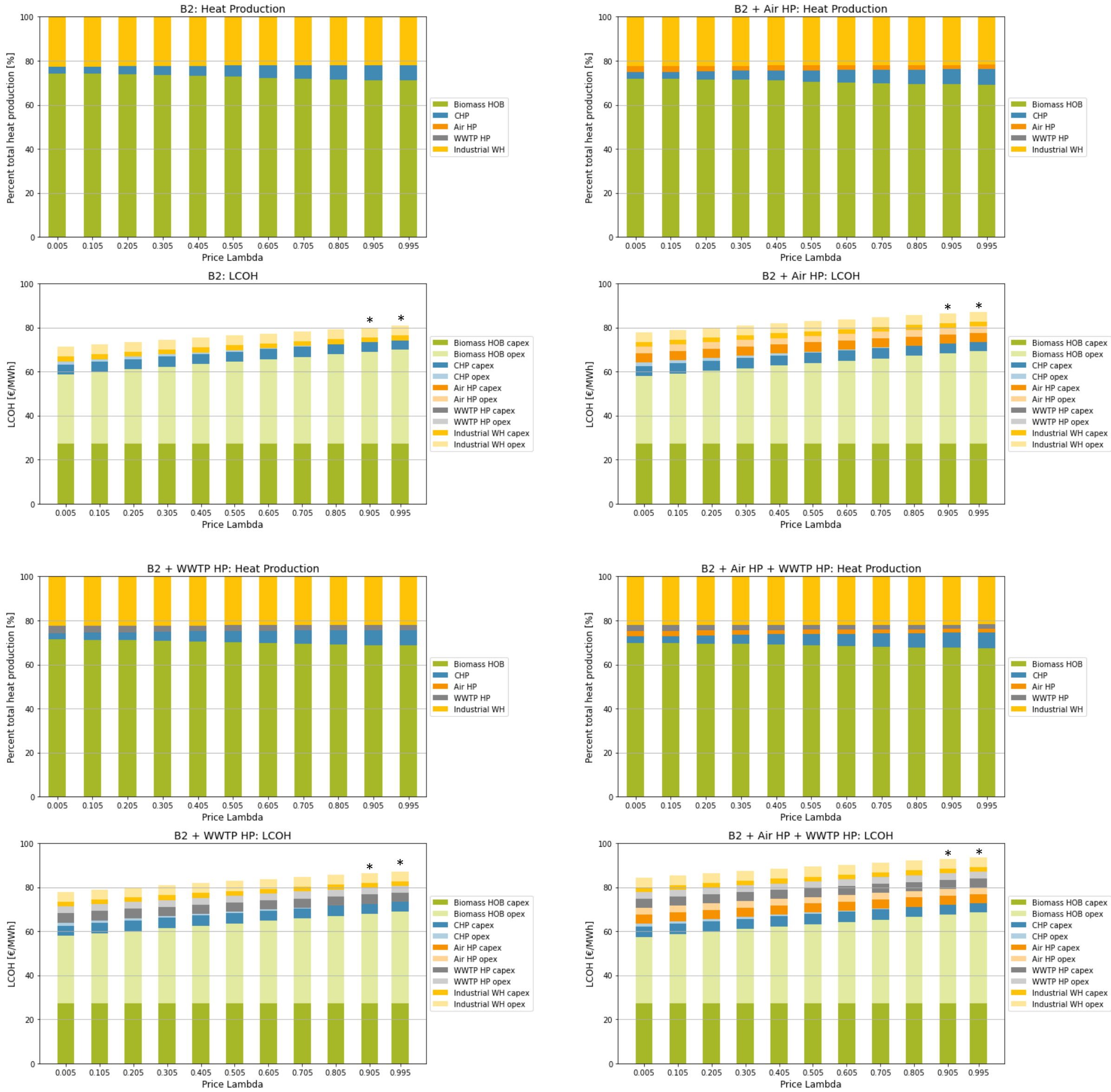

Figure B.2 Heat output per technology and levelized cost of heat (LCOH) broken down into capital expenditure (CAPEX) and operation expenditure (OPEX) across energy scenarios for system configurations in scenario B2. The asterisk (*) indicates high price scenarios where the CHP has a net revenue (negative OPEX) which is not shown.

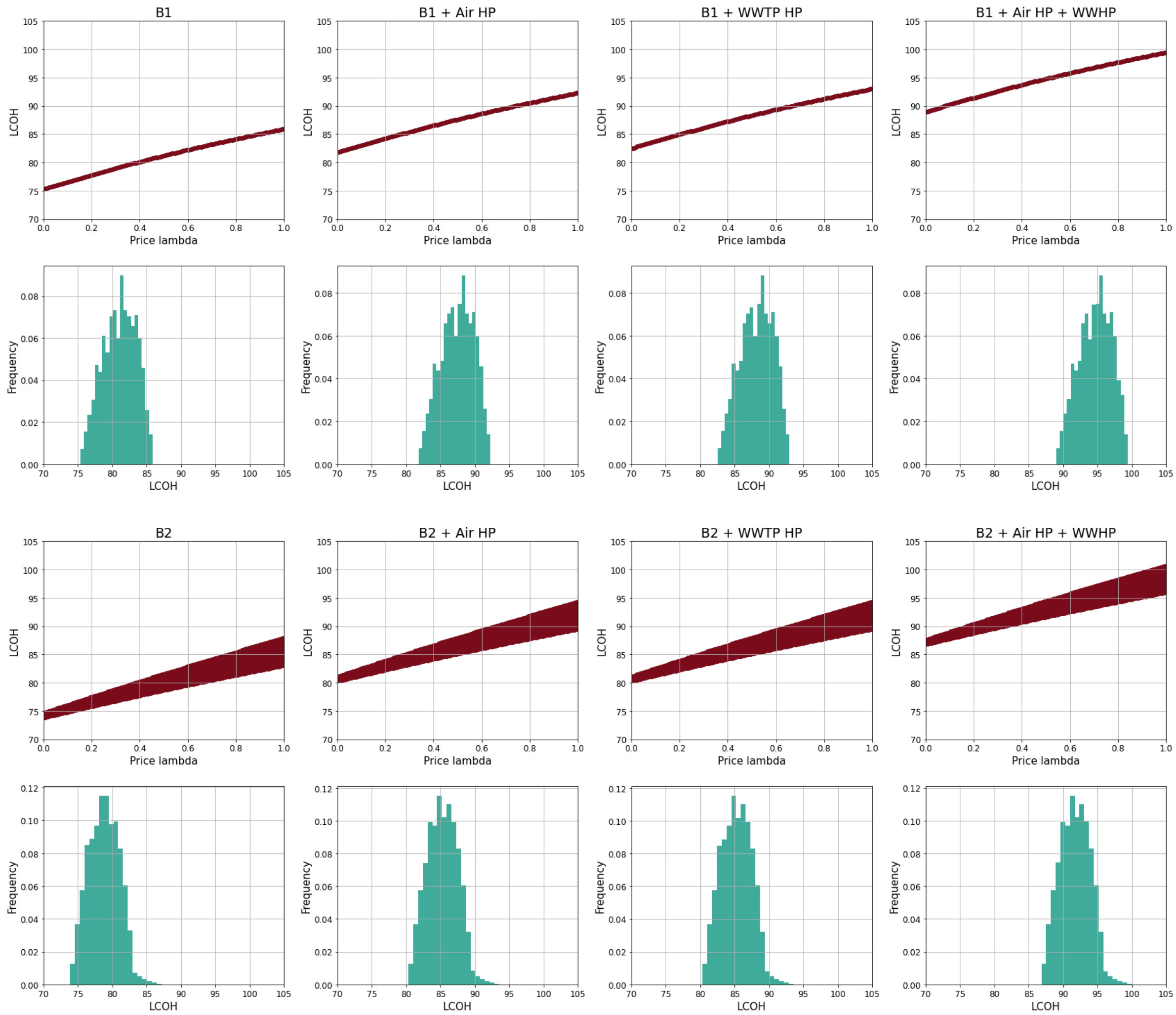

Figure B.3 Plots showing price lambda vs. levelized cost of heat (LCOH) and histogram of weighted LCOH for each energy price scenario and each WH cessation scenario modelled for the eight system configurations in the case study.

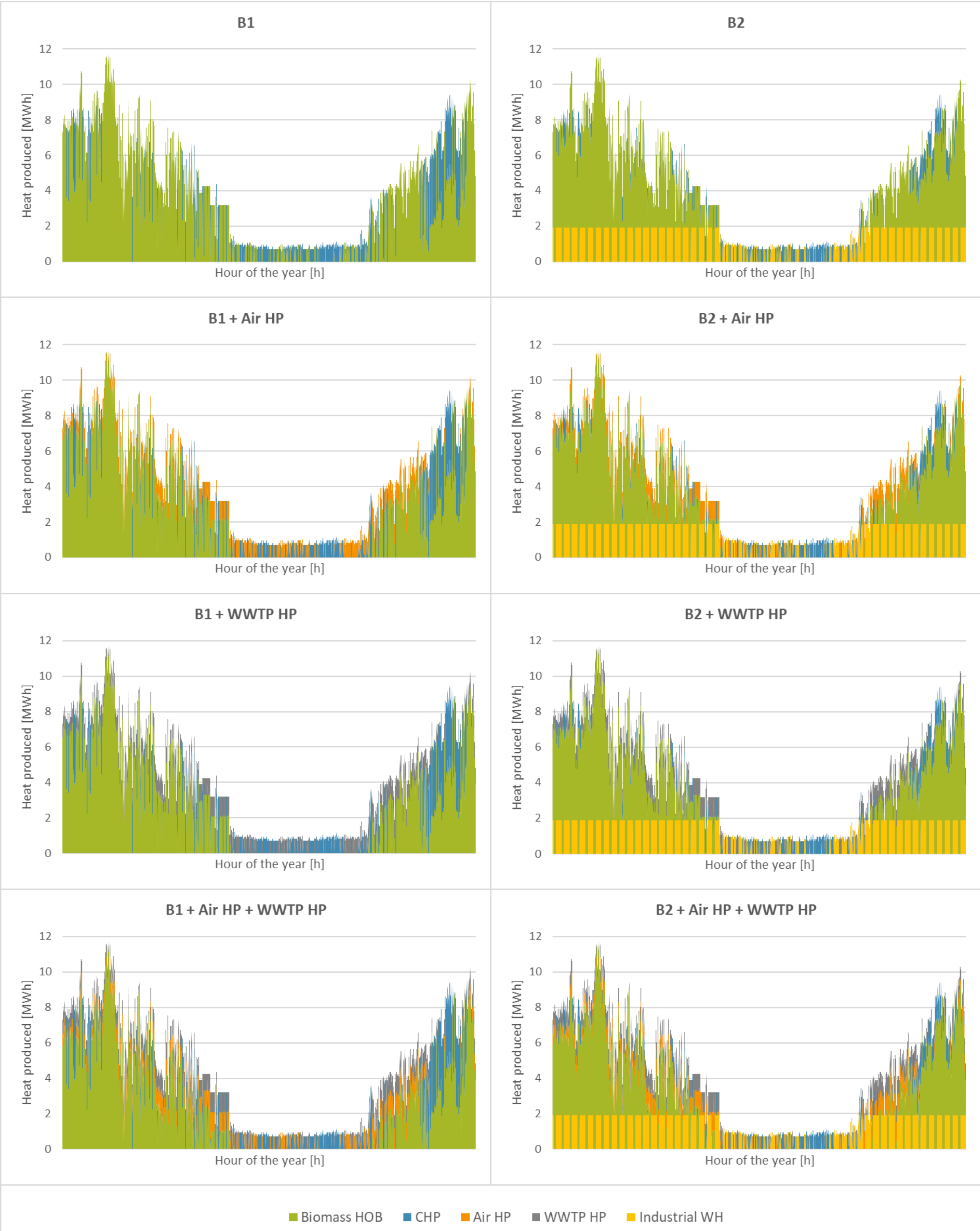

Figure B.4 Hourly heat production per technology for the eight system configurations in the case study in an average price scenario (price lambda of 0.505) and no waste heat cessation for the iron foundry under the ***low*** *biomass restriction scenario (biomass multiplication factor: 2).*

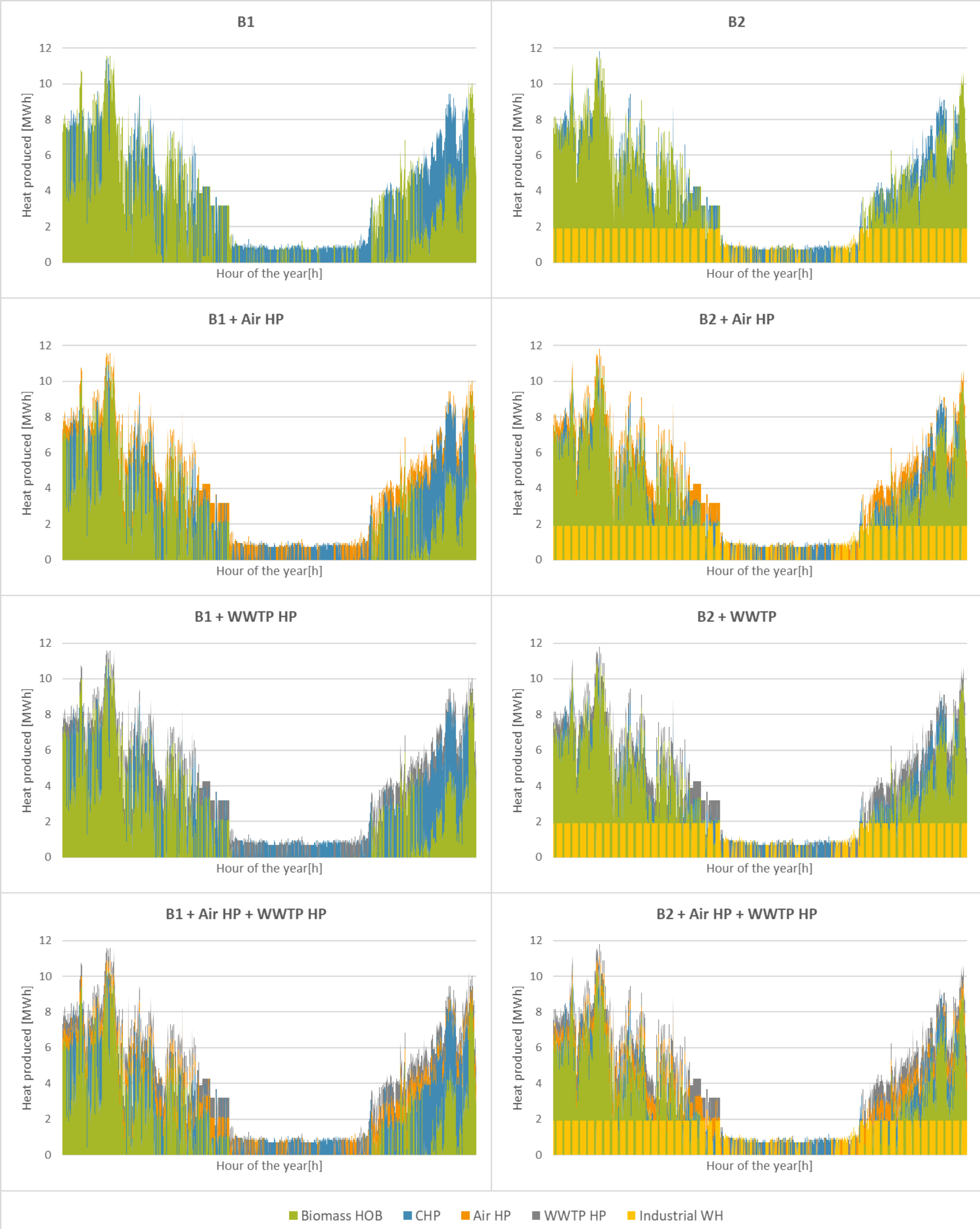

Figure B.5 Hourly heat production per technology for the eight system configurations in the case study in an average price scenario (price lambda of 0.505) and no waste heat cessation for the iron foundry under the ***medium*** *biomass restriction scenario (biomass multiplication factor: 3).*

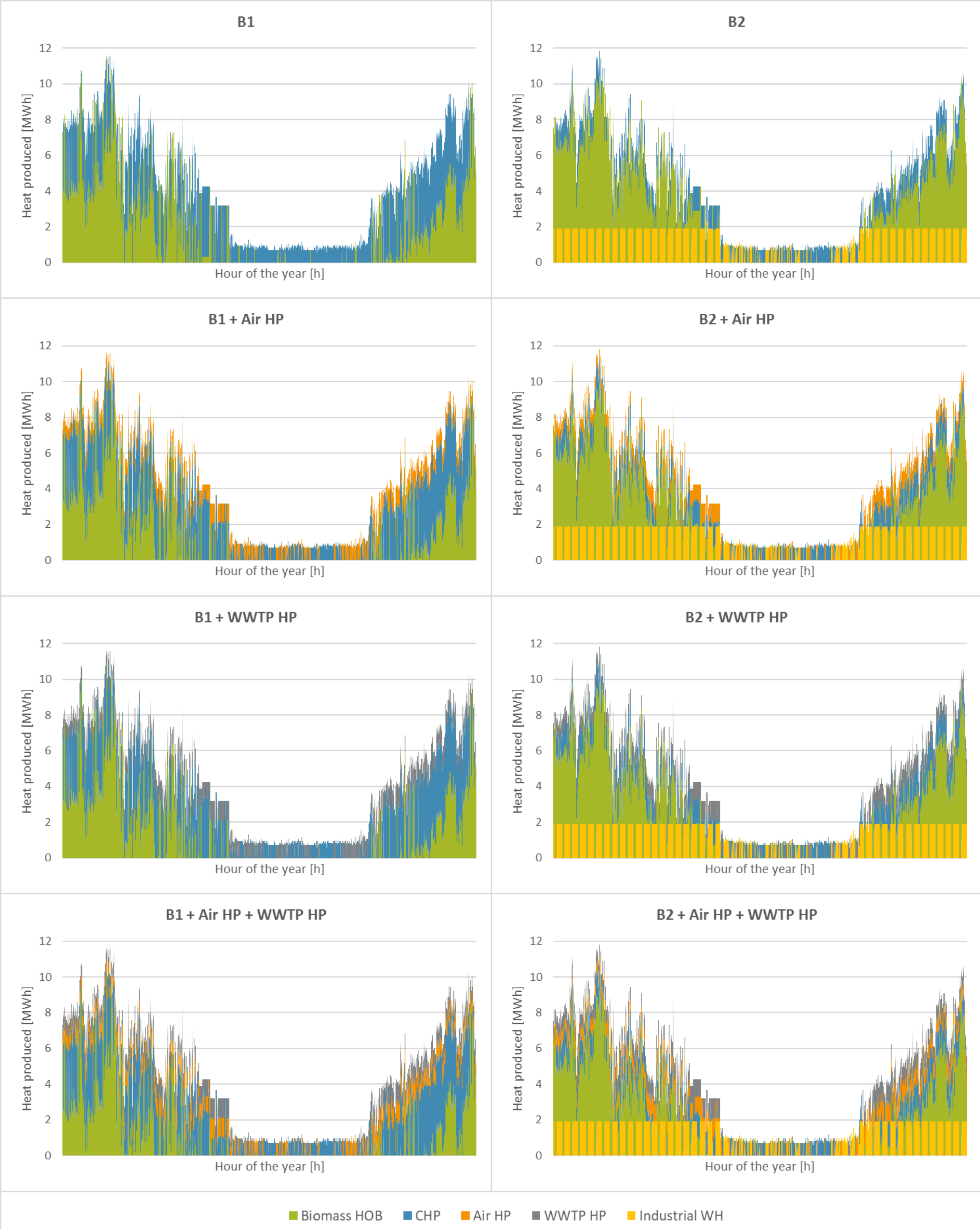

Figure B.6 Hourly heat production per technology for the eight system configurations in the case study in an average price scenario (price lambda of 0.505) and no waste heat cessation for the iron foundry under the ***high*** *biomass restriction scenario (biomass multiplication factor: 4).*

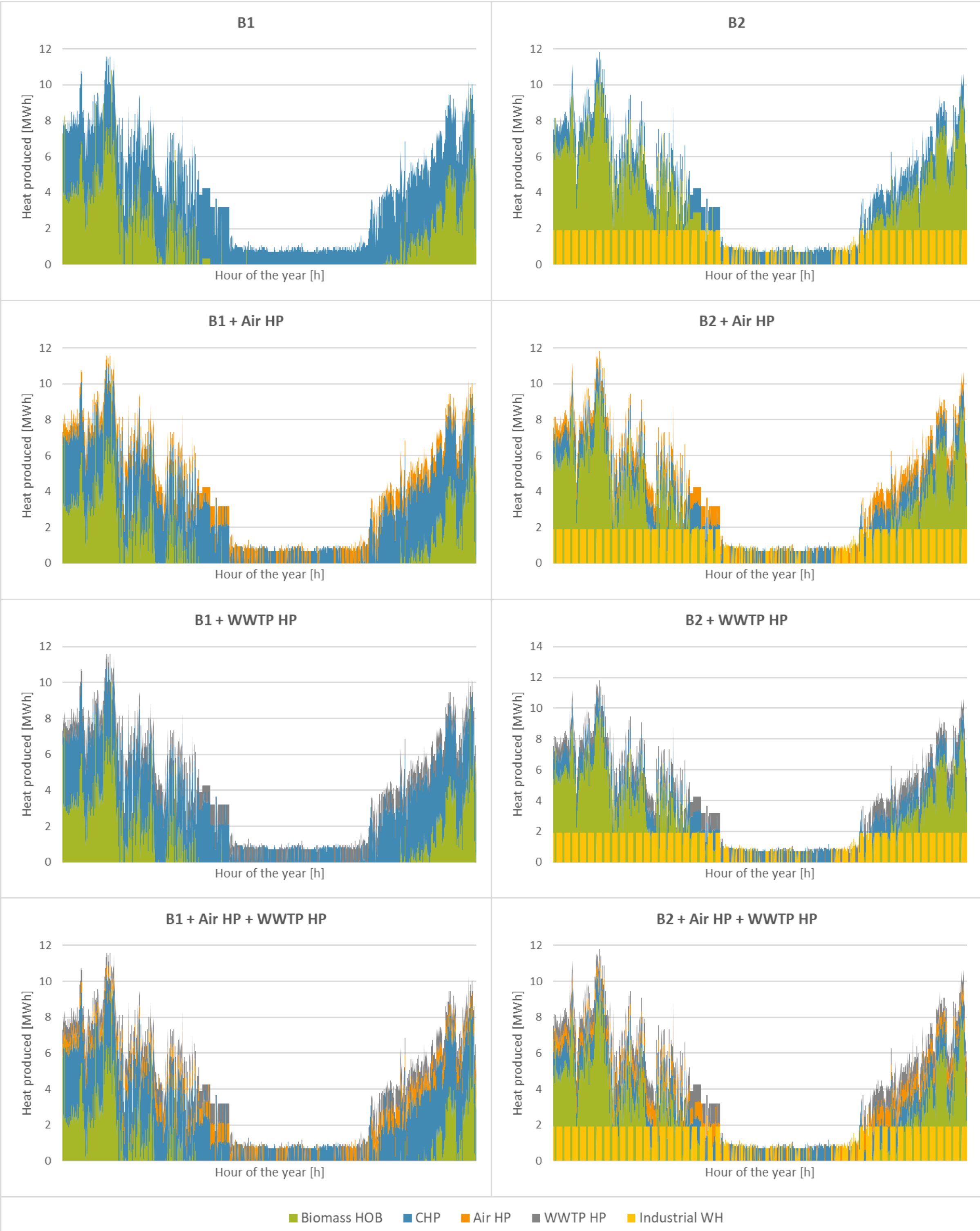

Figure B.7 Hourly heat production per technology for the eight system configurations in the case study in an average price scenario (price lambda of 0.505) and no waste heat cessation for the iron foundry under the ***very high*** *biomass restriction scenario (biomass multiplication factor: 5).*

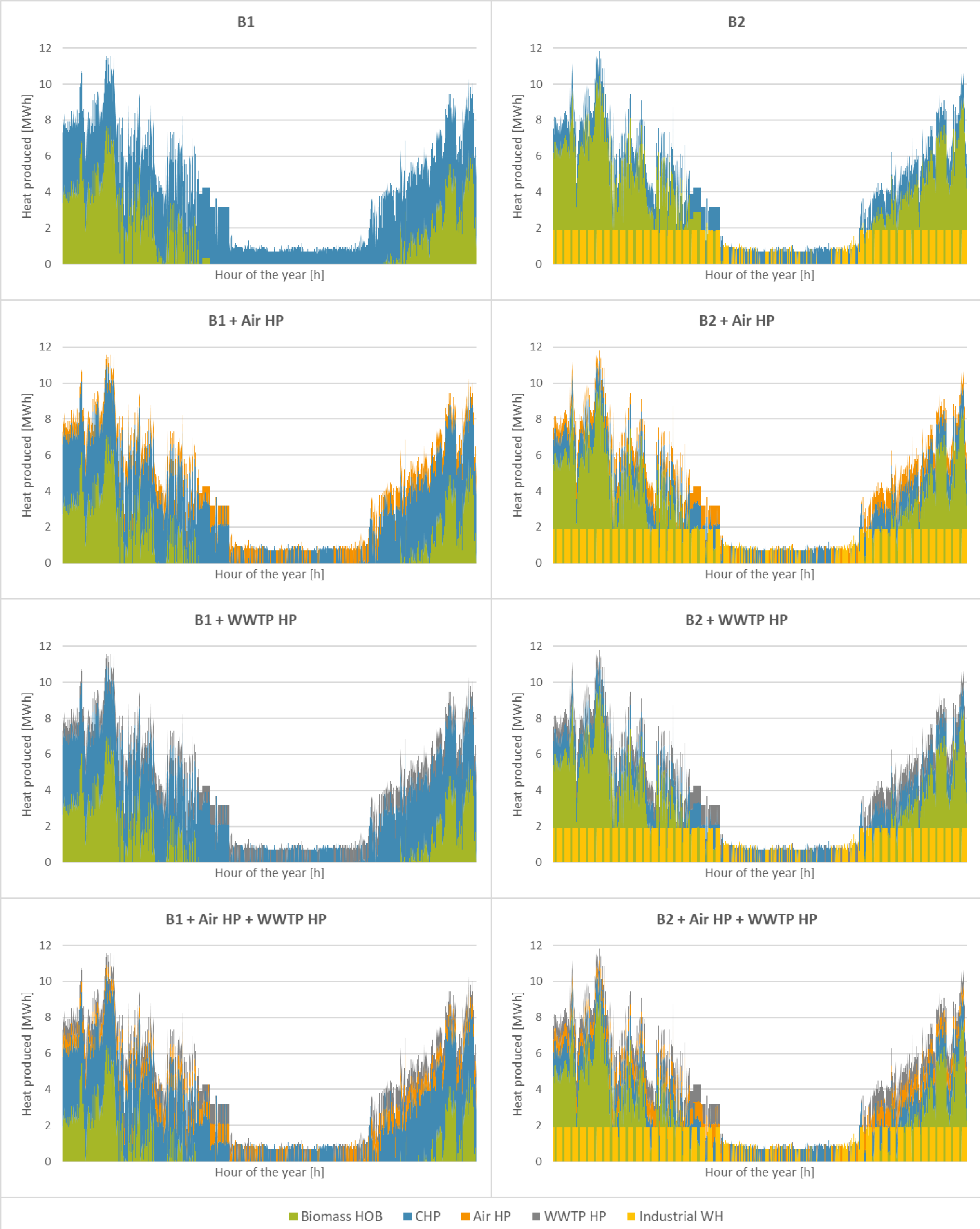

*Figure B.8 Hourly heat production per technology for the eight system configurations in the case study in an average price scenario (price lambda of 0.505) and no waste heat cessation for the iron foundry under the **maximum** biomass restriction scenario (biomass multiplication factor: 10).*

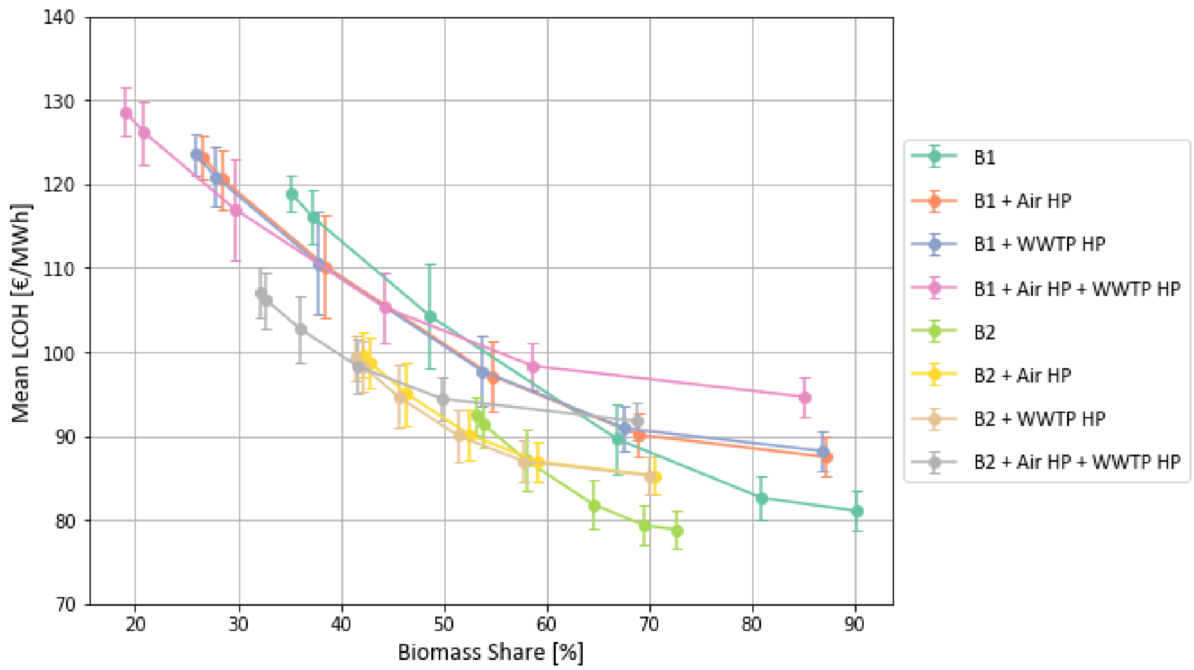

Figure B.9 Mean levelized cost of heat (LCOH) compared to the share of heat production from the biomass HOB as a percent of total heat production across the eight configurations studied for the case study. Each of the points modelled per system configuration represents a biomass restriction level (none, low, medium, high, very high, and maximum when moving from high biomass share to low biomass share). Error bars indicate standard deviation in mean LCOH.